Title

Measurement of top-quark pair production in association with charm quarks in proton—proton collisions at s = 13 TeV with the ATLAS detector

Authors

Aad, G

Aakvaag, E

Abbott, B

et al.

Publication Date

2025

DOI

10.1016/j.physletb.2024.139177

EUROPEAN ORGANISATION FOR NUCLEAR RESEARCH (CERN)

Phys. Lett. B 860 (2025) 139177
DOI: 10.1016/j.physletb.2024.139177

CERN-EP-2024-242
December 13, 2024

Measurement of top-quark pair production in association with charm quarks in proton–proton collisions at $\sqrt{s} = 13$ TeV with the ATLAS detector

The ATLAS Collaboration

Inclusive cross-sections for top-quark pair production in association with charm quarks are measured with proton–proton collision data at a center-of-mass energy of 13 TeV corresponding to an integrated luminosity of 140 fb^{-1}, collected with the ATLAS experiment at the LHC between 2015 and 2018. The measurements are performed by requiring one or two charged leptons (electrons and muons), two b-tagged jets, and at least one additional jet in the final state. A custom flavor-tagging algorithm is employed for the simultaneous identification of b-jets and c-jets. In a fiducial phase space that replicates the acceptance of the ATLAS detector, the cross-sections for $t\bar{t} + \geq 2c$ and $t\bar{t} + 1c$ production are measured to be $1.28^{+0.27}_{-0.24}$ pb and $6.4^{+1.0}_{-0.9}$ pb, respectively. The measurements are primarily limited by uncertainties in the modeling of inclusive $t\bar{t}$ and $t\bar{t} + b\bar{b}$ production, in the calibration of the flavor-tagging algorithm, and by data statistics. Cross-section predictions from various $t\bar{t}$ simulations are largely consistent with the measured cross-section values, though all underpredict the observed values by 0.5 to 2.0 standard deviations. In a phase-space volume without requirements on the $t\bar{t}$ decay products and the jet multiplicity, the cross-section ratios of $t\bar{t} + \geq 2c$ and $t\bar{t} + 1c$ to total $t\bar{t}$ + jets production are determined to be $(1.23 \pm 0.25)\%$ and $(8.8 \pm 1.3)\%$.

1 Introduction

Due to its pivotal role in the Standard Model (SM) of particle physics and its potential interactions with new physics in various beyond-SM frameworks, the study of the top quark (t) remains a cornerstone of contemporary particle physics research. In particular, the ATLAS [1] and CMS [2] experiments at the Large Hadron Collider (LHC) have directed their attention towards exploring rare final states involving top-quark pairs ($t\bar{t}$), such as associated production of $t\bar{t}$ with Higgs bosons ($t\bar{t}H$) or gauge bosons ($t\bar{t}W$, $t\bar{t}Z$, $t\bar{t}\gamma$), and four-top-quark production ($t\bar{t}t\bar{t}$). Measurements of $t\bar{t}H$ with $H \to b\bar{b}$ decay and $t\bar{t}t\bar{t}$ topologies with single-lepton or dilepton final states [3–7] encounter significant challenges due to substantial, irreducible background contributions stemming from $t\bar{t}$ production in association with heavy-flavor quarks, namely bottom (b) and charm (c) quarks. These heavy-flavor quarks can be produced via radiation of a gluon which then splits into a $b\bar{b}$ or $c\bar{c}$ pair. Depending on the kinematics, the $b\bar{b}$ or $c\bar{c}$ pair can form a jet each ($t\bar{t}+b\bar{b}/c\bar{c}$) or merge into a single jet ($t\bar{t}+1B/1C$). Single b-quark or c-quark production ($t\bar{t}+1b/c$) can also occur via a b-quark or c-quark originating from the initial state. Illustrative Feynman diagrams for these three production modes are shown in Figure 1.

Measurements of $t\bar{t}+b\bar{b}$ and $t\bar{t}+c\bar{c}$ production have been limited by the challenging modeling of these processes. While computations of the $t\bar{t}+b\bar{b}$ production cross-section are available at next-to-leading order (NLO) in quantum chromodynamics (QCD) [8–13], the uncertainties in the choice of the renormalization and factorization scales, denoted by μ_{R} and μ_{F}, remain sizable, primarily due to the distinct energy scales associated with the $t\bar{t}$ pair and the $b\bar{b}$ pair. Experimental measurements of $t\bar{t}+b\bar{b}$ production were conducted in proton–proton (pp) collision data at the LHC by the ATLAS and CMS experiments at a center-of-mass energy of $\sqrt{s}=13$ TeV [14–17]. These measurements, along with those of $t\bar{t}H$ ($H \to b\bar{b}$) and $t\bar{t}t\bar{t}$ production, frequently involve determining the $t\bar{t}+\geq 1c$ normalization *in situ* through a free parameter in the fit, compensating for the limited knowledge of this process. Recent ATLAS measurements of $t\bar{t}+b\bar{b}$ and $t\bar{t}H$ ($H \to b\bar{b}$) [5, 17] reported the $t\bar{t}+\geq 1c$ normalization factor to be larger than the value predicted by Monte Carlo (MC) simulations. CMS performed a dedicated $t\bar{t}+c\bar{c}$ measurement in $t\bar{t}$ final states with two charged leptons based on Run 2 data corresponding to 41.5 fb^{-1} [18], but did not explicitly measure the $t\bar{t}+1c/C$ cross-section. The rates of $t\bar{t}+b\bar{b}$, $t\bar{t}+c\bar{c}$, and $t\bar{t}+$ light jets were found to agree with predictions from MC simulations performed at NLO in the matrix element interfaced with a parton shower (PS) algorithm (NLO+PS) within one to two standard deviations of measurement uncertainties.

Using the complete LHC Run 2 data sample of pp collisions corresponding to an integrated luminosity of 140 fb^{-1}, this Letter presents the first ATLAS measurement of $t\bar{t}+\geq 1c$ production. The production rates of $t\bar{t}+\geq 2c$ and $t\bar{t}+1c$ are determined separately to facilitate more detailed comparisons with theoretical predictions, as these processes are expected to be sensitive to different production mechanisms (c.f. Figure 1). The first comprises all final states with two or more c-jets, e.g., $t\bar{t}+c\bar{c}$ production where both c-quarks form separate jets, while the second includes both $t\bar{t}+1c$ production via a c-quark from the initial state and $t\bar{t}+1C$ production. Events with one or two charged leptons in the final state are considered, targeting $t\bar{t}$ topologies where one or both W bosons from the top quarks decay leptonically. While topologies with one charged lepton (single-lepton) offer larger statistics, they introduce additional complexity due to the potential production of extra c-quarks from the hadronically decaying W boson. Conversely, final states with two charged leptons (dilepton) are rarer but expect less background contamination.

The probabilities for $t\bar{t}$ pairs with additional jets initiated by b-quarks, c-quarks, light quarks, and gluons to enter each analysis region are estimated through NLO+PS simulations of inclusive $t\bar{t}$ and of $t\bar{t}+b\bar{b}$ production. This measurement uses a custom flavor tagging algorithm, termed the b/c-tagger, tailored to simultaneous c-jet and b-jet identification, to define analysis regions sensitive to $t\bar{t}+\geq 2c$ and $t\bar{t}+1c$

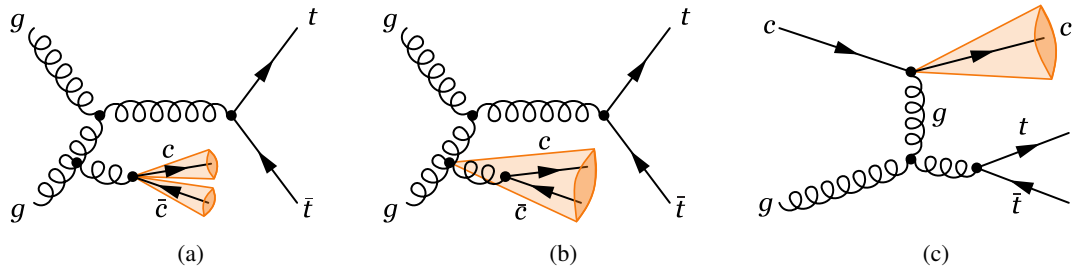

Figure 1: Illustrative Feynman diagrams for $t\bar{t}+\geq 2c$ and $t\bar{t}+1c$ production: (a) $t\bar{t}+c\bar{c}$ production via initial-state gluon radiation where both c-quarks form a jet each, (b) $t\bar{t}+c\bar{c}$ production via initial-state gluon radiation where the two c-quarks are in the same jet, (c) $t\bar{t}+1c$ production where the c-quark originates from the initial state.

production. The rates of these processes are then measured in a fiducial phase space designed to replicate the acceptance of the ATLAS detector and in a more inclusive volume. Furthermore, the ratios of $t\bar{t}+\geq 2c$, $t\bar{t}+1c$, and $t\bar{t}+\geq 1b$ to overall $t\bar{t}+$jets production are extracted and compared with NLO+PS simulations.

2 ATLAS detector

The ATLAS experiment [1] at the LHC is a multipurpose particle detector with a forward–backward symmetric cylindrical geometry and a near 4π coverage in solid angle.[1] It consists of an inner tracking detector (ID) surrounded by a thin superconducting solenoid providing a 2 T axial magnetic field, electromagnetic and hadronic calorimeters, and a muon spectrometer. The ID covers the pseudorapidity range $|\eta| < 2.5$. It consists of silicon pixel, silicon microstrip, and transition radiation tracking detectors. Lead/liquid-argon (LAr) sampling calorimeters provide electromagnetic (EM) energy measurements with high granularity within the region $|\eta| < 3.2$. A steel/scintillator-tile hadronic calorimeter covers the central pseudorapidity range ($|\eta| < 1.7$). The endcap and forward regions are instrumented with LAr calorimeters for EM and hadronic energy measurements up to $|\eta| = 4.9$. The muon spectrometer surrounds the calorimeters and is based on three large superconducting air-core toroidal magnets with eight coils each. The field integral of the toroids ranges between 2.0 and 6.0 T m across most of the detector. The muon spectrometer includes a system of precision tracking chambers up to $|\eta| = 2.7$ and fast detectors for triggering up to $|\eta| = 2.4$. The luminosity is measured mainly by the LUCID–2 [19] detector which is located close to the beampipe. A two-level trigger system is used to select events [20]. The first-level trigger is implemented in hardware and uses a subset of the detector information to accept events at a rate below 100 kHz. This is followed by a software-based trigger that reduces the accepted event rate to 1 kHz on average depending on the data-taking conditions. A software suite [21] is used in data simulation, in the reconstruction and analysis of real and simulated data, in detector operations, and in the trigger and data acquisition systems of the experiment.

[1] ATLAS uses a right-handed coordinate system with its origin at the nominal interaction point (IP) in the center of the detector and the z-axis along the beam pipe. The x-axis points from the IP to the center of the LHC ring, and the y-axis points upwards. Polar coordinates (r, ϕ) are used in the transverse plane, ϕ being the azimuthal angle around the z-axis. The pseudorapidity is defined in terms of the polar angle θ as $\eta = -\ln\tan(\theta/2)$ and is equal to the rapidity $y = \frac{1}{2}\ln\left(\frac{E+p_z}{E-p_z}\right)$ in the relativistic limit. Angular distance is measured in units of $\Delta R \equiv \sqrt{(\Delta y)^2 + (\Delta\phi)^2}$.

3 Simulation of signal and background processes

Samples of simulated events are used to model $t\bar{t}$ + jets production and most background processes. These MC simulated samples were generated employing either the full ATLAS detector simulation [22] based on GEANT4 [23], or a faster simulation where the GEANT4 simulation of the calorimeter response is replaced by a detailed parameterization of the shower shapes [22]. Both simulation methods were found to provide similar modeling for the observables used in this Letter. To account for the effects of multiple interactions in the same and neighboring bunch crossings (pileup), additional interactions were simulated using PYTHIA 8.186 [24] with a set of tuned parameters (*tune*) referred to as A3 [25] and superimposed onto the simulated hard-scatter event. Subsequently, simulated events were reweighted to replicate the pileup conditions observed in the full Run 2 data sample, with a mean number of pp interactions per bunch crossing of 34. All simulated events were processed through the same reconstruction algorithms and analysis chain as the data.

Unless specified otherwise, PYTHIA8 [26] was employed to simulate PS, hadronization, and multi-parton interactions (MPIs). For all samples using PYTHIA8 or HERWIG7 [27–29] for the simulation of the PS, hadronization and MPIs, the decays of b- and c-hadrons were simulated using the EVTGEN program [30]. PYTHIA8 setups use the A14 tune [31] and the NNPDF2.3LO parton distribution function (PDF) set [32]; HERWIG7 setups use the H7UE tune [28] or the default HERWIG tune alongside the MMHT2014LO PDF set [33]. The top-quark mass was set to $m_t = 172.5\,\text{GeV}$ and, unless stated otherwise, the five-flavor scheme (5FS) with massless b-quarks in the matrix element was used for all simulation setups and the corresponding PDF sets.

Inclusive $t\bar{t}$ events were generated with the POWHEG BOX2 [34–37] generator at NLO in QCD employing the NNPDF3.0NLO PDF set [38]. The h_{damp} parameter, which regulates the transverse momentum (p_{T}) of the first additional emission beyond the Born configuration, was set to $1.5\,m_t$ [39]. The hardness scale parameter, which determines the region of phase space vetoed during showering when matched to a PS, was fixed at $p_{\text{T}}^{\text{hard}} = 0$ [40, 41]. The scales μ_{R} and μ_{F} were set to the transverse mass of the top quark, $m_{\text{T}}(t) = \sqrt{m_t^2 + p_{\text{T},t}^2}$. In the following, this sample is referred to as $t\bar{t}$ POWHEG+PYTHIA8. To assess uncertainties in the modeling, alternative sets of $t\bar{t}$ events were generated with different configurations: with $p_{\text{T}}^{\text{hard}} = 1$; with $h_{\text{damp}} = 3\,m_t$; and with POWHEG BOX interfaced to HERWIG7 instead of PYTHIA8. To compare the result with another prediction, an additional set was generated with the MADGRAPH5_AMC@NLO 2.6.0 generator [42] at NLO in QCD, which uses the NNPDF3.0NLO PDF set, MADSPIN [43, 44] to simulate top-quark decays, and HERWIG7 for PS and hadronization [45]. All generated sets of events were reweighted to the predicted cross-section of $\sigma(t\bar{t}) = 832 \pm 51$ pb, as calculated with the Top++2.0 program to next-to-next-to-leading order (NNLO) in QCD, including soft-gluon resummation to next-to-next-to-leading-log order (see Ref. [46] and references therein). The uncertainties include independent variations of μ_{R} and μ_{F}, and variations in the PDF and α_S, following the PDF4LHC prescription with the MSTW2008 68% CL NNLO, CT10 NNLO and NNPDF2.3 5FS PDF sets (see Ref. [47] and references therein, and Refs. [32, 48, 49]).

The POWHEG BOX RES [11] generator and OPENLOOPS [50–52] were used to generate $t\bar{t} + b\bar{b}$ events in the four-flavor scheme (4FS) with massive b-quarks, where the generation of the additional $b\bar{b}$ pair is included in the matrix element, employing the NNPDF3.0NLO 4FS PDF set [38]. The μ_{R} scale was set to $\frac{1}{2}\sqrt[4]{\prod_{i=t,\bar{t},b,\bar{b}} m_{\text{T},i}}$ where $m_{\text{T},i}$ denotes the transverse mass for each parton i. The μ_{F} scale and the h_{damp} parameter were set to $0.5 \times \sum_i m_{\text{T},i}$ with $i \in \{t, \bar{t}, b, \bar{b}, j\}$ and $i \in \{t, \bar{t}, b, \bar{b}\}$, respectively, where j denotes extra partons. The $p_{\text{T}}^{\text{hard}}$ parameter was fixed to 0, and the Born-zero-damp parameter (h_{bzd}), regulating the

division between the finite and singular part of the real emission in the NLO calculation, was set to 5. In the following, this sample is referred to as $t\bar{t} + b\bar{b}$ POWHEG+PYTHIA8. To assess uncertainties in the modeling, alternative sets of $t\bar{t} + b\bar{b}$ events were generated with different configurations: with $p_{\mathrm{T}}^{\mathrm{hard}} = 1$; using the dipole recoil scheme instead of the nominal global recoil scheme [11, 53]; and interfacing POWHEG BOX RES with HERWIG7 instead of PYTHIA8. To compare the result with another prediction, alternative sets of $t\bar{t} + b\bar{b}$ events were generated with $h_{\mathrm{bzd}} = 2$. An additional alternative set of events was generated with the SHERPA 2.2.10 generator [54] in the 4FS, for which the virtual corrections for matrix elements at NLO accuracy were provided by COMIX [55] and OPENLOOPS. The SHERPA events were matched with the SHERPA PS algorithm [56] based on Catani–Seymour dipole factorization using the MEPS@NLO prescription [57–60] and a set of tuned parameters developed by the SHERPA authors. All generated sets of events were reweighted to the same prediction cross-section value as computed in POWHEG BOX RES at NLO in QCD.

A dedicated simulation of $t\bar{t} + c\bar{c}$ production in the three-flavor scheme (3FS) is not available. Hence, $t\bar{t} + c\bar{c}$ contributions are estimated solely using $t\bar{t}$ 5FS simulation, where only the gluon radiation process is simulated in the NLO matrix element, but its splitting into a $c\bar{c}$ pair is done in the PS.

Simulated $t\bar{t}$ and $t\bar{t} + b\bar{b}$ events are sorted into four $t\bar{t}$ + jets categories using particle-level information: $t\bar{t} + \geq 2c$, $t\bar{t} + 1c$, $t\bar{t} + \geq 1b$, and $t\bar{t}$ + light. For the categorization, jets are reconstructed from stable particles[2] following PS and hadronization, using the anti-k_t algorithm [61, 62] with a radius parameter $R = 0.4$. They are required to have $p_{\mathrm{T}} > 15$ GeV and $|\eta| < 2.5$. The flavor of a particle-level jet is determined by counting b- and c-hadrons with $p_{\mathrm{T}} > 5$ GeV that are *ghost-associated* [63, 64] with the jet. Jets with one or more associated b-hadrons are designated as b-jets, while those with one or more associated c-hadrons but no b-hadron are labeled as c-jets. Events are categorized based on the presence of additional particle-level b-jets and c-jets, excluding jets originating from decays of top quarks and W bosons.[3] Events with one or more b-jets are classified as $t\bar{t} + \geq 1b$, those with two or more c-jets but no b-jet are categorized as $t\bar{t} + \geq 2c$, and events with one c-jet but no b-jet are labeled as $t\bar{t} + 1c$. Any remaining events enter the $t\bar{t}$ + light category.

The $t\bar{t}$ + jets categorization at particle level is used to remove the overlap between the inclusive $t\bar{t}$ 5FS simulation and the $t\bar{t} + b\bar{b}$ 4FS simulation. The latter is expected to provide the more accurate modeling of $t\bar{t} + b\bar{b}$ production and is the preferable setup to simulate $t\bar{t} + \geq 1b$ contributions in this analysis. Thus, events are removed from any of the $t\bar{t}$ 5FS setups if they fall into the $t\bar{t} + \geq 1b$ category at particle level. All other events are retained to estimate contributions in the $t\bar{t} + \geq 2c$, $t\bar{t} + 1c$, and $t\bar{t}$ + light categories. Likewise, events from the $t\bar{t} + b\bar{b}$ 4FS simulation are removed if they fall into the $t\bar{t} + \geq 2c$, $t\bar{t} + 1c$, or $t\bar{t}$ + light categories at particle level. The individual cross-sections assigned to the $t\bar{t}$ and $t\bar{t} + b\bar{b}$ samples are retained, and no rescaling is performed after removing the overlapping events.

Various other processes involving top quarks can mimic $t\bar{t}$ + jets topologies. Single-top-quark t-channel, s-channel, and tW production were simulated using POWHEG BOX2 at NLO in QCD. For t-channel production, events were generated in the 4FS with the NNPDF3.0NLO 4FS PDF set. For s-channel and tW production, events were generated in the 5FS using the NNPDF3.0NLO 5FS PDF set. The tW simulation employed the diagram-removal scheme [65] to treat interference with $t\bar{t}$ production [39]. Additional sets of tW events were generated in different setups: using the diagram-subtraction scheme [39, 65]; using

[2] Particle-level objects are considered stable if $\tau > 3 \times 10^{-11}$ s.

[3] The procedure to exclude these jets is as follows: b-quarks and c-quarks originating directly from the decays of top quarks and W bosons are identified in the MC generator record. Then, the b- and c-hadrons closest in ΔR are flagged. Any jet *ghost-associated* with these hadrons is removed from the categorization.

Powheg Box2 interfaced with Herwig 7.04; and using MadGraph5_aMC@NLO 2.6.2 interfaced with Pythia8. Powheg Box2+Herwig7 setups were also generated for t-channel and s-channel production. $t\bar{t}H$ production was simulated with Powheg Box2 at NLO in QCD in the 5FS, using the NNPDF3.0nlo PDF set. Additionally, $t\bar{t}W$, $t\bar{t}Z$, tZq, and tWZ events were generated using the MadGraph5_aMC@NLO 2.3.3 generator at NLO in QCD with the NNPDF3.0nlo PDF set. Secondary sets of $t\bar{t}W$ and $t\bar{t}Z$ events were simulated with Sherpa 2.2.0 at leading order (LO) in QCD. In the following, these processes are collectively referred to as *Other Top*.

W+jets and Z+jets events were simulated using the Sherpa 2.2.1 generator employing NLO matrix elements for up to two partons and LO matrix elements for up to four partons, calculated with the Comix and OpenLoops libraries. Diboson events with semileptonic and fully leptonic decays were simulated using Sherpa 2.2.1 and Sherpa 2.2.2, employing NLO matrix elements for up to one additional parton and LO matrix elements for up to three additional partons. W+jets, Z+jets and diboson events were matched with the Sherpa PS algorithm based on Catani–Seymour dipole factorization using the MEPS@NLO prescription and a set of tuned parameters developed by the Sherpa authors. The NNPDF3.0nnlo PDF set [38] was used, and the cross-sections of the samples were reweighted to NNLO predictions [66]. In the following, W+jets, Z+jets and diboson processes are collectively referred to as *Non-Top*.

The cross-section measurements are conducted within a fiducial volume at particle level, closely resembling the detector-level acceptance, ensuring robustness against variations in acceptance predictions from MC simulations. Events in the single-lepton (dilepton) channel must exhibit five (three) or more jets with $p_{\mathrm{T}} > 25\,\mathrm{GeV}$ and $|\eta| < 2.5$, out of which at least two must be ghost-associated with b-hadrons. No specific requirements are imposed regarding the presence of additional b- or c-jets in the fiducial phase space, but the $t\bar{t}$+jets categorization is performed as described above. In the single-lepton channel, events must feature exactly one charged lepton ($\ell = e, \mu$), while in the dilepton channel, events must contain exactly two oppositely charged leptons. One lepton must have $p_{\mathrm{T}} > 27\,\mathrm{GeV}$, any additional lepton must carry $p_{\mathrm{T}} > 10\,\mathrm{GeV}$, and all are required to be within $|\eta| < 2.5$. Any event featuring a same-flavor lepton pair with an invariant mass below 15 GeV or within the range 83 to 99 GeV is rejected. Leptons are removed if their distance to a jet satisfies $\Delta R < 0.4$. The fiducial phase space accepts approximately 17% of the total number of simulated $t\bar{t} + \geq 1c$ events. The measurements are also performed in a more inclusive phase-space volume without requirements on the $t\bar{t}$ decay products and the jet multiplicity.

4 Event reconstruction and selection

Events are required to have at least one primary vertex with two or more tracks with $p_{\mathrm{T}} > 0.5\,\mathrm{GeV}$. For events with more than one primary vertex, the hard-scattering primary vertex is selected as the one with the highest sum of squared track p_{T} [67]. A suite of single-electron and single-muon triggers is used to select events with at least one charged lepton [68, 69].

Jets are reconstructed using the anti-k_t clustering algorithm with a radius parameter of $R = 0.4$ using particle flow jet constituents that combine measurements from both the ID and the calorimeter [70]. Jet candidates undergo calibration using simulations, with corrections derived from in situ techniques applied to data [71]. They are required to have $p_{\mathrm{T}} > 25\,\mathrm{GeV}$ and $|\eta| < 2.5$, with jets within $|\eta| < 2.4$ and $p_{\mathrm{T}} < 60\,\mathrm{GeV}$ further required to pass the tight working point of the jet vertex tagger [72] to reduce contribution from pileup jets.

Electron candidates are reconstructed from clusters of energy in the EM calorimeter associated with reconstructed tracks from the ID. Their reconstruction, identification, and calibration are detailed in Refs. [73, 74]. They must satisfy a set of likelihood-based identification criteria with $p_{\mathrm{T}} > 10\,\mathrm{GeV}$ and $|\eta_{\mathrm{cluster}}| < 2.47$. Electrons in the transition region between the end-caps and barrel region ($1.37 < |\eta_{\mathrm{cluster}}| < 1.52$) are vetoed. Tracks matched to electrons are required to be associated with the primary vertex and satisfy $|z_0 \sin\theta| < 0.5\,\mathrm{mm}$ and $|d_0|/\sigma(d_0) < 5$, where z_0 and d_0 are the longitudinal and transverse impact parameters of the electron track, respectively. For the analysis regions, the identification criteria are tightened, and electrons are required to satisfy a set of variable-radius isolation criteria to reduce contributions from misidentified jets, considering energy depositions in the calorimeter and tracks in the ID [73].

Muons are reconstructed by combining a track from the muon spectrometer with an ID track. Details regarding the reconstruction, identification and calibration of muons are summarized in Refs. [75, 76]. The ID tracks must be associated with the primary vertex by passing $|z_0 \sin\theta| < 0.5\,\mathrm{mm}$ and $|d_0|/\sigma(d_0) < 3$. They must fulfill $p_{\mathrm{T}} > 10\,\mathrm{GeV}$, $|\eta| < 2.5$, and satisfy a set of muon quality criteria. For the analysis regions, the quality criteria are tightened, and muons are required to pass a track-based isolation criterion to reduce contributions from misidentified jets [75].

An overlap removal procedure prevents double counting of energy deposits and improves object resolution and identification efficiencies. Electron candidates sharing tracks with a muon candidate are removed. The nearest jet within $\Delta R < 0.2$ of an electron candidate is removed in favor of the electron. Electrons within $\Delta R < 0.4$ of any jets after this selection are removed in favor of the jet. Muons are removed if they are within $\Delta R < 0.4$ of a jet to reduce contributions from heavy-flavor decays. However, if the jet has fewer than three associated tracks, the muon is kept in favor of the jet.

Jets containing b-hadrons are identified as b-tagged jets using the DL1r algorithm [77], which leverages distinctive b-hadron features like track impact parameters and the presence of displaced vertices in the ID. The algorithm also includes discriminating variables from a recurrent neural network that exploit spatial and kinematic correlations between tracks from the same b-hadron. The DL1r algorithm provides three output scores, p_b, p_c, and p_{light}, and in the standard DL1r calibration, jets are tagged as b-jets using a discriminant $\mathcal{D}_b$ that is built using the Neyman–Pearson lemma [78]:

$$\mathcal{D}_b = \log \frac{p_b}{f_c p_c + (1 - f_c) p_{\mathrm{light}}}.$$

The parameter f_c controls which background contributes more to the decision. To improve the efficiency of selecting jets originating from c-quarks without compromising the b-jet identification performance, the DL1r algorithm was reoptimized as a 2D binned discriminant, the b/c-tagger. This reoptimization was necessary because standard DL1r configurations do not provide calibrated c-tagging working points, requiring a tailored approach to achieve the desired balance between b-jet and c-jet identification. The axes of the discriminant, $\mathcal{D}_c$ and $\mathcal{D}_b$, are calculated from the p_b, p_c, and p_{light} scores following the above formula, with all b- and c-subscripts interchanged for the $\mathcal{D}_c$ discriminant. It was found that $f_b = 0.4$ provides good performance for the b/c-tagger as it leads to a balanced contamination of b-jets and light-flavor jets in the analysis regions; the value of $f_c = 0.018$ was chosen to align the admixture with the standard DL1r calibration.

The binning in $\mathcal{D}_c$ and $\mathcal{D}_b$ includes five working points (WPs), two of which are optimized for c-jet identification and two for b-jet identification. The WPs are designed to achieve an approximately constant efficiency for b-jet and c-jet identification across the jet p_{T} and $|\eta|$ range, with $p_{\mathrm{T}} > 20\,\mathrm{GeV}$. The c-tagging

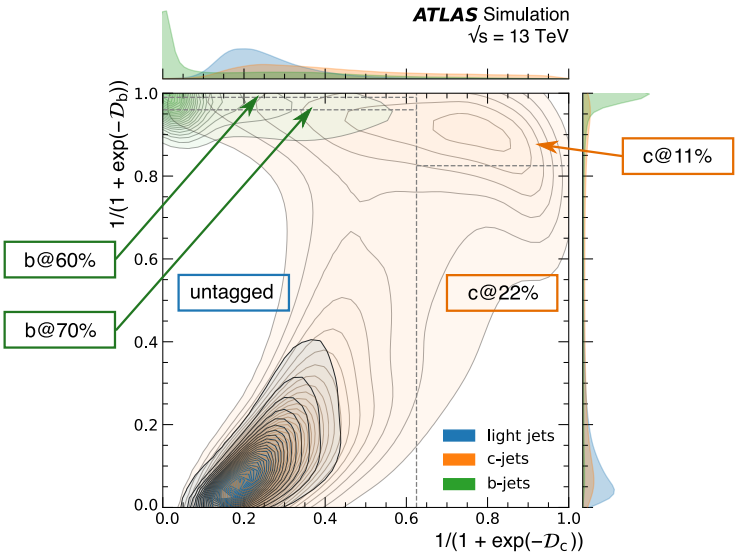

Figure 2: Distribution of light, c-, and b-jets for the 2D b/c-tagger in simulated $t\bar{t}$ events. Dashed lines correspond to the edges of the working points. For visualization purposes a standard logistic function is applied to both axes of the discriminant. The contours for each jet type are smoothed with a kernel density method to improve readability, with contours corresponding to lines of constant density. The two b-tagging bins comprise the top left corner of the discriminant, with the c-tagging bins to the right of the vertical dashed line. Untagged jets are located in the bottom left corner.

WPs are separated from the others by $\mathcal{D}_c' \geq 0.625$, where the prime indicates that a standard logistic function is applied to the discriminant: $\mathcal{D}_c' = 1/(1+\exp(-\mathcal{D}_c))$. The tight c-tagging WP includes a tighter cut on $\mathcal{D}_b'$ to increase the light-flavor rejection rate and is designed to achieve an exclusive efficiency of 11% (denoted c@11%).[4] The loose c-tagging WP, which includes c@11%, achieves an inclusive efficiency of 22% (c@22%). The c@11% and c@22% WPs yield b-jet rejection rates of 28.7 and 18.9 and light-flavor rejection rates of 1051 and 104 in simulated $t\bar{t}$ events, respectively. The b-tagging WPs, defined for $\mathcal{D}_c' < 0.625$, use the same $\mathcal{D}_b'$ cuts as the two tightest b-tagging WPs in the standard DL1r calibration. The tighter b-tagging WP is designed to achieve an exclusive efficiency of 60% (b@60%), the looser, which includes b@60%, to achieve an inclusive b-tagging efficiency of 70% (b@70%), with c-jet rejection rates of 37.1 and 12.2 and light-flavor rejection rates of 2320 and 573, respectively. Jets not entering any of the four WP bins are classified as untagged. Consequently, the b/c-tagger comprises a total of five orthogonal bins, with the distribution of light, c- and b-jets illustrated in Figure 2.

The calibration of the five b/c-tagger WPs follows standard procedures applied to the DL1r algorithm [79–81]. Jets originating from b- and c-quarks are calibrated in data using $t\bar{t}$ events, both selections being orthogonal to the events analyzed in this study by limiting the number of jets to four (two) in single-lepton (dilepton) final states. All b-tagging calibration scale factors (SFs) are close to unity, with statistical uncertainties dominating the high p_{T} regime. The c-tagging calibration yields more variation in the SF values. For the b@70% WP, the SFs average around 0.9 and some bins in jet p_{T} are incompatible with unity within their uncertainties. Light-flavor jet calibration employs the *negative-tag* method [82, 83] in conjunction with a *flip-tagger* approach following Ref. [81], and all SFs are compatible with unity within uncertainties. For the b@60% working point, the light-flavor SFs cannot be determined due to the

[4] Tightening the cut on $\mathcal{D}_c'$ instead of $\mathcal{D}_b'$ would lead to a more balanced increase in the b-jet and light-flavor rejection rate, but it was found that a focus on higher light-flavor rejection rates yields better $t\bar{t}+\geq 1c$ signal sensitivity.

Table 1: Jet multiplicity and tagging criteria for the signal regions (SRs) and control regions (CRs) in the single-lepton and dilepton channels. All single-lepton regions are defined in the 5-jet-exclusive and 6-jet-inclusive jet selections, all dilepton regions in the 3-jet-exclusive and 4-jet-inclusive jet selections. By construction, $\mathrm{SR}^{2\ell}_{\mathrm{tight}}$ only exists for the 4-jet-inclusive selection. Identical requirements on inclusive and exclusive working points, e.g., one c@22% and one c@11% in the $\mathrm{CR}^{1\ell}_{1}$, indicate a veto of additional tags at the inclusive working point.

	$\mathrm{CR}^{1\ell}_{1}$	$\mathrm{CR}^{1\ell}_{2}$	$\mathrm{CR}^{1\ell}_{3}$	$\mathrm{SR}^{1\ell}_{\mathrm{loose}}$	$\mathrm{SR}^{1\ell}_{\mathrm{tight}}$	$\mathrm{CR}^{2\ell}_{1}$	$\mathrm{CR}^{2\ell}_{2}$	$\mathrm{CR}^{2\ell}_{3}$	$\mathrm{SR}^{2\ell}_{\mathrm{loose}}$	$\mathrm{SR}^{2\ell}_{\mathrm{tight}}$
N_{jets}	$= 5$ or ≥ 6					$= 3$ or ≥ 4				≥ 4
b@70%	2	–	–	2	2	2	–	≥ 3	2	2
b@60%	–	≥ 3	3	–	–	–	≥ 3	≤ 2	–	–
c@22%	1	0	1	≥ 2	–	0	–	–	1	≥ 2
c@11%	1	–	1	1	≥ 2	–	–	–	–	–

large b-jet contamination and so, following the procedure in Ref. [81], are set to unity with additional uncertainties. The c@11% WP also has large uncertainties due to high contamination of heavy-flavor jets and low statistics. Simulation-to-simulation SFs are derived in bins of jet p_{T} and $|\eta|$ to account for differences between tagging efficiencies for different PS and hadronization algorithms [84].

A preselection is applied and requires at least one electron or muon with $p_{\mathrm{T}} > 27$ GeV that is matched to the trigger object. The single-lepton channel selects events with exactly one lepton, while the dilepton channel selects those with exactly two oppositely charged leptons. Events must have at least five (three) jets in the single-lepton (dilepton) channel, with at least three (two) b-tagged or c-tagged jets using the b@70% or c@22% working points. For dilepton final states with identical lepton flavors, the same invariant-mass criteria as those applied in the fiducial selection at particle level are imposed. In the single-lepton channel, events are split into those with exactly five jets (5-jet-exclusive) and those with six or more jets (6-jet-inclusive). Similarly, in the dilepton channel, events are categorized as either 3-jet-exclusive or 4-jet-inclusive. Based on the number of identified b- and c-tagged jets, events are further classified into signal regions (SRs) enriched in $t\bar{t}$ + ≥2c and $t\bar{t}$ + 1c events, and control regions (CRs), which determine the normalization of the $t\bar{t}$ + ≥1b and $t\bar{t}$ + light background. An overview of the seven SRs and 12 CRs is shown in Table 1. Approximately 5.3% of the simulated $t\bar{t}$ + ≥1c events passing the fiducial selection criteria are reconstructed in the analysis regions.

There are four SRs in the single-lepton channel and three SRs in the dilepton channel with different degrees of purity in $t\bar{t}$ + ≥2c and $t\bar{t}$ + 1c events. The $\mathrm{SR}^{1\ell}_{\mathrm{tight}}$ and $\mathrm{SR}^{2\ell}_{\mathrm{tight}}$ regions target $t\bar{t}$ + ≥2c events, while $\mathrm{SR}^{1\ell}_{\mathrm{loose}}$ and $\mathrm{SR}^{2\ell}_{\mathrm{loose}}$ are dominated by $t\bar{t}$ + 1c. All seven regions require exactly two b-tagged jets at b@70%. In the single-lepton channel, events featuring at least two c-tagged jets at c@22% with exactly one satisfying the c@11% working point enter the $\mathrm{SR}^{1\ell}_{\mathrm{loose}}$ regions. Events with two or more c-tagged jets at c@11% are classified into $\mathrm{SR}^{1\ell}_{\mathrm{tight}}$. The expected purity in $t\bar{t}$ + ≥2c events in the single-lepton SRs ranges between 10% and 28%, while the predicted $t\bar{t}$ + 1c contributions are between 29% and 38%. In the dilepton channel, events with exactly one c-tagged jet at c@22% are sorted into $\mathrm{SR}^{2\ell}_{\mathrm{loose}}$, while events with at least two enter $\mathrm{SR}^{2\ell}_{\mathrm{tight}}$, which is only defined in the 4-jet-inclusive selection. In the dilepton regions, the expected purity in $t\bar{t}$ + ≥2c and $t\bar{t}$ + 1c events is between 4% and 46%, and between 16% and 38%, respectively.

In the single-lepton channel, three CRs with varying compositions in $t\bar{t}$ + ≥1b and $t\bar{t}$ + light are defined for each of the two jet multiplicity selections. The $\mathrm{CR}^{1\ell}_{1}$ regions select exactly two b-tagged jets at b@70% and exactly one c-tagged jet passing c@22% and c@11%. They are dominated by $t\bar{t}$ + light events. The $\mathrm{CR}^{1\ell}_{2}$ regions are characterized by events with three or more b-tagged jets at b@60%, with a veto on c-tagged

jets, leading to a mix of $t\bar{t}$ + ≥1b and $t\bar{t}$ + light. The $\mathrm{CR}_3^{1\ell}$ regions are pure in $t\bar{t}$ + ≥1b and select events with exactly three b-tagged jets at b@60% and exactly one c-tagged jet satisfying c@22% and c@11%.

Similarly, the dilepton channel features three CRs for each of the two jet multiplicity selections. The $\mathrm{CR}_1^{2\ell}$ regions require exactly two b-tagged jets at b@70% and veto c-tagged jets. They are dominated by $t\bar{t}$ + light events. The $\mathrm{CR}_2^{2\ell}$ regions are pure in $t\bar{t}$ + ≥1b and select events with three or more b-tagged jets at b@60%. The $\mathrm{CR}_3^{2\ell}$ regions show a mix of $t\bar{t}$ + ≥1b and $t\bar{t}$ + light by requiring at least three b-tagged jets at b@70%, with no more than two satisfying the b@60% criteria.

Contributions from processes with non-prompt or misidentified leptons to the single-lepton selection, in the following termed *fake leptons*, were estimated by using the data-driven *matrix method* [85] in dedicated CRs. Prompt-lepton efficiencies were derived in data using a tag-and-probe method in Z-boson decays. Fake-lepton efficiencies were estimated in data in bins of lepton p_{T} and $|\eta|$ using events with at least three jets, at least two b-tagged jets at the 70% working point of the DL1r tagger, and one lepton fulfilling the looser identification and quality criteria. The isolation requirements were completely dropped. To enrich the selection in fake leptons, only events where the scalar sum of the magnitude of the missing-transverse-momentum vector and the leptonically decaying W-boson mass is no larger than 60 GeV were considered.[5] The fake-lepton contributions to the analysis were then estimated by inverting the efficiency matrix and applying it to the observed event yields in the analysis regions using the looser and the nominal lepton identification and isolation criteria. Fake-lepton contributions to the dilepton selection mainly arise from W+jets and single-lepton $t\bar{t}$ + jets events and were estimated from MC simulation.

5 Systematic uncertainties

The extraction of the $t\bar{t}$ + ≥2c and $t\bar{t}$ + 1c cross-sections is subject to various sources of uncertainties, impacting either the overall event yields in a region, the shape of observable distributions considered in the fit, or both.

Experimental sources of uncertainties include uncertainties in the value of the integrated luminosity of the Run 2 data, the simulation of pileup events, and effects related to the reconstruction and identification of physics objects used in the analysis. The uncertainty in the combined 2015–2018 integrated luminosity is 0.83% [87], obtained using the LUCID-2 detector [19] for the primary luminosity measurements, complemented by measurements using the inner detector and calorimeters. Uncertainties in the modeling of pileup are evaluated by varying the pileup reweighting in MC simulations within its associated uncertainties. Furthermore, lepton identification and isolation efficiencies, momentum scale and resolution, and lepton trigger efficiencies are varied within their uncertainties to evaluate their impact on the measurement [73–76]. The uncertainty in the jet energy scale (JES) is derived from a combination of simulations, test-beam data, and in situ measurements [71]. This uncertainty incorporates contributions from various sources such as jet-flavor composition, η-intercalibration, punch-through, single-particle response, calorimeter response to different jet flavors, and pileup. It comprises 30 uncorrelated JES uncertainty subcomponents. Additionally, the jet energy resolution in simulation is varied by its corresponding uncertainty, which is divided into thirteen uncorrelated sources. The uncertainty associated with the jet vertex tagger is determined by varying its efficiency correction factors [72]. Moreover, uncertainties in the calibration of

[5] The magnitude of the missing-transverse-momentum vector, denoted $E_{\mathrm{T}}^{\mathrm{miss}}$, is defined as the negative sum of the transverse momenta of the reconstructed and calibrated physical objects, plus a *soft term* built from all other tracks associated with the primary vertex [86] and not matched to a reconstructed object. The mass of the leptonically decaying W boson is calculated from the kinematics of the lepton and the missing transverse momentum.

the b/c-tagger are separately determined for b-jets, c-jets, and light-flavor jets, following the procedures detailed in Refs. [79–81]. They are derived as a function of jet p_{T} and separately for each WP, yielding a total of 45 components for b-jets and 20 each for c-jets and light-flavor jets. For jets with p_{T} values above the range covered by the calibration, extrapolation uncertainties derived from MC simulation are applied.

Uncertainties in the modeling of $t\bar{t}+\geq 2c$, $t\bar{t}+1c$, and $t\bar{t}+$ light are considered through several alternative inclusive $t\bar{t}$ simulation setups. The alternative set of events with $p_{\mathrm{T}}^{\mathrm{hard}} = 1$ is used to assess the uncertainty in the NLO matching between the matrix elements and the PS. The $h_{\mathrm{damp}} = 3\,m_t$ sample assesses the uncertainty in the choice of that parameter. The Powheg+Herwig7 setup evaluates the uncertainty in the choice of the PS and hadronization algorithm. Additionally, the nominal set of events is reweighted to scenarios where μ_{R} and μ_{F} in the matrix element are halved and doubled independently to assess the uncertainty in the choice of these parameters. To estimate uncertainties in the modeling of initial-state radiation (ISR) and final-state radiation (FSR), the factorized parameter α_S^{ISR} is varied using the *var3c* variation of the A14 tune, and the renormalization scale associated with α_S^{FSR} is varied to 0.625 and 2 relative to its nominal setting. The uncertainty in the PDF set is estimated by using 30 PDF variations of the PDF4LHC prescription.

Uncertainties in the modeling of the $t\bar{t}+\geq 1b$ contributions are considered through a similar suite of alternative $t\bar{t}+b\bar{b}$ simulation setups. The alternative set of events with $p_{\mathrm{T}}^{\mathrm{hard}} = 1$ is used to assess the uncertainty in the NLO matching between the matrix elements and the PS. The uncertainty in the choice of the recoil scheme is evaluated with the set of events generated with the alternative dipole recoil scheme. The Powheg+Herwig7 setup is used to evaluate the uncertainty in the selection of the PS and hadronization algorithm. Event weight variations identical to those applied in $t\bar{t}$ simulations, including μ_{R}, μ_{F}, ISR, FSR, and the PDF set, are considered for $t\bar{t}+b\bar{b}$.

All uncertainties considered in the modeling of $t\bar{t}+$jets production are treated as uncorrelated between the $t\bar{t}+\geq 1b$, $t\bar{t}+\geq 1c$, and $t\bar{t}+$ light processes. Moreover, the NLO matching and PS uncertainties for $t\bar{t}+\geq 1c$ ($t\bar{t}+\geq 1b$) are parameterized independently for the $t\bar{t}+\geq 2c$ and $t\bar{t}+1c$ ($t\bar{t}+\geq 2b$ and $t\bar{t}+1b$) components as the components are sensitive to different effects. Additionally, the $t\bar{t}+$light PS uncertainty is parameterized separately for the 3-jet-exclusive, 4-jet-inclusive, 5-jet-exclusive, and 6-jet-inclusive regions to avoid strong constraints arising from region-to-region migration effects.

For t-channel, s-channel, and tW single-top-quark production, the Powheg+Herwig7 setups are used to assess the uncertainty in the choice of the PS and hadronization algorithm. For tW production, the set of events with the diagram-subtraction scheme is used to gauge the uncertainty in the treatment of the interference with $t\bar{t}$, and the NLO matching uncertainty is evaluated using events generated with MadGraph5_aMC@NLO+Pythia8. An additional 5% normalization uncertainty is assigned to accommodate the uncertainty in the cross-section value [88]. For the t-channel and s-channel predictions, normalization uncertainties of 50% are assigned to cover NLO matching and cross-section uncertainties. The difference between the sets of $t\bar{t}W$ and $t\bar{t}Z$ events generated with MadGraph5_aMC@NLO+Pythia8 and Sherpa is used as an uncertainty in the prediction for these processes. Additionally, uncertainties of approximately 13% and 11% are assigned to $t\bar{t}W$ and $t\bar{t}Z$, respectively, to accommodate uncertainties in the assigned cross-section values [89]. Conservative normalization uncertainties of 50% are assigned to each of the remaining top-quark processes considered ($t\bar{t}H$, tWZ, tZq) to cover potential mismodeling of the rates of these processes in the probed fiducial phase space. For the $W+$jets, $Z+$jets and diboson background, the assigned uncertainties follow those used in previous ATLAS measurements [90]. Normalization uncertainties of 40% and 35% are considered for $W+$jets and $Z+$jets processes, based on variations of the μ_{R} and μ_{F} scales and of the matching parameters in the Sherpa generator. Additional 40% uncertainties are assigned to $W+$jets events with exactly two heavy-flavor jets and at least three heavy-flavor jets based on the

same variations. A 50% uncertainty is assigned to the diboson background, which includes uncertainties in the inclusive cross-section and additional jet production [91–93]. None of the modeling uncertainties of the *Other Top* and *Non-Top* categories have any significant impact on the $t\bar{t}+\geq 2c$ and $t\bar{t}+1c$ cross-section measurements.

The fake-lepton estimate in the single-lepton channel is derived from a data sample with finite statistics, leading to bin-by-bin statistical uncertainties for the fake-electron and fake-muon contributions. In addition, conservative 50% normalization uncertainties are assigned to the data-driven single-lepton and MC-based dilepton estimates.

6 Results

The data from all 19 analysis regions are simultaneously fit using a binned profile likelihood approach using the HistFactory [94] and RooFit [95] toolkits. Systematic uncertainties are incorporated as nuisance parameters in the fit and are constrained by a Gaussian penalty term present in the likelihood function. The statistical uncertainty arising from the limited number of simulated events is included in the likelihood in the form of additional nuisance parameters with Poisson constraint terms. To determine the production cross-sections of the $t\bar{t}+\geq 2c$ and $t\bar{t}+1c$ processes, and to control the $t\bar{t}+\geq 1b$ and $t\bar{t}+$ light background processes, normalization factors are defined for all four $t\bar{t}+$jets categories. These factors, μ_i, serve as unconstrained normalization factors in the profile likelihood fit, and they are applied to both fiducial and non-fiducial $t\bar{t}+$jets events. The inclusive $t\bar{t}+$jets normalization factor is computed following

$$\mu(t\bar{t}+\text{jets}) = \sum_i \mu_i R_i^{\text{MC}} \quad \text{for } i \in \{t\bar{t}+\geq 1b, t\bar{t}+\geq 2c, t\bar{t}+1c, t\bar{t}+\text{light}\}, \tag{1}$$

where R_i^{MC} is the predicted cross-section ratio of process i to overall $t\bar{t}+$jets production in MC simulation.

Each of the 12 CRs is represented as a single bin in the fit. $\text{SR}^{1\ell 5\text{j}}_{\text{loose}}$ and $\text{SR}^{1\ell 5\text{j}}_{\text{tight}}$ use the invariant mass between the two geometrically closest c-tagged jets to increase sensitivity to differences between the $t\bar{t}+\geq 2c$, $t\bar{t}+1c$, and $t\bar{t}+$ light contributions (only considering c-tagged jets passing $c@11\%$ in $\text{SR}^{1\ell 5\text{j}}_{\text{tight}}$). Due to c-jets originating from the decay of the W boson, the contribution from $t\bar{t}+$ light is enhanced around the W-boson mass. $\text{SR}^{2\ell 3\text{j}}_{\text{loose}}$ uses the invariant mass between the c-tagged jet and the geometrically closest b-tagged jet. All three regions use four bins with varying width to maximize sensitivity to the $t\bar{t}+\geq 2c$ and $t\bar{t}+1c$ contributions. In the 4-jet-inclusive and 6-jet-inclusive SRs, the jet multiplicity is used to enhance the separation between $t\bar{t}+\geq 1b$, $t\bar{t}+\geq 2c$, $t\bar{t}+1c$, and $t\bar{t}+$ light processes, fitting $6 \leq N_{\text{jets}} \leq 9$ and $4 \leq N_{\text{jets}} \leq 7$ in the single-lepton and dilepton channels, respectively. Overflow events are included in the last bin of each distribution.

Post-fit comparisons between data and simulation for all regions are depicted in Figure 3. The fitted observable distributions of the SRs are shown in Figures 4 and 5. Good agreement between data and simulation is observed in all regions and observables with varying relative contributions of the $t\bar{t}+$jets categories. The goodness of fit was evaluated using a *saturated model* [96] and the compatibility with data was found to be 98%.

The $t\bar{t}+\geq 2c$ and $t\bar{t}+1c$ normalization factors obtained from this fit are used to extract the observed fiducial cross-sections by scaling them with the predicted cross-sections for the fiducial phase space introduced in Section 3. Theoretical uncertainties in the predicted cross-sections owing to the μ_{R} and μ_{F} scale

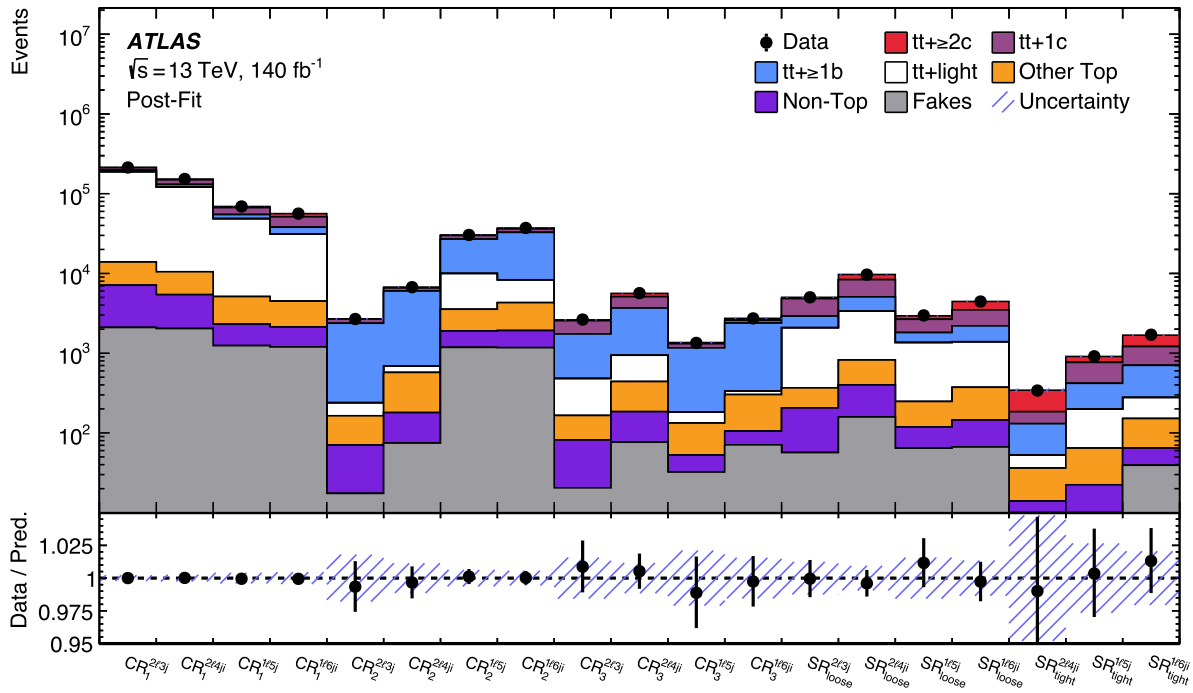

Figure 3: Post-fit agreement between data and MC simulation in the 12 control regions (CRs) and seven signal regions (SRs). The error bars indicate data statistical uncertainties. The hatched uncertainty bands include all uncertainties and their correlations. *Other Top* includes single-top-quark production and associated production of $t\bar{t}$ and single top quarks with bosons. *Non-Top* includes W+jets, Z+jets, and diboson processes.

choice and the used PDF set are not propagated to the extracted fiducial cross-section values. The fiducial cross-sections for $t\bar{t}+\geq 2c$ and $t\bar{t}+1c$ processes are determined to be

$$\sigma^{\text{fid}}(t\bar{t}+\geq 2c) = 1.28\,^{+0.16}_{-0.10}\,(\text{stat})\,^{+0.21}_{-0.22}\,(\text{syst})\ \text{pb} = 1.28\,^{+0.27}_{-0.24}\ \text{pb}, \tag{2}$$

$$\sigma^{\text{fid}}(t\bar{t}+1c) = 6.4\,^{+0.5}_{-0.4}\,(\text{stat})\ \pm 0.8\,(\text{syst})\ \text{pb} = 6.4\,^{+1.0}_{-0.9}\ \text{pb}. \tag{3}$$

The breakdown into statistical and systematic uncertainties is estimated from the covariance matrix of the profile likelihood fit, following Ref. [97]. The precision of the measured $t\bar{t}+\geq 2c$ and $t\bar{t}+1c$ cross-sections is limited by uncertainties in the modeling of $t\bar{t}+\geq 1c$, $t\bar{t}+\geq 1b$, and $t\bar{t}+$light, in particular in the NLO matching and the PS, by uncertainties in the b/c-tagger calibration, as well as by data statistics. Table 2 provides a detailed breakdown of the uncertainties that affect the $t\bar{t}+\geq 2c$ and $t\bar{t}+1c$ cross-sections in the fiducial phase space. The uncertainty in the $t\bar{t}+\geq 1b$ and $t\bar{t}+$light normalization factors on the $t\bar{t}+\geq 2c$ and $t\bar{t}+1c$ cross-sections is included in the data statistics entry. The fit constrains several nuisance parameters that strongly impact the $t\bar{t}+\geq 2c$ and $t\bar{t}+1c$ cross-sections, with none falling below 50% of their prior values. Noteworthy constraints are placed on the $t\bar{t}+\geq 1c$ FSR and $t\bar{t}+1c$ PS nuisance parameters, which arise primarily from discrepancies between the predicted rates of $t\bar{t}+\geq 2c$ and $t\bar{t}+1c$ events in the signal regions. No significant pulls of the nuisance parameters are observed in the fit. The measured $t\bar{t}+\geq 1b$ normalization factor is compatible with those obtained in a dedicated ATLAS $t\bar{t}+b\bar{b}$ measurement performed in a fiducial phase space targeting $e+\mu$ final states [17], reaching a similar level of relative precision.

The measured values for the four processes and the overall $t\bar{t}+$jets production are depicted in Figure 6 and

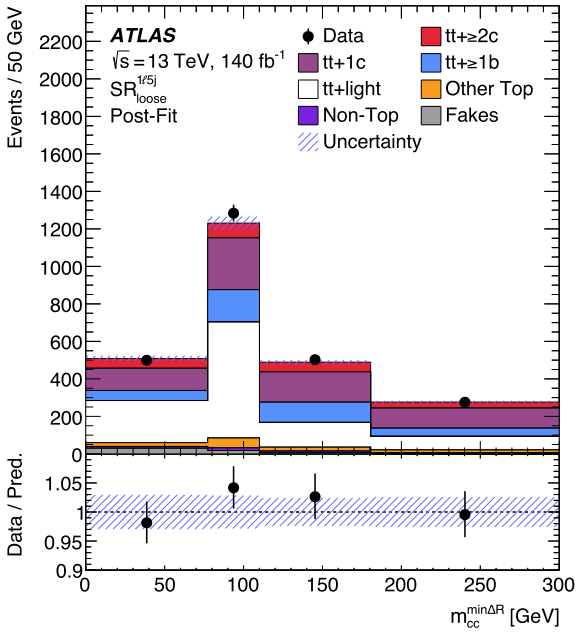

(a)

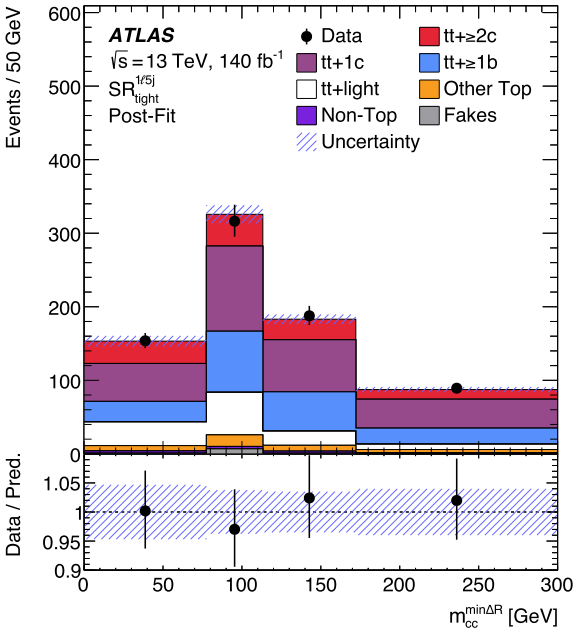

(b)

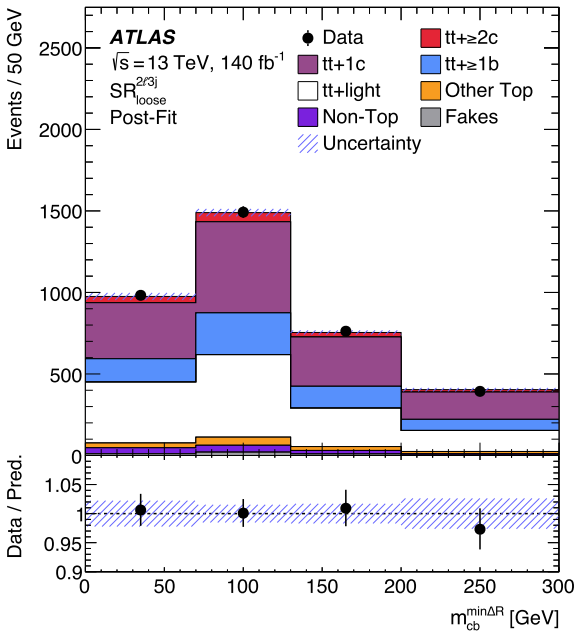

(c)

Figure 4: Post-fit agreement between data and MC prediction for the observables used in the 5-jet-exclusive and 3-jet-exclusive signal regions (SRs): (a) $\mathrm{SR}^{1\ell 5\mathrm{j}}_{\mathrm{loose}}$ and (b) $\mathrm{SR}^{1\ell 5\mathrm{j}}_{\mathrm{tight}}$, both using the invariant mass of the two geometrically closest c-tagged jets, $m_{cc}^{\mathrm{min}\Delta R}$, for the latter only considering c-tagged jets passing $c@11\%$; (c) $\mathrm{SR}^{2\ell 3\mathrm{j}}_{\mathrm{loose}}$ using the invariant mass of the selected c-tagged jet and the geometrically closest b-tagged jet, $m_{cb}^{\mathrm{min}\Delta R}$. The hatched uncertainty bands include all uncertainties and their correlations. The last bins contain overflow events. *Other Top* includes single-top-quark production and associated production of $t\bar{t}$ and single top quarks with bosons. *Non-Top* includes $W+$jets, $Z+$jets, and diboson processes.

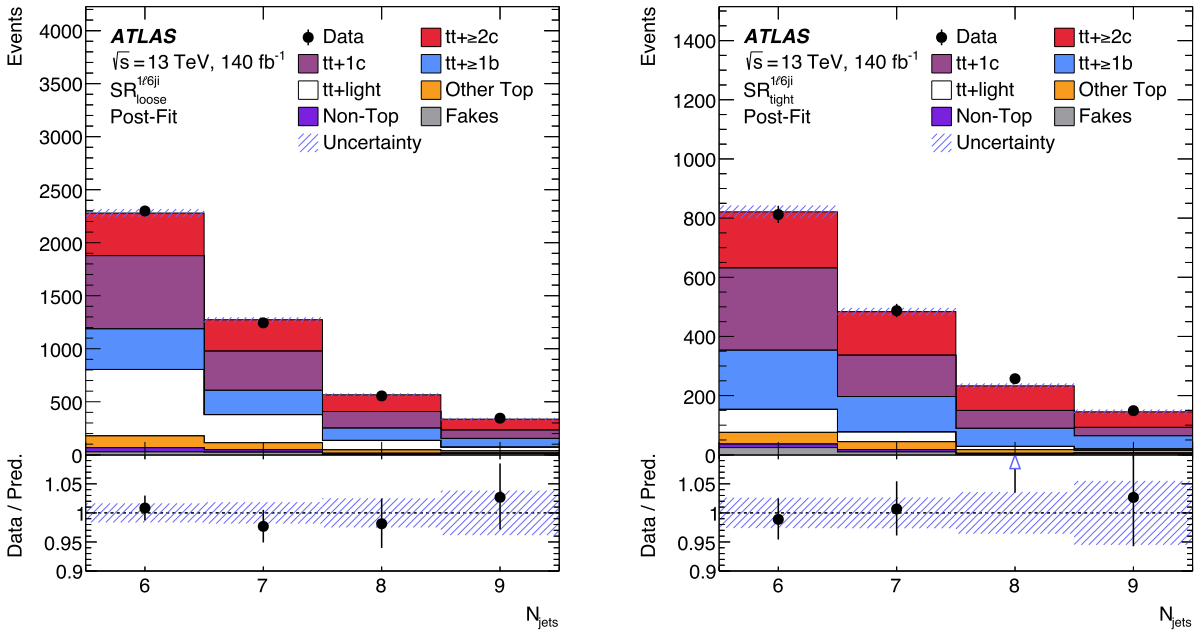

(a)

(b)

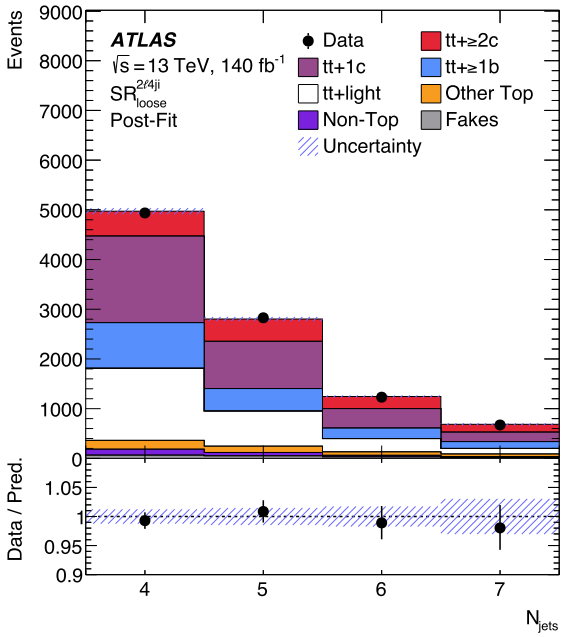

(c)

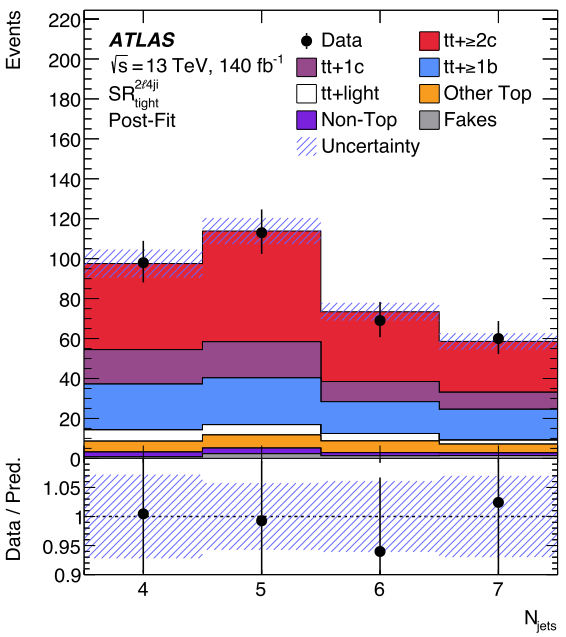

(d)

Figure 5: Post-fit agreement between data and MC prediction for the observables used in the (a) loose 6-jet-inclusive, (b) tight 6-jet-inclusive, (c) loose 4-jet-inclusive, and (d) tight 4-jet-inclusive signal regions (SRs). All regions use the jet multiplicity, N_{jets}, as a fit observable. The hatched uncertainty bands include all uncertainties and their correlations. The last bins contain overflow events. *Other Top* includes single-top-quark production and associated production of $t\bar{t}$ and single top quarks with bosons. *Non-Top* includes W+ jets, Z + jets, and diboson processes.

Table 2: Breakdown of the fiducial $t\bar{t}+\geq 2c$ and $t\bar{t}+1c$ cross-section uncertainties. Systematic uncertainties are grouped into signal and background modeling, instrumental, and MC statistics categories. The table lists the fractional uncertainty in the measured cross-sections in percent and is estimated from the covariance matrix of the profile likelihood fit, following Ref. [97]. Individual groups of uncertainties can be added in quadrature to obtain the total uncertainty. JES and JER denote the jet energy scale and resolution uncertainties, respectively. The fractional uncertainties in the fitted $t\bar{t}+\geq 1b$ and $t\bar{t}+$ light normalization factors are included in the data statistics category. For presentation purposes, all uncertainties are symmetrized.

Uncertainty group	Fractional uncertainty [%] on $\sigma^{\text{fid}}(t\bar{t}+\geq 2c)$	$\sigma^{\text{fid}}(t\bar{t}+1c)$
$t\bar{t}+\geq 1c$ modeling	9	8
Background modeling:		
$t\bar{t}+\geq 1b$	4	4
$t\bar{t}+$ light	6	4
Others	2.5	1.7
Instrumental:		
b-tagging	2.2	1.8
c-tagging	9	4
light mis-tagging	2.2	3.4
JES/JER	6	3.5
Others	1.3	0.9
MC statistics	3.1	2.5
Total systematic uncertainty	17	12
Data statistical uncertainty	11	7
Total	20	14

listed in Table 3, along with several NLO+PS predictions from different MC simulations. The predictions for $t\bar{t}+\geq 2c$ and $t\bar{t}+1c$ are largely consistent with the measurements, but underpredict the observed cross-sections by 0.5 to 2.0 standard deviations. Considering variations of the μ_{R} and μ_{F} scales and uncertainties in the PDF choice of the predictions, the Powheg+Pythia8 setups agree with the measured $t\bar{t}+\geq 2c$ ($t\bar{t}+1c$) values within 0.5 to 0.8 (0.9 to 1.1) standard deviations of measurement and prediction uncertainties. In contrast, Powheg+Herwig7 and MadGraph5_aMC@NLO+Herwig7 fall short by 25% to 40%, aligning with the measured values at 1.2 to 2.0 standard deviations. For $t\bar{t}+\geq 1b$, $t\bar{t}+$ light, and $t\bar{t}+$ jets, most NLO+PS predictions agree with the measured cross-sections within measurement uncertainties.

To test the compatibility of the two channels, an additional fit was performed where the $t\bar{t}+\geq 2c$ and $t\bar{t}+1c$ normalization factors were parameterized independently in the single-lepton and dilepton regions. The single-lepton channel measures $\sigma^{\text{fid}}(t\bar{t}+\geq 2c) = (1.5 \pm 0.4)$ pb and $\sigma^{\text{fid}}(t\bar{t}+1c) = (6.4 \pm 1.1)$ pb, and the dilepton channel $\sigma^{\text{fid}}(t\bar{t}+\geq 2c) = (1.18 \pm 0.25)$ pb and $\sigma^{\text{fid}}(t\bar{t}+1c) = (6.4 \pm 1.0)$ pb. The results in both channels are consistent with the nominal results within their uncertainties. The compatibility of this fit with the nominal setup was evaluated by performing a χ^2 test on the log-likelihood difference, yielding a compatibility of 58%. In a second test, the $t\bar{t}+\geq 2c$ and $t\bar{t}+1c$ normalization factors were parameterized through one joint parameter of interest, and the NLO matching and PS uncertainties of the two processes were treated as correlated. The resulting cross-section of $\sigma^{\text{fid}}(t\bar{t}+\geq 1c) = (8.2 \pm 0.9)$ pb is consistent with the sum of the $t\bar{t}+\geq 2c$ and $t\bar{t}+1c$ cross-sections in the nominal setup within uncertainties, but shows increased relative precision.

A measurement of the cross-sections in the more inclusive phase space yields $\sigma^{\text{inc}}(t\bar{t}+\geq 2c) = (5.4 \pm 1.1)$ pb

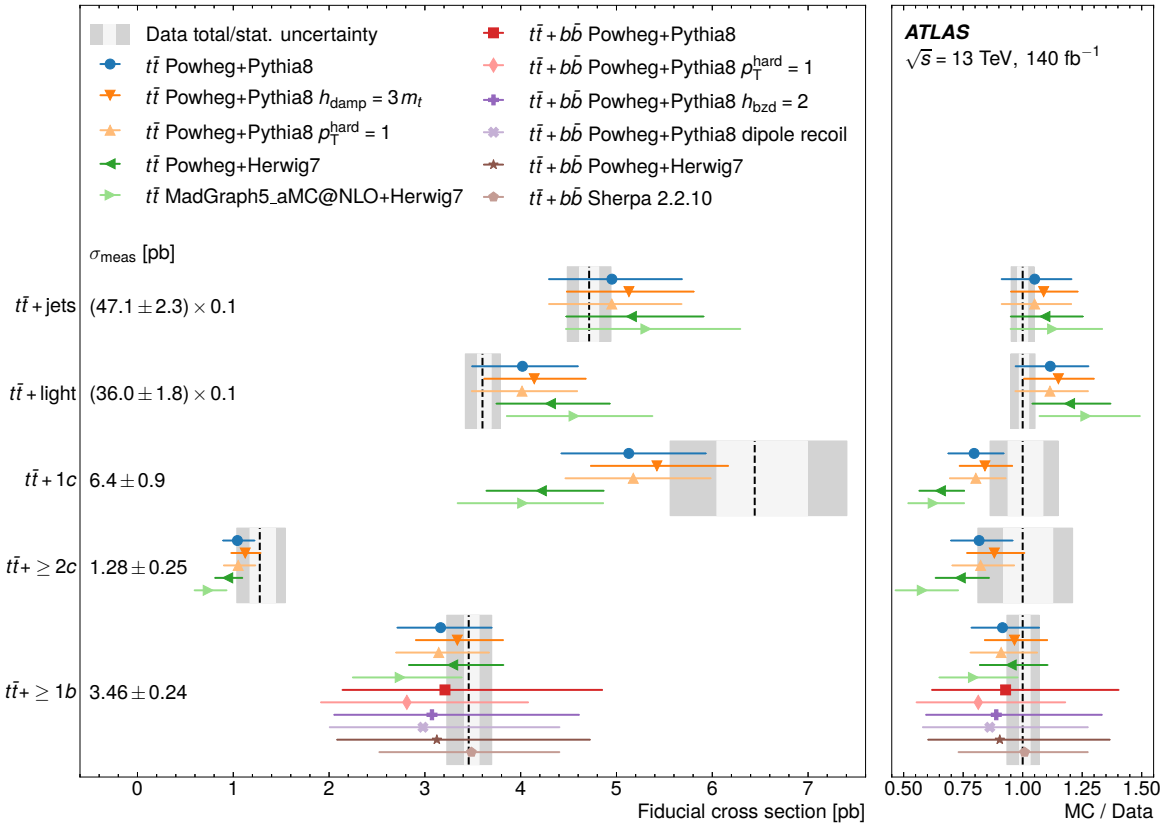

Figure 6: Measured fiducial cross-section values in comparison with various NLO+PS predictions from inclusive $t\bar{t}$ and $t\bar{t}+b\bar{b}$ simulations. The boxes in the background represent the statistical and total uncertainties of the values extracted from data. The uncertainty bars of the predictions include independent and simultaneous variations of the μ_{R} and μ_{F} scales and uncertainties in the choice of the PDF set, but no uncertainties in the parton shower or hadronization. The measured and computed values for $t\bar{t}$ + jets and $t\bar{t}$ + light are scaled by a factor of 0.1 to facilitate visualization. For presentation purposes, the quoted measurement uncertainties are symmetrized.

and $\sigma^{\text{inc}}(t\bar{t}+1c) = (38 \pm 6)$ pb, showing moderately increased relative uncertainties compared with the fiducial cross-sections.

The normalization factors $\mu(t\bar{t}+\geq 1b)$, $\mu(t\bar{t}+\geq 2c)$, $\mu(t\bar{t}+1c)$, and $\mu(t\bar{t}+\text{light})$ are used to determine the cross-section ratios of these processes to total $t\bar{t}$ + jets production. These measurements benefit from the cancelation of several systematic uncertainties related to detector instrumentation and calibrations, potentially reducing the overall systematic uncertainties. In the more inclusive phase space, the measurement yields ratios of $R^{\text{inc}}_{t\bar{t}+\geq 2c} = (1.23 \pm 0.25)\%$ and $R^{\text{inc}}_{t\bar{t}+1c} = (8.8 \pm 1.3)\%$. In the fiducial phase space, these ratios increase to $R^{\text{fid}}_{t\bar{t}+\geq 2c} = (2.7 \pm 0.5)\%$ and $R^{\text{fid}}_{t\bar{t}+1c} = (13.7 \pm 1.8)\%$. In both phase spaces, the Powheg+Pythia8 simulations underpredict the ratios, but agree with the measured $R^{\text{inc}}_{t\bar{t}+\geq 2c}$ and $R^{\text{inc}}_{t\bar{t}+1c}$ values within 0.9 and 1.1 standard deviations, and in the fiducial phase space within 1.0 and 1.4 standard deviations, respectively. A summary of all results is given in Table 4.

Table 3: Measured fiducial cross-section values in comparison with various NLO+PS predictions. The uncertainties in the predictions include independent and simultaneous variations of the μ_R and μ_F scales and uncertainties in the choice of the PDF set, but no uncertainties in the parton shower or hadronization. The uncertainties in the measured values include all statistical and systematic uncertainties. For presentation purposes, the quoted measurement and prediction uncertainties are symmetrized.

	$t\bar{t}+\geq 2c$ [pb]	$t\bar{t}+1c$ [pb]	$t\bar{t}+\geq 1b$ [pb]	$t\bar{t}$ + light [pb]	$t\bar{t}$ + jets [pb]
$t\bar{t}$ Powheg+Pythia 8	1.04 ± 0.18	5.1 ± 0.8	3.2 ± 0.5	40 ± 6	50 ± 7
$t\bar{t}$ Powheg+Pythia 8, $h_{\text{damp}} = 3\,m_t$	1.12 ± 0.16	5.4 ± 0.7	3.3 ± 0.5	41 ± 5	51 ± 7
$t\bar{t}$ Powheg+Pythia 8, $p_{\text{T}}^{\text{hard}} = 1$	1.05 ± 0.18	5.2 ± 0.8	3.1 ± 0.5	40 ± 6	50 ± 7
$t\bar{t}$ Powheg+Herwig 7	0.94 ± 0.16	4.2 ± 0.7	3.3 ± 0.5	43 ± 6	52 ± 8
$t\bar{t}$ MadGraph5_aMC@NLO+Herwig 7	0.74 ± 0.19	4.0 ± 0.8	2.7 ± 0.6	46 ± 8	53 ± 10
$t\bar{t}+b\bar{b}$ Powheg+Pythia 8	—	—	3.2 ± 1.6	—	—
$t\bar{t}+b\bar{b}$ Powheg+Pythia 8, $p_{\text{T}}^{\text{hard}} = 1$	—	—	2.8 ± 1.3	—	—
$t\bar{t}+b\bar{b}$ Powheg+Pythia 8, $h_{\text{bzd}} = 2$	—	—	3.1 ± 1.5	—	—
$t\bar{t}+b\bar{b}$ Powheg+Pythia 8, dipole recoil	—	—	3.0 ± 1.4	—	—
$t\bar{t}+b\bar{b}$ Powheg+Herwig 7	—	—	3.1 ± 1.6	—	—
$t\bar{t}+b\bar{b}$ Sherpa 2.2.10	—	—	3.5 ± 1.0	—	—
Data	1.28 ± 0.25	6.4 ± 0.9	3.46 ± 0.24	36.0 ± 1.8	47.1 ± 2.3

Table 4: Measured and predicted values for the $t\bar{t}+\geq 1b$, $t\bar{t}+\geq 2c$, and $t\bar{t}+1c$ cross-sections and for the cross-section ratios of these processes to total $t\bar{t}$ + jets production. The quoted uncertainties in the measurements include statistical and systematic uncertainties. The predictions are taken from the nominal setup using inclusive $t\bar{t}$ Powheg+Pythia8 predictions for the $t\bar{t}+\geq 2c$, $t\bar{t}+1c$, and $t\bar{t}$ + light processes, and $t\bar{t}+b\bar{b}$ Powheg+Pythia8 predictions for the $t\bar{t}+\geq 1b$ process. The first use the five-flavor scheme (5FS), the latter the four-flavor scheme (4FS), where the b-quarks are treated as massive particles and are included in the matrix element calculation. The uncertainties in the predictions include independent and simultaneous variations of the μ_R and μ_F scales and uncertainties in the choice of the PDF set.

	Measured	$t\bar{t}$ or $t\bar{t}+b\bar{b}$ Powheg+Pythia8
$\sigma^{\text{fid}}(t\bar{t}+\geq 1b)$ [pb]	3.46 ± 0.24	3.2 ± 1.6
$\sigma^{\text{fid}}(t\bar{t}+\geq 2c)$ [pb]	1.28 ± 0.25	1.04 ± 0.18
$\sigma^{\text{fid}}(t\bar{t}+1c)$ [pb]	6.4 ± 0.9	5.1 ± 0.8
$\sigma^{\text{inc}}(t\bar{t}+\geq 1b)$ [pb]	13.0 ± 0.9	12 ± 4
$\sigma^{\text{inc}}(t\bar{t}+\geq 2c)$ [pb]	5.4 ± 1.1	4.4 ± 0.7
$\sigma^{\text{inc}}(t\bar{t}+1c)$ [pb]	38 ± 6	31 ± 4
$R^{\text{fid}}_{t\bar{t}+\geq 1b}$ [%]	7.2 ± 0.4	6.5 ± 3.3
$R^{\text{fid}}_{t\bar{t}+\geq 2c}$ [%]	2.7 ± 0.5	2.1 ± 0.4
$R^{\text{fid}}_{t\bar{t}+1c}$ [%]	13.7 ± 1.8	10.3 ± 1.6
$R^{\text{inc}}_{t\bar{t}+\geq 1b}$ [%]	3.14 ± 0.23	2.6 ± 0.8
$R^{\text{inc}}_{t\bar{t}+\geq 2c}$ [%]	1.23 ± 0.25	0.97 ± 0.16
$R^{\text{inc}}_{t\bar{t}+1c}$ [%]	8.8 ± 1.3	6.9 ± 1.0

7 Conclusion

The production of $t\bar{t}$ pairs in association with heavy-flavor jets, $t\bar{t}+b\bar{b}$ and $t\bar{t}+c\bar{c}$, is a background in many measurements of rare SM processes and searches for new physics, yet a challenging process to model precisely. This Letter presents a measurement of the production of $t\bar{t}$ with additional jets initiated by charm quarks with the ATLAS experiment at the LHC. The analysis exploits the full ATLAS Run 2 pp collision data sample at a center-of-mass energy of 13 TeV, corresponding to an integrated luminosity of 140 fb^{-1}, and considers events with one or two charged leptons in the final state. A custom flavor tagging algorithm, termed the b/c-tagger, tailored to simultaneously tag c-jets and b-jets, is employed to define analysis regions sensitive to both $t\bar{t}+\geq 2c$ and $t\bar{t}+1c$ production which are determined separately for the first time. Using a profile likelihood fit approach, the cross-sections for $t\bar{t}$ production with two or more additional c-jets and one additional c-jet are found to be $\sigma^{\text{fid}}(t\bar{t}+\geq 2c) = 1.28^{+0.27}_{-0.24}$ pb and $\sigma^{\text{fid}}(t\bar{t}+1c) = 6.4^{+1.0}_{-0.9}$ pb in a fiducial volume that mimics the acceptance of the ATLAS detector. NLO+PS predictions for $t\bar{t}+\geq 2c$ and $t\bar{t}+1c$ are largely consistent with the measurements, though all underpredict the observed values. Powheg+Pythia8 setups agree with the measured values within 0.5 to 1.1 standard deviations, while Powheg+Herwig7 and MadGraph5_aMC@NLO+Herwig7 predict cross-sections up to 40% lower than the measurements, with agreement observed at the level of up to 2.0 standard deviations. The precision of the measured cross-sections is limited by uncertainties in the modeling of $t\bar{t}+\geq 1c$, $t\bar{t}+\geq 1b$, and $t\bar{t}+$light, and in the b/c-tagger calibration, as well as by data statistics. The cross-section ratios of $t\bar{t}+\geq 2c$ and $t\bar{t}+1c$ to total $t\bar{t}+$jets production are found to be $R^{\text{inc}}_{t\bar{t}+\geq 2c} = (1.23 \pm 0.25)\%$ and $R^{\text{inc}}_{t\bar{t}+1c} = (8.8 \pm 1.3)\%$ in a phase-space volume without requirements on the $t\bar{t}$ decay products and the jet multiplicity. These results provide crucial inputs for improving the modeling of $t\bar{t}$ production with additional c-jets, which would benefit from 3FS $t\bar{t}+c\bar{c}$ simulations that incorporate the gluon splitting to a $c\bar{c}$ pair into the matrix element calculation. Understanding $t\bar{t}+\geq 1c$ production is essential for precision measurements of even rarer SM processes and for searches for physics beyond the SM, where $t\bar{t}+\geq 1c$ is an important background.

Acknowledgements

We thank CERN for the very successful operation of the LHC and its injectors, as well as the support staff at CERN and at our institutions worldwide without whom ATLAS could not be operated efficiently.

The crucial computing support from all WLCG partners is acknowledged gratefully, in particular from CERN, the ATLAS Tier-1 facilities at TRIUMF/SFU (Canada), NDGF (Denmark, Norway, Sweden), CC-IN2P3 (France), KIT/GridKA (Germany), INFN-CNAF (Italy), NL-T1 (Netherlands), PIC (Spain), RAL (UK) and BNL (USA), the Tier-2 facilities worldwide and large non-WLCG resource providers. Major contributors of computing resources are listed in Ref. [98].

We gratefully acknowledge the support of ANPCyT, Argentina; YerPhI, Armenia; ARC, Australia; BMWFW and FWF, Austria; ANAS, Azerbaijan; CNPq and FAPESP, Brazil; NSERC, NRC and CFI, Canada; CERN; ANID, Chile; CAS, MOST and NSFC, China; Minciencias, Colombia; MEYS CR, Czech Republic; DNRF and DNSRC, Denmark; IN2P3-CNRS and CEA-DRF/IRFU, France; SRNSFG, Georgia; BMBF, HGF and MPG, Germany; GSRI, Greece; RGC and Hong Kong SAR, China; ISF and Benoziyo Center, Israel; INFN, Italy; MEXT and JSPS, Japan; CNRST, Morocco; NWO, Netherlands; RCN, Norway; MNiSW, Poland; FCT, Portugal; MNE/IFA, Romania; MSTDI, Serbia; MSSR, Slovakia; ARIS and MVZI, Slovenia; DSI/NRF, South Africa; MICIU/AEI, Spain; SRC and Wallenberg Foundation, Sweden; SERI, SNSF

and Cantons of Bern and Geneva, Switzerland; NSTC, Taipei; TENMAK, Türkiye; STFC/UKRI, United Kingdom; DOE and NSF, United States of America.

Individual groups and members have received support from BCKDF, CANARIE, CRC and DRAC, Canada; CERN-CZ, FORTE and PRIMUS, Czech Republic; COST, ERC, ERDF, Horizon 2020, ICSC-NextGenerationEU and Marie Skłodowska-Curie Actions, European Union; Investissements d'Avenir Labex, Investissements d'Avenir Idex and ANR, France; DFG and AvH Foundation, Germany; Herakleitos, Thales and Aristeia programmes co-financed by EU-ESF and the Greek NSRF, Greece; BSF-NSF and MINERVA, Israel; NCN and NAWA, Poland; La Caixa Banking Foundation, CERCA Programme Generalitat de Catalunya and PROMETEO and GenT Programmes Generalitat Valenciana, Spain; Göran Gustafssons Stiftelse, Sweden; The Royal Society and Leverhulme Trust, United Kingdom.

In addition, individual members wish to acknowledge support from Armenia: Yerevan Physics Institute (FAPERJ); CERN: European Organization for Nuclear Research (CERN PJAS); Chile: Agencia Nacional de Investigación y Desarrollo (FONDECYT 1230812, FONDECYT 1230987, FONDECYT 1240864); China: Chinese Ministry of Science and Technology (MOST-2023YFA1605700), National Natural Science Foundation of China (NSFC - 12175119, NSFC 12275265, NSFC-12075060); Czech Republic: Czech Science Foundation (GACR - 24-11373S), Ministry of Education Youth and Sports (FORTE CZ.02.01.01/00/22_008/0004632), PRIMUS Research Programme (PRIMUS/21/SCI/017); EU: H2020 European Research Council (ERC - 101002463); European Union: European Research Council (ERC - 948254, ERC 101089007), European Union, Future Artificial Intelligence Research (FAIR-NextGenerationEU PE00000013), Italian Center for High Performance Computing, Big Data and Quantum Computing (ICSC, NextGenerationEU); France: Agence Nationale de la Recherche (ANR-20-CE31-0013, ANR-21-CE31-0013, ANR-21-CE31-0022, ANR-22-EDIR-0002); Germany: Baden-Württemberg Stiftung (BW Stiftung-Postdoc Eliteprogramme), Deutsche Forschungsgemeinschaft (DFG - 469666862, DFG - CR 312/5-2); Italy: Istituto Nazionale di Fisica Nucleare (ICSC, NextGenerationEU), Ministero dell'Università e della Ricerca (PRIN - 20223N7F8K - PNRR M4.C2.1.1); Japan: Japan Society for the Promotion of Science (JSPS KAKENHI JP22H01227, JSPS KAKENHI JP22H04944, JSPS KAKENHI JP22KK0227, JSPS KAKENHI JP23KK0245); Netherlands: Netherlands Organisation for Scientific Research (NWO Veni 2020 - VI.Veni.202.179); Norway: Research Council of Norway (RCN-314472); Poland: Ministry of Science and Higher Education (IDUB AGH, POB8, D4 no 9722), Polish National Agency for Academic Exchange (PPN/PPO/2020/1/00002/U/00001), Polish National Science Centre (NCN 2021/42/E/ST2/00350, NCN OPUS 2023/51/B/ST2/02507, NCN OPUS nr 2022/47/B/ST2/03059, NCN UMO-2019/34/E/ST2/00393, NCN & H2020 MSCA 945339, UMO-2020/37/B/ST2/01043, UMO-2021/40/C/ST2/00187, UMO-2022/47/O/ST2/00148, UMO-2023/49/B/ST2/04085, UMO-2023/51/B/ST2/00920); Slovenia: Slovenian Research Agency (ARIS grant J1-3010); Spain: Generalitat Valenciana (Artemisa, FEDER, IDIFEDER/2018/048), Ministry of Science and Innovation (MCIN & NextGenEU PCI2022-135018-2, MICIN & FEDER PID2021-125273NB, RYC2019-028510-I, RYC2020-030254-I, RYC2021-031273-I, RYC2022-038164-I); Sweden: Carl Trygger Foundation (Carl Trygger Foundation CTS 22:2312), Swedish Research Council (Swedish Research Council 2023-04654, VR 2018-00482, VR 2022-03845, VR 2022-04683, VR 2023-03403, VR grant 2021-03651), Knut and Alice Wallenberg Foundation (KAW 2018.0458, KAW 2019.0447, KAW 2022.0358); Switzerland: Swiss National Science Foundation (SNSF - PCEFP2_194658); United Kingdom: Leverhulme Trust (Leverhulme Trust RPG-2020-004), Royal Society (NIF-R1-231091); United States of America: U.S. Department of Energy (ECA DE-AC02-76SF00515), Neubauer Family Foundation.

References

[1] ATLAS Collaboration, *The ATLAS Experiment at the CERN Large Hadron Collider*, JINST **3** (2008) S08003.

[2] CMS Collaboration, *The CMS Experiment at the CERN LHC*, JINST **3** (2008) S08004.

[3] CMS Collaboration, *Search for $t\bar{t}H$ production in the all-jet final state in proton–proton collisions at $\sqrt{s} = 13$ TeV*, JHEP **06** (2018) 101, arXiv: 1803.06986 [hep-ex].

[4] CMS Collaboration, *Search for $t\bar{t}H$ production in the $H \to b\bar{b}$ decay channel with leptonic $t\bar{t}$ decays in proton–proton collisions at $\sqrt{s} = 13$ TeV*, JHEP **03** (2019) 026, arXiv: 1804.03682 [hep-ex].

[5] ATLAS Collaboration, *Measurement of the associated production of a top-antitop-quark pair and a Higgs boson decaying into a $b\bar{b}$ pair in pp collisions at $\sqrt{s} = 13$ TeV using the ATLAS detector at the LHC*, (2024), arXiv: 2407.10904 [hep-ex].

[6] ATLAS Collaboration, *Measurement of the $t\bar{t}t\bar{t}$ production cross section in pp collisions at $\sqrt{s} = 13$ TeV with the ATLAS detector*, JHEP **11** (2021) 118, arXiv: 2106.11683 [hep-ex].

[7] CMS Collaboration, *Evidence for four-top quark production in proton–proton collisions at $\sqrt{s} = 13$ TeV*, Phys. Lett. B **844** (2023) 138076, arXiv: 2303.03864 [hep-ex].

[8] A. Bredenstein, A. Denner, S. Dittmaier, and S. Pozzorini, *NLO QCD corrections to $t\bar{t}b\bar{b}$ production at the LHC: 1. quark-antiquark annihilation*, JHEP **08** (2008) 108, arXiv: 0807.1248 [hep-ph].

[9] A. Bredenstein, A. Denner, S. Dittmaier, and S. Pozzorini, *Next-To-Leading Order QCD Corrections to $pp \to t\bar{t}b\bar{b} + X$ at the LHC*, Phys. Rev. Lett. **103** (2009) 012002, arXiv: 0905.0110 [hep-ph].

[10] F. Cascioli, P. Maierhöfer, N. Moretti, S. Pozzorini, and F. Siegert, *NLO matching for $t\bar{t}b\bar{b}$ production with massive b-quarks*, Phys. Lett. B **734** (2014) 210, arXiv: 1309.5912 [hep-ph].

[11] T. Ježo, J. M. Lindert, N. Moretti, and S. Pozzorini, *New NLOPS predictions for $t\bar{t}$ + b-jet production at the LHC*, Eur. Phys. J. C **78** (2018) 502, arXiv: 1802.00426 [hep-ph].

[12] F. Buccioni, S. Kallweit, S. Pozzorini, and M. F. Zoller, *NLO QCD predictions for $t\bar{t}b\bar{b}$ production in association with a light jet at the LHC*, JHEP **12** (2019) 015, arXiv: 1907.13624 [hep-ph].

[13] G. Bevilacqua et al., *$t\bar{t}b\bar{b}$ at the LHC: On the size of off-shell effects and prompt b-jet identification*, Phys. Rev. D **107** (2023) 014028, arXiv: 2202.11186 [hep-ph].

[14] ATLAS Collaboration, *Measurements of inclusive and differential fiducial cross-sections of $t\bar{t}$ production with additional heavy-flavour jets in proton–proton collisions at $\sqrt{s} = 13$ TeV with the ATLAS detector*, JHEP **04** (2019) 046, arXiv: 1811.12113 [hep-ex].

[15] CMS Collaboration, *Measurement of the $t\bar{t}b\bar{b}$ production cross section in the all-jet final state in pp collisions at $\sqrt{s} = 13$ TeV*, Phys. Lett. B **803** (2020) 135285, arXiv: 1909.05306 [hep-ex].

[16] CMS Collaboration, *Inclusive and differential cross section measurements of $t\bar{t}b\bar{b}$ production in the lepton+jets channel at $\sqrt{s}$ = 13 TeV*, JHEP **05** (2024) 042, arXiv: 2309.14442 [hep-ex].

[17] ATLAS Collaboration, *Measurement of $t\bar{t}$ production in association with additional b-jets in the $e\mu$ final state in proton–proton collisions at $\sqrt{s}$ = 13 TeV with the ATLAS detector*, (2024), arXiv: 2407.13473 [hep-ex].

[18] CMS Collaboration, *First measurement of the cross section for top quark pair production with additional charm jets using dileptonic final states in pp collisions at $\sqrt{s}$ = 13 TeV*, Phys. Lett. B **820** (2021) 136565, arXiv: 2012.09225 [hep-ex].

[19] G. Avoni et al., *The new LUCID-2 detector for luminosity measurement and monitoring in ATLAS*, JINST **13** (2018) P07017.

[20] ATLAS Collaboration, *Performance of the ATLAS trigger system in 2015*, Eur. Phys. J. C **77** (2017) 317, arXiv: 1611.09661 [hep-ex].

[21] ATLAS Collaboration, *Software and computing for Run 3 of the ATLAS experiment at the LHC*, (2024), arXiv: 2404.06335 [hep-ex].

[22] ATLAS Collaboration, *The ATLAS Simulation Infrastructure*, Eur. Phys. J. C **70** (2010) 823, arXiv: 1005.4568 [physics.ins-det].

[23] S. Agostinelli et al., *GEANT4 – a simulation toolkit*, Nucl. Instrum. Meth. A **506** (2003) 250.

[24] T. Sjöstrand, S. Mrenna, and P. Skands, *A brief introduction to PYTHIA 8.1*, Comput. Phys. Commun. **178** (2008) 852, arXiv: 0710.3820 [hep-ph].

[25] ATLAS Collaboration, *The Pythia 8 A3 tune description of ATLAS minimum bias and inelastic measurements incorporating the Donnachie–Landshoff diffractive model*, ATL-PHYS-PUB-2016-017, 2016, URL: https://cds.cern.ch/record/2206965.

[26] T. Sjöstrand et al., *An introduction to PYTHIA 8.2*, Comput. Phys. Commun. **191** (2015) 159, arXiv: 1410.3012 [hep-ph].

[27] M. Bähr et al., *Herwig++ physics and manual*, Eur. Phys. J. C **58** (2008) 639, arXiv: 0803.0883 [hep-ph].

[28] J. Bellm et al., *Herwig 7.0/Herwig++ 3.0 release note*, Eur. Phys. J. C **76** (2016) 196, arXiv: 1512.01178 [hep-ph].

[29] J. Bellm et al., *Herwig 7.1 Release Note*, (2017), arXiv: 1705.06919 [hep-ph].

[30] D. J. Lange, *The EvtGen particle decay simulation package*, Nucl. Instrum. Meth. A **462** (2001) 152.

[31] ATLAS Collaboration, *ATLAS Pythia 8 tunes to 7 TeV data*, ATL-PHYS-PUB-2014-021, 2014, URL: https://cds.cern.ch/record/1966419.

[32] NNPDF Collaboration, R. D. Ball, et al., *Parton distributions with LHC data*, Nucl. Phys. B **867** (2013) 244, arXiv: 1207.1303 [hep-ph].

[33] L. A. Harland-Lang, A. D. Martin, P. Motylinski, and R. S. Thorne, *Parton distributions in the LHC era: MMHT 2014 PDFs*, Eur. Phys. J. C **75** (2015) 204, arXiv: 1412.3989 [hep-ph].

[34] S. Frixione, G. Ridolfi, and P. Nason, *A positive-weight next-to-leading-order Monte Carlo for heavy flavour hadroproduction*, JHEP **09** (2007) 126, arXiv: 0707.3088 [hep-ph].

[35] P. Nason, *A new method for combining NLO QCD with shower Monte Carlo algorithms*, JHEP **11** (2004) 040, arXiv: hep-ph/0409146.

[36] S. Frixione, P. Nason, and C. Oleari, *Matching NLO QCD computations with parton shower simulations: the POWHEG method*, JHEP **11** (2007) 070, arXiv: 0709.2092 [hep-ph].

[37] S. Alioli, P. Nason, C. Oleari, and E. Re, *A general framework for implementing NLO calculations in shower Monte Carlo programs: the POWHEG BOX*, JHEP **06** (2010) 043, arXiv: 1002.2581 [hep-ph].

[38] NNPDF Collaboration, R. D. Ball, et al., *Parton distributions for the LHC run II*, JHEP **04** (2015) 040, arXiv: 1410.8849 [hep-ph].

[39] ATLAS Collaboration, *Studies on top-quark Monte Carlo modelling for Top2016*, ATL-PHYS-PUB-2016-020, 2016, URL: https://cds.cern.ch/record/2216168.

[40] S. Höche, S. Mrenna, S. Payne, C. T. Preuss, and P. Skands, *A Study of QCD Radiation in VBF Higgs Production with Vincia and Pythia*, SciPost Phys. **12** (2022) 010, arXiv: 2106.10987 [hep-ph].

[41] ATLAS Collaboration, *Studies on the improvement of the matching uncertainty definition in top-quark processes simulated with Powheg+Pythia8*, ATL-PHYS-PUB-2023-029, 2013, URL: https://cds.cern.ch/record/2872787.

[42] J. Alwall et al., *The automated computation of tree-level and next-to-leading order differential cross sections, and their matching to parton shower simulations*, JHEP **07** (2014) 079, arXiv: 1405.0301 [hep-ph].

[43] S. Frixione, E. Laenen, P. Motylinski, and B. R. Webber, *Angular correlations of lepton pairs from vector boson and top quark decays in Monte Carlo simulations*, JHEP **04** (2007) 081, arXiv: hep-ph/0702198.

[44] P. Artoisenet, R. Frederix, O. Mattelaer, and R. Rietkerk, *Automatic spin-entangled decays of heavy resonances in Monte Carlo simulations*, JHEP **03** (2013) 015, arXiv: 1212.3460 [hep-ph].

[45] ATLAS Collaboration, *Studies on top-quark Monte Carlo modelling with Sherpa and MG5_aMC@NLO*, ATL-PHYS-PUB-2017-007, 2017, URL: https://cds.cern.ch/record/2261938.

[46] M. Czakon and A. Mitov, *Top++: A program for the calculation of the top-pair cross-section at hadron colliders*, Comput. Phys. Commun. **185** (2014) 2930, arXiv: 1112.5675 [hep-ph].

[47] J. Butterworth et al., *PDF4LHC recommendations for LHC Run II*, J. Phys. G **43** (2016) 023001, arXiv: 1510.03865 [hep-ph].

[48] A. D. Martin, W. J. Stirling, R. S. Thorne, and G. Watt, *Uncertainties on α_S in global PDF analyses and implications for predicted hadronic cross sections*, Eur. Phys. J. C **64** (2009) 653, arXiv: 0905.3531 [hep-ph].

[49] J. Gao et al., *CT10 next-to-next-to-leading order global analysis of QCD*, Phys. Rev. D **89** (2014) 033009, arXiv: 1302.6246 [hep-ph].

[50] F. Cascioli, P. Maierhöfer, and S. Pozzorini, *Scattering Amplitudes with Open Loops*, Phys. Rev. Lett. **108** (2012) 111601, arXiv: 1111.5206 [hep-ph].

[51] A. Denner, S. Dittmaier, and L. Hofer,
COLLIER: A fortran-based complex one-loop library in extended regularizations,
Comput. Phys. Commun. **212** (2017) 220, arXiv: 1604.06792 [hep-ph].

[52] F. Buccioni et al., *OpenLoops 2*, Eur. Phys. J. C **79** (2019) 866, arXiv: 1907.13071 [hep-ph].

[53] ATLAS Collaboration, *Study of $t\bar{t}bb$ and $t\bar{t}W$ background modelling for $t\bar{t}H$ analyses*,
ATL-PHYS-PUB-2022-026, 2022, URL: https://cds.cern.ch/record/2810864.

[54] E. Bothmann et al., *Event generation with Sherpa 2.2*, SciPost Phys. **7** (2019) 034,
arXiv: 1905.09127 [hep-ph].

[55] T. Gleisberg and S. Höche, *Comix, a new matrix element generator*, JHEP **12** (2008) 039,
arXiv: 0808.3674 [hep-ph].

[56] S. Schumann and F. Krauss,
A parton shower algorithm based on Catani–Seymour dipole factorisation, JHEP **03** (2008) 038,
arXiv: 0709.1027 [hep-ph].

[57] S. Höche, F. Krauss, M. Schönherr, and F. Siegert,
A critical appraisal of NLO+PS matching methods, JHEP **09** (2012) 049,
arXiv: 1111.1220 [hep-ph].

[58] S. Höche, F. Krauss, M. Schönherr, and F. Siegert,
QCD matrix elements + parton showers. The NLO case, JHEP **04** (2013) 027,
arXiv: 1207.5030 [hep-ph].

[59] S. Catani, F. Krauss, B. R. Webber, and R. Kuhn, *QCD Matrix Elements + Parton Showers*,
JHEP **11** (2001) 063, arXiv: hep-ph/0109231.

[60] S. Höche, F. Krauss, S. Schumann, and F. Siegert, *QCD matrix elements and truncated showers*,
JHEP **05** (2009) 053, arXiv: 0903.1219 [hep-ph].

[61] M. Cacciari, G. P. Salam, and G. Soyez, *The anti-k_t jet clustering algorithm*, JHEP **04** (2008) 063,
arXiv: 0802.1189 [hep-ph].

[62] M. Cacciari, G. P. Salam, and G. Soyez, *FastJet user manual*, Eur. Phys. J. C **72** (2012) 1896,
arXiv: 1111.6097 [hep-ph].

[63] M. Cacciari and G. P. Salam, *Pileup subtraction using jet areas*, Phys. Lett. B **659** (2008) 119,
arXiv: 0707.1378 [hep-ph].

[64] M. Cacciari, G. P. Salam, and G. Soyez, *The Catchment Area of Jets*, JHEP **04** (2008) 005,
arXiv: 0802.1188 [hep-ph].

[65] S. Frixione, E. Laenen, P. Motylinski, C. White, and B. R. Webber,
Single-top hadroproduction in association with a W boson, JHEP **07** (2008) 029,
arXiv: 0805.3067 [hep-ph].

[66] C. Anastasiou, L. Dixon, K. Melnikov, and F. Petriello, *High-precision QCD at hadron colliders:
Electroweak gauge boson rapidity distributions at next-to-next-to leading order*,
Phys. Rev. D **69** (2004) 094008, arXiv: hep-ph/0312266.

[67] ATLAS Collaboration, *Vertex Reconstruction Performance of the ATLAS Detector at $\sqrt{s}$ = 13 TeV*,
ATL-PHYS-PUB-2015-026, 2015, URL: https://cds.cern.ch/record/2037717.

[68] ATLAS Collaboration, *Performance of electron and photon triggers in ATLAS during LHC Run 2*,
Eur. Phys. J. C **80** (2020) 47, arXiv: 1909.00761 [hep-ex].

[69] ATLAS Collaboration, *Performance of the ATLAS muon triggers in Run 2*, JINST **15** (2020) P09015, arXiv: 2004.13447 [physics.ins-det].

[70] ATLAS Collaboration, *Jet reconstruction and performance using particle flow with the ATLAS Detector*, Eur. Phys. J. C **77** (2017) 466, arXiv: 1703.10485 [hep-ex].

[71] ATLAS Collaboration, *Jet energy scale and resolution measured in proton–proton collisions at* $\sqrt{s} = 13$ *TeV with the ATLAS detector*, Eur. Phys. J. C **81** (2021) 689, arXiv: 2007.02645 [hep-ex].

[72] ATLAS Collaboration, *Performance of pile-up mitigation techniques for jets in* pp *collisions at* $\sqrt{s} = 8$ *TeV using the ATLAS detector*, Eur. Phys. J. C **76** (2016) 581, arXiv: 1510.03823 [hep-ex].

[73] ATLAS Collaboration, *Electron and photon performance measurements with the ATLAS detector using the 2015–2017 LHC proton–proton collision data*, JINST **14** (2019) P12006, arXiv: 1908.00005 [hep-ex].

[74] ATLAS Collaboration, *Electron and photon efficiencies in LHC Run 2 with the ATLAS experiment*, JHEP **05** (2024) 162, arXiv: 2308.13362 [hep-ex].

[75] ATLAS Collaboration, *Muon reconstruction and identification efficiency in ATLAS using the full Run 2* pp *collision data set at* $\sqrt{s} = 13$ *TeV*, Eur. Phys. J. C **81** (2021) 578, arXiv: 2012.00578 [hep-ex].

[76] ATLAS Collaboration, *Studies of the muon momentum calibration and performance of the ATLAS detector with* pp *collisions at* $\sqrt{s} = 13$ *TeV*, Eur. Phys. J. C **83** (2023) 686, arXiv: 2212.07338 [hep-ex].

[77] ATLAS Collaboration, *ATLAS flavour-tagging algorithms for the LHC Run 2* pp *collision dataset*, Eur. Phys. J. C **83** (2023) 681, arXiv: 2211.16345 [physics.data-an].

[78] J. Neyman and E. S. Pearson, *On the problem of the most efficient tests of statistical hypotheses*, Phil. Trans. R. Soc. A **231** (1933) 289.

[79] ATLAS Collaboration, *ATLAS b-jet identification performance and efficiency measurement with* $t\bar{t}$ *events in* pp *collisions at* $\sqrt{s} = 13$ *TeV*, Eur. Phys. J. C **79** (2019) 970, arXiv: 1907.05120 [hep-ex].

[80] ATLAS Collaboration, *Measurement of the c-jet mistagging efficiency in* $t\bar{t}$ *events using* pp *collision data at* $\sqrt{s} = 13$ *TeV collected with the ATLAS detector*, Eur. Phys. J. C **82** (2022) 95, arXiv: 2109.10627 [hep-ex].

[81] ATLAS Collaboration, *Calibration of the light-flavour jet mistagging efficiency of the b-tagging algorithms with Z+jets events using* $139\,fb^{-1}$ *of ATLAS proton–proton collision data at* $\sqrt{s} = 13$ *TeV*, Eur. Phys. J. C **83** (2023) 728, arXiv: 2301.06319 [hep-ex].

[82] ATLAS Collaboration, *Calibration of the performance of b-tagging for c and light-flavour jets in the 2012 ATLAS data*, ATLAS-CONF-2014-046, 2014, URL: https://cds.cern.ch/record/1741020.

[83] D0 Collaboration, *Measurement of the* $t\bar{t}$ *production cross section in* $p\overline{p}$ *collisions at* $\sqrt{s} = 1.96$ *TeV using secondary vertex b tagging*, Phys. Rev. D **74** (2006) 112004, arXiv: hep-ex/0611002.

[84] ATLAS Collaboration,
Monte Carlo to Monte Carlo scale factors for flavour tagging efficiency calibration,
ATL-PHYS-PUB-2020-009, 2020, URL: https://cds.cern.ch/record/2718610.

[85] ATLAS Collaboration,
Tools for estimating fake/non-prompt lepton backgrounds with the ATLAS detector at the LHC,
JINST **18** (2023) T11004, arXiv: 2211.16178 [hep-ex].

[86] ATLAS Collaboration, *The performance of missing transverse momentum reconstruction and its significance with the ATLAS detector using* $140\,fb^{-1}$ *of* $\sqrt{s} = 13$ *TeV* pp *collisions*, (2024),
arXiv: 2402.05858 [hep-ex].

[87] ATLAS Collaboration,
Luminosity determination in pp *collisions at* $\sqrt{s} = 13$ *TeV using the ATLAS detector at the LHC*,
Eur. Phys. J. C **83** (2023) 982, arXiv: 2212.09379 [hep-ex].

[88] N. Kidonakis and N. Yamanaka,
Higher-order corrections for tW production at high-energy hadron colliders, JHEP **05** (2021) 278,
arXiv: 2102.11300 [hep-ph].

[89] D. de Florian et al.,
Handbook of LHC Higgs Cross Sections: 4. Deciphering the Nature of the Higgs Sector, (2017),
arXiv: 1610.07922 [hep-ph].

[90] ATLAS Collaboration, *Probing the* CP *nature of the top-Higgs Yukawa coupling in* $t\bar{t}H$ *and* tH *events with* $H \to b\bar{b}$ *decays using the ATLAS detector at the LHC*, Phys. Lett. B **849** (2024) 138469,
arXiv: 2303.05974 [hep-ex].

[91] M. Grazzini, S. Kallweit, D. Rathlev, and M. Wiesemann,
$W^{\pm}Z$ *production at hadron colliders in NNLO QCD*, Phys. Lett. B **761** (2016) 179,
arXiv: 1604.08576 [hep-ph].

[92] ATLAS Collaboration, *Multi-boson simulation for* 13 *TeV ATLAS analyses*,
ATL-PHYS-PUB-2016-002, 2016, URL: https://cds.cern.ch/record/2119986.

[93] ATLAS Collaboration, *Measurement of* $W^{\pm}Z$ *production cross sections and gauge boson polarisation in* pp *collisions at* $\sqrt{s} = 13$ *TeV with the ATLAS detector*,
Eur. Phys. J. C **79** (2019) 535, arXiv: 1902.05759 [hep-ex].

[94] K. Cranmer, G. Lewis, L. Moneta, A. Shibata, and W. Verkerke,
HistFactory: A tool for creating statistical models for use with RooFit and RooStats,
CERN-OPEN-2012-016, 2012, URL: https://cds.cern.ch/record/1456844.

[95] W. Verkerke and D. Kirkby, *The RooFit toolkit for data modeling*, 2003,
arXiv: physics/0306116 [physics.data-an].

[96] S. Baker and R. D. Cousins,
Clarification of the use of CHI-square and likelihood functions in fits to histograms,
Nucl. Instrum. Methods Phys. Res. **221** (1984) 437.

[97] A. Pinto et al., *Uncertainty components in profile likelihood fits*, Eur. Phys. J. C **84** (2024) 593,
arXiv: 2307.04007 [physics.data-an].

[98] ATLAS Collaboration, *ATLAS Computing Acknowledgements*, ATL-SOFT-PUB-2023-001, 2023,
URL: https://cds.cern.ch/record/2869272.

The ATLAS Collaboration

G. Aad [105], E. Aakvaag [17], B. Abbott [124], S. Abdelhameed [120a], K. Abeling [57], N.J. Abicht [51], S.H. Abidi [30], M. Aboelela [46], A. Aboulhorma [36e], H. Abramowicz [156], H. Abreu [155], Y. Abulaiti [121], B.S. Acharya [71a,71b,k], A. Ackermann [65a], C. Adam Bourdarios [4], L. Adamczyk [88a], S.V. Addepalli [148], M.J. Addison [104], J. Adelman [119], A. Adiguzel [22c], T. Adye [138], A.A. Affolder [140], Y. Afik [41], M.N. Agaras [13], A. Aggarwal [103], C. Agheorghiesei [28c], F. Ahmadov [40,y], S. Ahuja [98], X. Ai [64e], G. Aielli [78a,78b], A. Aikot [168], M. Ait Tamlihat [36e], B. Aitbenchikh [36a], M. Akbiyik [103], T.P.A. Åkesson [101], A.V. Akimov [150], D. Akiyama [173], N.N. Akolkar [25], S. Aktas [22a], K. Al Khoury [43], G.L. Alberghi [24b], J. Albert [170], P. Albicocco [55], G.L. Albouy [62], S. Alderweireldt [54], Z.L. Alegria [125], M. Aleksa [37], I.N. Aleksandrov [40], C. Alexa [28b], T. Alexopoulos [10], F. Alfonsi [24b], M. Algren [58], M. Alhroob [172], B. Ali [136], H.M.J. Ali [94,s], S. Ali [32], S.W. Alibocus [95], M. Aliev [34c], G. Alimonti [73a], W. Alkakhi [57], C. Allaire [68], B.M.M. Allbrooke [151], J.S. Allen [104], J.F. Allen [54], C.A. Allendes Flores [141f], P.P. Allport [21], A. Aloisio [74a,74b], F. Alonso [93], C. Alpigiani [143], Z.M.K. Alsolami [94], M. Alvarez Estevez [102], A. Alvarez Fernandez [103], M. Alves Cardoso [58], M.G. Alviggi [74a,74b], M. Aly [104], Y. Amaral Coutinho [85b], A. Ambler [107], C. Amelung [37], M. Amerl [104], C.G. Ames [112], D. Amidei [109], B. Amini [56], K.J. Amirie [159], S.P. Amor Dos Santos [134a], K.R. Amos [168], D. Amperiadou [157], S. An [86], V. Ananiev [129], C. Anastopoulos [144], T. Andeen [11], J.K. Anders [37], A.C. Anderson [61], S.Y. Andrean [49a,49b], A. Andreazza [73a,73b], S. Angelidakis [9], A. Angerami [43], A.V. Anisenkov [39], A. Annovi [76a], C. Antel [58], E. Antipov [150], M. Antonelli [55], F. Anulli [77a], M. Aoki [86], T. Aoki [158], M.A. Aparo [151], L. Aperio Bella [50], C. Appelt [156], A. Apyan [27], S.J. Arbiol Val [89], C. Arcangeletti [55], A.T.H. Arce [53], J-F. Arguin [111], S. Argyropoulos [157], J.-H. Arling [50], O. Arnaez [4], H. Arnold [150], G. Artoni [77a,77b], H. Asada [114], K. Asai [122], S. Asai [158], N.A. Asbah [37], R.A. Ashby Pickering [172], K. Assamagan [30], R. Astalos [29a], K.S.V. Astrand [101], S. Atashi [163], R.J. Atkin [34a], H. Atmani [36f], P.A. Atmasiddha [132], K. Augsten [136], A.D. Auriol [21], V.A. Austrup [104], G. Avolio [37], K. Axiotis [58], G. Azuelos [111,ac], D. Babal [29b], H. Bachacou [139], K. Bachas [157,o], A. Bachiu [35], E. Bachmann [52], A. Badea [41], T.M. Baer [109], P. Bagnaia [77a,77b], M. Bahmani [19], D. Bahner [56], K. Bai [127], J.T. Baines [138], L. Baines [97], O.K. Baker [177], E. Bakos [16], D. Bakshi Gupta [8], L.E. Balabram Filho [85b], V. Balakrishnan [124], R. Balasubramanian [4], E.M. Baldin [39], P. Balek [88a], E. Ballabene [24b,24a], F. Balli [139], L.M. Baltes [65a], W.K. Balunas [33], J. Balz [103], I. Bamwidhi [120b], E. Banas [89], M. Bandieramonte [133], A. Bandyopadhyay [25], S. Bansal [25], L. Barak [156], M. Barakat [50], E.L. Barberio [108], D. Barberis [59b,59a], M. Barbero [105], M.Z. Barel [118], T. Barillari [113], M-S. Barisits [37], T. Barklow [148], P. Baron [126], D.A. Baron Moreno [104], A. Baroncelli [64a], A.J. Barr [130], J.D. Barr [99], F. Barreiro [102], J. Barreiro Guimarães da Costa [14], M.G. Barros Teixeira [134a], S. Barsov [39], F. Bartels [65a], R. Bartoldus [148], A.E. Barton [94], P. Bartos [29a], A. Basan [103], M. Baselga [51], A. Bassalat [68,b], M.J. Basso [160a], S. Bataju [46], R. Bate [169], R.L. Bates [61], S. Batlamous [102], B. Batool [146], M. Battaglia [140], D. Battulga [19], M. Bauce [77a,77b], M. Bauer [81], P. Bauer [25], L.T. Bazzano Hurrell [31], J.B. Beacham [53], T. Beau [131], J.Y. Beaucamp [93], P.H. Beauchemin [162], P. Bechtle [25], H.P. Beck [20,n], K. Becker [172], A.J. Beddall [84], V.A. Bednyakov [40], C.P. Bee [150], L.J. Beemster [16], T.A. Beermann [37], M. Begalli [85d], M. Begel [30], A. Behera [150], J.K. Behr [50], J.F. Beirer [37], F. Beisiegel [25], M. Belfkir [120b], G. Bella [156], L. Bellagamba [24b], A. Bellerive [35], P. Bellos [21], K. Beloborodov [39], D. Benchekroun [36a], F. Bendebba [36a], Y. Benhammou [156],

K.C. Benkendorfer[63], L. Beresford[50], M. Beretta[55], E. Bergeaas Kuutmann[166], N. Berger[4], B. Bergmann[136], J. Beringer[18a], G. Bernardi[5], C. Bernius[148], F.U. Bernlochner[25], F. Bernon[37], A. Berrocal Guardia[13], T. Berry[98], P. Berta[137], A. Berthold[52], S. Bethke[113], A. Betti[77a,77b], A.J. Bevan[97], N.K. Bhalla[56], S. Bhatta[150], D.S. Bhattacharya[171], P. Bhattarai[148], Z.M. Bhatti[121], K.D. Bhide[56], V.S. Bhopatkar[125], R.M. Bianchi[133], G. Bianco[24b,24a], O. Biebel[112], M. Biglietti[79a], C.S. Billingsley[46], Y. Bimgdi[36f], M. Bindi[57], A. Bingham[176], A. Bingul[22b], C. Bini[77a,77b], G.A. Bird[33], M. Birman[174], M. Biros[137], S. Biryukov[151], T. Bisanz[51], E. Bisceglie[45b,45a], J.P. Biswal[138], D. Biswas[146], I. Bloch[50], A. Blue[61], U. Blumenschein[97], J. Blumenthal[103], V.S. Bobrovnikov[39], M. Boehler[56], B. Boehm[171], D. Bogavac[37], A.G. Bogdanchikov[39], L.S. Boggia[131], C. Bohm[49a], V. Boisvert[98], P. Bokan[37], T. Bold[88a], M. Bomben[5], M. Bona[97], M. Boonekamp[139], A.G. Borbély[61], I.S. Bordulev[39], G. Borissov[94], D. Bortoletto[130], D. Boscherini[24b], M. Bosman[13], K. Bouaouda[36a], N. Bouchhar[168], L. Boudet[4], J. Boudreau[133], E.V. Bouhova-Thacker[94], D. Boumediene[42], R. Bouquet[59b,59a], A. Boveia[123], J. Boyd[37], D. Boye[30], I.R. Boyko[40], L. Bozianu[58], J. Bracinik[21], N. Brahimi[4], G. Brandt[176], O. Brandt[33], B. Brau[106], J.E. Brau[127], R. Brener[174], L. Brenner[118], R. Brenner[166], S. Bressler[174], G. Brianti[80a,80b], D. Britton[61], D. Britzger[113], I. Brock[25], R. Brock[110], G. Brooijmans[43], A.J. Brooks[70], E.M. Brooks[160b], E. Brost[30], L.M. Brown[170], L.E. Bruce[63], T.L. Bruckler[130], P.A. Bruckman de Renstrom[89], B. Brüers[50], A. Bruni[24b], G. Bruni[24b], D. Brunner[49a,49b], M. Bruschi[24b], N. Bruscino[77a,77b], T. Buanes[17], Q. Buat[143], D. Buchin[113], A.G. Buckley[61], O. Bulekov[39], B.A. Bullard[148], S. Burdin[95], C.D. Burgard[51], A.M. Burger[37], B. Burghgrave[8], O. Burlayenko[56], J. Burleson[167], J.T.P. Burr[33], J.C. Burzynski[147], E.L. Busch[43], V. Büscher[103], P.J. Bussey[61], J.M. Butler[26], C.M. Buttar[61], J.M. Butterworth[99], W. Buttinger[138], C.J. Buxo Vazquez[110], A.R. Buzykaev[39], S. Cabrera Urbán[168], L. Cadamuro[68], D. Caforio[60], H. Cai[133], Y. Cai[14,115c], Y. Cai[115a], V.M.M. Cairo[37], O. Cakir[3a], N. Calace[37], P. Calafiura[18a], G. Calderini[131], P. Calfayan[35], G. Callea[61], L.P. Caloba[85b], D. Calvet[42], S. Calvet[42], R. Camacho Toro[131], S. Camarda[37], D. Camarero Munoz[27], P. Camarri[78a,78b], M.T. Camerlingo[74a,74b], D. Cameron[37], C. Camincher[170], M. Campanelli[99], A. Camplani[44], V. Canale[74a,74b], A.C. Canbay[3a], E. Canonero[98], J. Cantero[168], Y. Cao[167], F. Capocasa[27], M. Capua[45b,45a], A. Carbone[73a,73b], R. Cardarelli[78a], J.C.J. Cardenas[8], M.P. Cardiff[27], G. Carducci[45b,45a], T. Carli[37], G. Carlino[74a], J.I. Carlotto[13], B.T. Carlson[133,p], E.M. Carlson[170,160a], J. Carmignani[95], L. Carminati[73a,73b], A. Carnelli[139], M. Carnesale[37], S. Caron[117], E. Carquin[141f], I.B. Carr[108], S. Carrá[73a], G. Carratta[24b,24a], A.M. Carroll[127], M.P. Casado[13,h], M. Caspar[50], F.L. Castillo[4], L. Castillo Garcia[13], V. Castillo Gimenez[168], N.F. Castro[134a,134e], A. Catinaccio[37], J.R. Catmore[129], T. Cavaliere[4], V. Cavaliere[30], L.J. Caviedes Betancourt[23b], Y.C. Cekmecelioglu[50], E. Celebi[84], S. Cella[37], V. Cepaitis[58], K. Cerny[126], A.S. Cerqueira[85a], A. Cerri[151], L. Cerrito[78a,78b], F. Cerutti[18a], B. Cervato[146], A. Cervelli[24b], G. Cesarini[55], S.A. Cetin[84], P.M. Chabrillat[131], D. Chakraborty[119], J. Chan[18a], W.Y. Chan[158], J.D. Chapman[33], E. Chapon[139], B. Chargeishvili[154b], D.G. Charlton[21], M. Chatterjee[20], C. Chauhan[137], Y. Che[115a], S. Chekanov[6], S.V. Chekulaev[160a], G.A. Chelkov[40,a], A. Chen[109], B. Chen[156], B. Chen[170], H. Chen[115a], H. Chen[30], J. Chen[64c], J. Chen[147], M. Chen[130], S. Chen[90], S.J. Chen[115a], X. Chen[64c], X. Chen[15,ab], Y. Chen[64a], C.L. Cheng[175], H.C. Cheng[66a], S. Cheong[148], A. Cheplakov[40], E. Cheremushkina[50], E. Cherepanova[118], R. Cherkaoui El Moursli[36e], E. Cheu[7], K. Cheung[67], L. Chevalier[139], V. Chiarella[55], G. Chiarelli[76a], N. Chiedde[105], G. Chiodini[72a], A.S. Chisholm[21], A. Chitan[28b], M. Chitishvili[168], M.V. Chizhov[40,q], K. Choi[11], Y. Chou[143],

E.Y.S. Chow [117], K.L. Chu [174], M.C. Chu [66a], X. Chu [14,115c], Z. Chubinidze [55], J. Chudoba [135], J.J. Chwastowski [89], D. Cieri [113], K.M. Ciesla [88a], V. Cindro [96], A. Ciocio [18a], F. Cirotto [74a,74b], Z.H. Citron [174], M. Citterio [73a], D.A. Ciubotaru[28b], A. Clark [58], P.J. Clark [54], N. Clarke Hall [99], C. Clarry [159], J.M. Clavijo Columbie [50], S.E. Clawson [50], C. Clement [49a,49b], Y. Coadou [105], M. Cobal [71a,71c], A. Coccaro [59b], R.F. Coelho Barrue [134a], R. Coelho Lopes De Sa [106], S. Coelli [73a], L.S. Colangeli [159], B. Cole [43], J. Collot [62], P. Conde Muiño [134a,134g], M.P. Connell [34c], S.H. Connell [34c], E.I. Conroy [130], F. Conventi [74a,ad], H.G. Cooke [21], A.M. Cooper-Sarkar [130], F.A. Corchia [24b,24a], A. Cordeiro Oudot Choi [131], L.D. Corpe [42], M. Corradi [77a,77b], F. Corriveau [107,x], A. Cortes-Gonzalez [19], M.J. Costa [168], F. Costanza [4], D. Costanzo [144], B.M. Cote [123], J. Couthures [4], G. Cowan [98], K. Cranmer [175], L. Cremer [51], D. Cremonini [24b,24a], S. Crépé-Renaudin [62], F. Crescioli [131], M. Cristinziani [146], M. Cristoforetti [80a,80b], V. Croft [118], J.E. Crosby [125], G. Crosetti [45b,45a], A. Cueto [102], H. Cui [99], Z. Cui [7], W.R. Cunningham [61], F. Curcio [168], J.R. Curran [54], P. Czodrowski [37], M.J. Da Cunha Sargedas De Sousa [59b,59a], J.V. Da Fonseca Pinto [85b], C. Da Via [104], W. Dabrowski [88a], T. Dado [37], S. Dahbi [153], T. Dai [109], D. Dal Santo [20], C. Dallapiccola [106], M. Dam [44], G. D'amen [30], V. D'Amico [112], J. Damp [103], J.R. Dandoy [35], D. Dannheim [37], M. Danninger [147], V. Dao [150], G. Darbo [59b], S.J. Das [30], F. Dattola [50], S. D'Auria [73a,73b], A. D'Avanzo [74a,74b], C. David [34a], T. Davidek [137], I. Dawson [97], H.A. Day-hall [136], K. De [8], C. De Almeida Rossi [159], R. De Asmundis [74a], N. De Biase [50], S. De Castro [24b,24a], N. De Groot [117], P. de Jong [118], H. De la Torre [119], A. De Maria [115a], A. De Salvo [77a], U. De Sanctis [78a,78b], F. De Santis [72a,72b], A. De Santo [151], J.B. De Vivie De Regie [62], J. Debevc [96], D.V. Dedovich[40], J. Degens [95], A.M. Deiana [46], F. Del Corso [24b,24a], J. Del Peso [102], L. Delagrange [131], F. Deliot [139], C.M. Delitzsch [51], M. Della Pietra [74a,74b], D. Della Volpe [58], A. Dell'Acqua [37], L. Dell'Asta [73a,73b], M. Delmastro [4], C.C. Delogu [103], P.A. Delsart [62], S. Demers [177], M. Demichev [40], S.P. Denisov [39], L. D'Eramo [42], D. Derendarz [89], F. Derue [131], P. Dervan [95], K. Desch [25], C. Deutsch [25], F.A. Di Bello [59b,59a], A. Di Ciaccio [78a,78b], L. Di Ciaccio [4], A. Di Domenico [77a,77b], C. Di Donato [74a,74b], A. Di Girolamo [37], G. Di Gregorio [37], A. Di Luca [80a,80b], B. Di Micco [79a,79b], R. Di Nardo [79a,79b], K.F. Di Petrillo [41], M. Diamantopoulou [35], F.A. Dias [118], T. Dias Do Vale [147], M.A. Diaz [141a,141b], A.R. Didenko [40], M. Didenko [168], E.B. Diehl [109], S. Díez Cornell [50], C. Diez Pardos [146], C. Dimitriadi [166], A. Dimitrievska [21], J. Dingfelder [25], T. Dingley [130], I-M. Dinu [28b], S.J. Dittmeier [65b], F. Dittus [37], M. Divisek [137], B. Dixit [95], F. Djama [105], T. Djobava [154b], C. Doglioni [104,101], A. Dohnalova [29a], Z. Dolezal [137], K. Domijan [88a], K.M. Dona [41], M. Donadelli [85d], B. Dong [110], J. Donini [42], A. D'Onofrio [74a,74b], M. D'Onofrio [95], J. Dopke [138], A. Doria [74a], N. Dos Santos Fernandes [134a], P. Dougan [104], M.T. Dova [93], A.T. Doyle [61], M.A. Draguet [130], M.P. Drescher [57], E. Dreyer [174], I. Drivas-koulouris [10], M. Drnevich [121], M. Drozdova [58], D. Du [64a], T.A. du Pree [118], F. Dubinin [39], M. Dubovsky [29a], E. Duchovni [174], G. Duckeck [112], O.A. Ducu [28b], D. Duda [54], A. Dudarev [37], E.R. Duden [27], M. D'uffizi [104], L. Duflot [68], M. Dührssen [37], I. Duminica [28g], A.E. Dumitriu [28b], M. Dunford [65a], S. Dungs [51], K. Dunne [49a,49b], A. Duperrin [105], H. Duran Yildiz [3a], M. Düren [60], A. Durglishvili [154b], B.L. Dwyer [119], G.I. Dyckes [18a], M. Dyndal [88a], B.S. Dziedzic [37], Z.O. Earnshaw [151], G.H. Eberwein [130], B. Eckerova [29a], S. Eggebrecht [57], E. Egidio Purcino De Souza [85e], L.F. Ehrke [58], G. Eigen [17], K. Einsweiler [18a], T. Ekelof [166], P.A. Ekman [101], S. El Farkh [36b], Y. El Ghazali [64a], H. El Jarrari [37], A. El Moussaouy [36a], V. Ellajosyula [166], M. Ellert [166], F. Ellinghaus [176], N. Ellis [37], J. Elmsheuser [30], M. Elsawy [120a], M. Elsing [37], D. Emeliyanov [138], Y. Enari [86], I. Ene [18a], S. Epari [13], P.A. Erland [89], D. Ernani Martins Neto [89], M. Errenst [176], M. Escalier [68], C. Escobar [168], E. Etzion [156],

G. Evans [134a], H. Evans [70], L.S. Evans [98], A. Ezhilov [39], S. Ezzarqtouni [36a], F. Fabbri [24b,24a], L. Fabbri [24b,24a], G. Facini [99], V. Fadeyev [140], R.M. Fakhrutdinov [39], D. Fakoudis [103], S. Falciano [77a], L.F. Falda Ulhoa Coelho [134a], F. Fallavollita [113], G. Falsetti [45b,45a], J. Faltova [137], C. Fan [167], K.Y. Fan [66b], Y. Fan [14], Y. Fang [14,115c], M. Fanti [73a,73b], M. Faraj [71a,71b], Z. Farazpay [100], A. Farbin [8], A. Farilla [79a], T. Farooque [110], J.N. Farr [177], S.M. Farrington [138,54], F. Fassi [36e], D. Fassouliotis [9], M. Faucci Giannelli [78a,78b], W.J. Fawcett [33], L. Fayard [68], P. Federic [137], P. Federicova [135], O.L. Fedin [39,a], M. Feickert [175], L. Feligioni [105], D.E. Fellers [127], C. Feng [64b], Z. Feng [118], M.J. Fenton [163], L. Ferencz [50], R.A.M. Ferguson [94], P. Fernandez Martinez [69], M.J.V. Fernoux [105], J. Ferrando [94], A. Ferrari [166], P. Ferrari [118,117], R. Ferrari [75a], D. Ferrere [58], C. Ferretti [109], M.P. Fewell [1], D. Fiacco [77a,77b], F. Fiedler [103], P. Fiedler [136], S. Filimonov [39], A. Filipčič [96], E.K. Filmer [160a], F. Filthaut [117], M.C.N. Fiolhais [134a,134c,c], L. Fiorini [168], W.C. Fisher [110], T. Fitschen [104], P.M. Fitzhugh [139], I. Fleck [146], P. Fleischmann [109], T. Flick [176], M. Flores [34d,z], L.R. Flores Castillo [66a], L. Flores Sanz De Acedo [37], F.M. Follega [80a,80b], N. Fomin [33], J.H. Foo [159], A. Formica [139], A.C. Forti [104], E. Fortin [37], A.W. Fortman [18a], M.G. Foti [18a], L. Fountas [9,i], D. Fournier [68], H. Fox [94], P. Francavilla [76a,76b], S. Francescato [63], S. Franchellucci [58], M. Franchini [24b,24a], S. Franchino [65a], D. Francis [37], L. Franco [117], V. Franco Lima [37], L. Franconi [50], M. Franklin [63], G. Frattari [27], Y.Y. Frid [156], J. Friend [61], N. Fritzsche [37], A. Froch [58], D. Froidevaux [37], J.A. Frost [130], Y. Fu [64a], S. Fuenzalida Garrido [141f], M. Fujimoto [105], K.Y. Fung [66a], E. Furtado De Simas Filho [85e], M. Furukawa [158], J. Fuster [168], A. Gaa [57], A. Gabrielli [24b,24a], A. Gabrielli [159], P. Gadow [37], G. Gagliardi [59b,59a], L.G. Gagnon [18a], S. Gaid [165], S. Galantzan [156], J. Gallagher [1], E.J. Gallas [130], A.L. Gallen [166], B.J. Gallop [138], K.K. Gan [123], S. Ganguly [158], Y. Gao [54], F.M. Garay Walls [141a,141b], B. Garcia [30], C. García [168], A. Garcia Alonso [118], A.G. Garcia Caffaro [177], J.E. García Navarro [168], M. Garcia-Sciveres [18a], G.L. Gardner [132], R.W. Gardner [41], N. Garelli [162], R.B. Garg [148], J.M. Gargan [54], C.A. Garner [159], C.M. Garvey [34a], V.K. Gassmann [162], G. Gaudio [75a], V. Gautam [13], P. Gauzzi [77a,77b], J. Gavranovic [96], I.L. Gavrilenko [39], A. Gavrilyuk [39], C. Gay [169], G. Gaycken [127], E.N. Gazis [10], A.A. Geanta [28b], A. Gekow [123], C. Gemme [59b], M.H. Genest [62], A.D. Gentry [116], S. George [98], W.F. George [21], T. Geralis [48], A.A. Gerwin [124], P. Gessinger-Befurt [37], M.E. Geyik [176], M. Ghani [172], K. Ghorbanian [97], A. Ghosal [146], A. Ghosh [163], A. Ghosh [7], B. Giacobbe [24b], S. Giagu [77a,77b], T. Giani [118], A. Giannini [64a], S.M. Gibson [98], M. Gignac [140], D.T. Gil [88b], A.K. Gilbert [88a], B.J. Gilbert [43], D. Gillberg [35], G. Gilles [118], L. Ginabat [131], D.M. Gingrich [2,ac], M.P. Giordani [71a,71c], P.F. Giraud [139], G. Giugliarelli [71a,71c], D. Giugni [73a], F. Giuli [78a,78b], I. Gkialas [9,i], L.K. Gladilin [39], C. Glasman [102], G.R. Gledhill [127], G. Glemža [50], M. Glisic [127], I. Gnesi [45b], Y. Go [30], M. Goblirsch-Kolb [37], B. Gocke [51], D. Godin [111], B. Gokturk [22a], S. Goldfarb [108], T. Golling [58], M.G.D. Gololo [34g], D. Golubkov [39], J.P. Gombas [110], A. Gomes [134a,134b], G. Gomes Da Silva [146], A.J. Gomez Delegido [168], R. Gonçalo [134a], L. Gonella [21], A. Gongadze [154c], F. Gonnella [21], J.L. Gonski [148], R.Y. González Andana [54], S. González de la Hoz [168], R. Gonzalez Lopez [95], C. Gonzalez Renteria [18a], M.V. Gonzalez Rodrigues [50], R. Gonzalez Suarez [166], S. Gonzalez-Sevilla [58], L. Goossens [37], B. Gorini [37], E. Gorini [72a,72b], A. Gorišek [96], T.C. Gosart [132], A.T. Goshaw [53], M.I. Gostkin [40], S. Goswami [125], C.A. Gottardo [37], S.A. Gotz [112], M. Gouighri [36b], V. Goumarre [50], A.G. Goussiou [143], N. Govender [34c], R.P. Grabarczyk [130], I. Grabowska-Bold [88a], K. Graham [35], E. Gramstad [129], S. Grancagnolo [72a,72b], C.M. Grant [1,139], P.M. Gravila [28f], F.G. Gravili [72a,72b], H.M. Gray [18a], M. Greco [72a,72b], M.J. Green [1], C. Grefe [25], A.S. Grefsrud [17], I.M. Gregor [50], K.T. Greif [163], P. Grenier [148], S.G. Grewe [113], A.A. Grillo [140], K. Grimm [32], S. Grinstein [13,t], J.-F. Grivaz [68],

E. Gross[174], J. Grosse-Knetter[57], L. Guan[109], J.G.R. Guerrero Rojas[168], G. Guerrieri[37], R. Gugel[103], J.A.M. Guhit[109], A. Guida[19], E. Guilloton[172], S. Guindon[37], F. Guo[14,115c], J. Guo[64c], L. Guo[50], L. Guo[14], Y. Guo[109], A. Gupta[51], R. Gupta[133], S. Gurbuz[25], S.S. Gurdasani[56], G. Gustavino[77a,77b], M. Guth[58], P. Gutierrez[124], L.F. Gutierrez Zagazeta[132], M. Gutsche[52], C. Gutschow[99], C. Gwenlan[130], C.B. Gwilliam[95], E.S. Haaland[129], A. Haas[121], M. Habedank[61], C. Haber[18a], H.K. Hadavand[8], A. Hadef[52], A.I. Hagan[94], J.J. Hahn[146], E.H. Haines[99], M. Haleem[171], J. Haley[125], G.D. Hallewell[105], L. Halser[20], K. Hamano[170], M. Hamer[25], E.J. Hampshire[98], J. Han[64b], L. Han[115a], L. Han[64a], S. Han[18a], Y.F. Han[159], K. Hanagaki[86], M. Hance[140], D.A. Hangal[43], H. Hanif[147], M.D. Hank[132], J.B. Hansen[44], P.H. Hansen[44], D. Harada[58], T. Harenberg[176], S. Harkusha[178], M.L. Harris[106], Y.T. Harris[25], J. Harrison[13], N.M. Harrison[123], P.F. Harrison[172], N.M. Hartman[113], N.M. Hartmann[112], R.Z. Hasan[98,138], Y. Hasegawa[145], F. Haslbeck[130], S. Hassan[17], R. Hauser[110], C.M. Hawkes[21], R.J. Hawkings[37], Y. Hayashi[158], D. Hayden[110], C. Hayes[109], R.L. Hayes[118], C.P. Hays[130], J.M. Hays[97], H.S. Hayward[95], F. He[64a], M. He[14,115c], Y. He[50], Y. He[99], N.B. Heatley[97], V. Hedberg[101], A.L. Heggelund[129], N.D. Hehir[97,*], C. Heidegger[56], K.K. Heidegger[56], J. Heilman[35], S. Heim[50], T. Heim[18a], J.G. Heinlein[132], J.J. Heinrich[127], L. Heinrich[113,aa], J. Hejbal[135], A. Held[175], S. Hellesund[17], C.M. Helling[169], S. Hellman[49a,49b], R.C.W. Henderson[94], L. Henkelmann[33], A.M. Henriques Correia[37], H. Herde[101], Y. Hernández Jiménez[150], L.M. Herrmann[25], T. Herrmann[52], G. Herten[56], R. Hertenberger[112], L. Hervas[37], M.E. Hesping[103], N.P. Hessey[160a], J. Hessler[113], M. Hidaoui[36b], N. Hidic[137], E. Hill[159], S.J. Hillier[21], J.R. Hinds[110], F. Hinterkeuser[25], M. Hirose[128], S. Hirose[161], D. Hirschbuehl[176], T.G. Hitchings[104], B. Hiti[96], J. Hobbs[150], R. Hobincu[28e], N. Hod[174], M.C. Hodgkinson[144], B.H. Hodkinson[130], A. Hoecker[37], D.D. Hofer[109], J. Hofer[168], T. Holm[25], M. Holzbock[37], L.B.A.H. Hommels[33], B.P. Honan[104], J.J. Hong[70], J. Hong[64c], T.M. Hong[133], B.H. Hooberman[167], W.H. Hopkins[6], M.C. Hoppesch[167], Y. Horii[114], M.E. Horstmann[113], S. Hou[153], M.R. Housenga[167], A.S. Howard[96], J. Howarth[61], J. Hoya[6], M. Hrabovsky[126], A. Hrynevich[50], T. Hryn'ova[4], P.J. Hsu[67], S.-C. Hsu[143], T. Hsu[68], M. Hu[18a], Q. Hu[64a], S. Huang[33], X. Huang[14,115c], Y. Huang[144], Y. Huang[103], Y. Huang[14], Z. Huang[104], Z. Hubacek[136], M. Huebner[25], F. Huegging[25], T.B. Huffman[130], M. Hufnagel Maranha De Faria[85a], C.A. Hugli[50], M. Huhtinen[37], S.K. Huiberts[17], R. Hulsken[107], N. Huseynov[12,f], J. Huston[110], J. Huth[63], R. Hyneman[148], G. Iacobucci[58], G. Iakovidis[30], L. Iconomidou-Fayard[68], J.P. Iddon[37], P. Iengo[74a,74b], R. Iguchi[158], Y. Iiyama[158], T. Iizawa[130], Y. Ikegami[86], D. Iliadis[157], N. Ilic[159], H. Imam[85c], G. Inacio Goncalves[85d], T. Ingebretsen Carlson[49a,49b], J.M. Inglis[97], G. Introzzi[75a,75b], M. Iodice[79a], V. Ippolito[77a,77b], R.K. Irwin[95], M. Ishino[158], W. Islam[175], C. Issever[19], S. Istin[22a,ag], H. Ito[173], R. Iuppa[80a,80b], A. Ivina[174], J.M. Izen[47], V. Izzo[74a], P. Jacka[135], P. Jackson[1], C.S. Jagfeld[112], G. Jain[160a], P. Jain[50], K. Jakobs[56], T. Jakoubek[174], J. Jamieson[61], W. Jang[158], M. Javurkova[106], P. Jawahar[104], L. Jeanty[127], J. Jejelava[154a], P. Jenni[56,e], C.E. Jessiman[35], C. Jia[64b], H. Jia[169], J. Jia[150], X. Jia[14,115c], Z. Jia[115a], C. Jiang[54], S. Jiggins[50], J. Jimenez Pena[13], S. Jin[115a], A. Jinaru[28b], O. Jinnouchi[142], P. Johansson[144], K.A. Johns[7], J.W. Johnson[140], F.A. Jolly[50], D.M. Jones[151], E. Jones[50], K.S. Jones[8], P. Jones[33], R.W.L. Jones[94], T.J. Jones[95], H.L. Joos[57,37], R. Joshi[123], J. Jovicevic[16], X. Ju[18a], J.J. Junggeburth[37], T. Junkermann[65a], A. Juste Rozas[13,t], M.K. Juzek[89], S. Kabana[141e], A. Kaczmarska[89], M. Kado[113], H. Kagan[123], M. Kagan[148], A. Kahn[132], C. Kahra[103], T. Kaji[158], E. Kajomovitz[155], N. Kakati[174], I. Kalaitzidou[56], C.W. Kalderon[30], N.J. Kang[140], D. Kar[34g], K. Karava[130], M.J. Kareem[160b], E. Karentzos[25],

O. Karkout[118], S.N. Karpov[40], Z.M. Karpova[40], V. Kartvelishvili[94], A.N. Karyukhin[39], E. Kasimi[157], J. Katzy[50], S. Kaur[35], K. Kawade[145], M.P. Kawale[124], C. Kawamoto[90], T. Kawamoto[64a], E.F. Kay[37], F.I. Kaya[162], S. Kazakos[110], V.F. Kazanin[39], Y. Ke[150], J.M. Keaveney[34a], R. Keeler[170], G.V. Kehris[63], J.S. Keller[35], J.J. Kempster[151], O. Kepka[135], J. Kerr[160b], B.P. Kerridge[138], S. Kersten[176], B.P. Kerševan[96], L. Keszeghova[29a], S. Ketabchi Haghighat[159], R.A. Khan[133], A. Khanov[125], A.G. Kharlamov[39], T. Kharlamova[39], E.E. Khoda[143], M. Kholodenko[134a], T.J. Khoo[19], G. Khoriauli[171], J. Khubua[154b,*], Y.A.R. Khwaira[131], B. Kibirige[34g], D. Kim[6], D.W. Kim[49a,49b], Y.K. Kim[41], N. Kimura[99], M.K. Kingston[57], A. Kirchhoff[57], C. Kirfel[25], F. Kirfel[25], J. Kirk[138], A.E. Kiryunin[113], S. Kita[161], C. Kitsaki[10], O. Kivernyk[25], M. Klassen[162], C. Klein[35], L. Klein[171], M.H. Klein[46], S.B. Klein[58], U. Klein[95], A. Klimentov[30], T. Klioutchnikova[37], P. Kluit[118], S. Kluth[113], E. Kneringer[81], T.M. Knight[159], A. Knue[51], D. Kobylianskii[174], S.F. Koch[130], M. Kocian[148], P. Kodyš[137], D.M. Koeck[127], P.T. Koenig[25], T. Koffas[35], O. Kolay[52], I. Koletsou[4], T. Komarek[89], K. Köneke[57], A.X.Y. Kong[1], T. Kono[122], N. Konstantinidis[99], P. Kontaxakis[58], B. Konya[101], R. Kopeliansky[43], S. Koperny[88a], K. Korcyl[89], K. Kordas[157,d], A. Korn[99], S. Korn[57], I. Korolkov[13], N. Korotkova[39], B. Kortman[118], O. Kortner[113], S. Kortner[113], W.H. Kostecka[119], V.V. Kostyukhin[146], A. Kotsokechagia[37], A. Kotwal[53], A. Koulouris[37], A. Kourkoumeli-Charalampidi[75a,75b], C. Kourkoumelis[9], E. Kourlitis[113,aa], O. Kovanda[127], R. Kowalewski[170], W. Kozanecki[127], A.S. Kozhin[39], V.A. Kramarenko[39], G. Kramberger[96], P. Kramer[25], M.W. Krasny[131], A. Krasznahorkay[37], A.C. Kraus[119], J.W. Kraus[176], J.A. Kremer[50], T. Kresse[52], L. Kretschmann[176], J. Kretzschmar[95], K. Kreul[19], P. Krieger[159], K. Krizka[21], K. Kroeninger[51], H. Kroha[113], J. Kroll[135], J. Kroll[132], K.S. Krowpman[110], U. Kruchonak[40], H. Krüger[25], N. Krumnack[83], M.C. Kruse[53], O. Kuchinskaia[39], S. Kuday[3a], S. Kuehn[37], R. Kuesters[56], T. Kuhl[50], V. Kukhtin[40], Y. Kulchitsky[40], S. Kuleshov[141d,141b], M. Kumar[34g], N. Kumari[50], P. Kumari[160b], A. Kupco[135], T. Kupfer[51], A. Kupich[39], O. Kuprash[56], H. Kurashige[87], L.L. Kurchaninov[160a], O. Kurdysh[68], Y.A. Kurochkin[38], A. Kurova[39], M. Kuze[142], A.K. Kvam[106], J. Kvita[126], T. Kwan[107], N.G. Kyriacou[109], L.A.O. Laatu[105], C. Lacasta[168], F. Lacava[77a,77b], H. Lacker[19], D. Lacour[131], N.N. Lad[99], E. Ladygin[40], A. Lafarge[42], B. Laforge[131], T. Lagouri[177], F.Z. Lahbabi[36a], S. Lai[57], J.E. Lambert[170], S. Lammers[70], W. Lampl[7], C. Lampoudis[157,d], G. Lamprinoudis[103], A.N. Lancaster[119], E. Lançon[30], U. Landgraf[56], M.P.J. Landon[97], V.S. Lang[56], O.K.B. Langrekken[129], A.J. Lankford[163], F. Lanni[37], K. Lantzsch[25], A. Lanza[75a], M. Lanzac Berrocal[168], J.F. Laporte[139], T. Lari[73a], F. Lasagni Manghi[24b], M. Lassnig[37], V. Latonova[135], S.D. Lawlor[144], Z. Lawrence[104], R. Lazaridou[172], M. Lazzaroni[73a,73b], H.D.M. Le[110], E.M. Le Boulicaut[177], L.T. Le Pottier[18a], B. Leban[24b,24a], A. Lebedev[83], M. LeBlanc[104], F. Ledroit-Guillon[62], S.C. Lee[153], S. Lee[49a,49b], T.F. Lee[95], L.L. Leeuw[34c], M. Lefebvre[170], C. Leggett[18a], G. Lehmann Miotto[37], M. Leigh[58], W.A. Leight[106], W. Leinonen[117], A. Leisos[157,r], M.A.L. Leite[85c], C.E. Leitgeb[19], R. Leitner[137], K.J.C. Leney[46], T. Lenz[25], S. Leone[76a], C. Leonidopoulos[54], A. Leopold[149], R. Les[110], C.G. Lester[33], M. Levchenko[39], J. Levêque[4], L.J. Levinson[174], G. Levrini[24b,24a], M.P. Lewicki[89], C. Lewis[143], D.J. Lewis[4], L. Lewitt[144], A. Li[30], B. Li[64b], C. Li[64a], C-Q. Li[113], H. Li[64a], H. Li[64b], H. Li[115a], H. Li[15], H. Li[64b], J. Li[64c], K. Li[14], L. Li[64c], M. Li[14,115c], S. Li[14,115c], S. Li[64d,64c], T. Li[5], X. Li[107], Z. Li[158], Z. Li[14,115c], Z. Li[64a], S. Liang[14,115c], Z. Liang[14], M. Liberatore[139], B. Liberti[78a], K. Lie[66c], J. Lieber Marin[85e], H. Lien[70], H. Lin[109], K. Lin[110], L. Linden[112], R.E. Lindley[7], J.H. Lindon[2], J. Ling[63], E. Lipeles[132], A. Lipniacka[17], A. Lister[169], J.D. Little[70], B. Liu[14], B.X. Liu[115b], D. Liu[64d,64c],

E.H.L. Liu [21], J.B. Liu [64a], J.K.K. Liu [33], K. Liu [64d], K. Liu [64d,64c], M. Liu [64a], M.Y. Liu [64a], P. Liu [14], Q. Liu [64d,143,64c], X. Liu [64a], X. Liu [64b], Y. Liu [115b,115c], Y.L. Liu [64b], Y.W. Liu [64a], S.L. Lloyd [97], E.M. Lobodzinska [50], P. Loch [7], E. Lodhi [159], T. Lohse [19], K. Lohwasser [144], E. Loiacono [50], J.D. Lomas [21], J.D. Long [43], I. Longarini [163], R. Longo [167], I. Lopez Paz [69], A. Lopez Solis [50], N.A. Lopez-canelas [7], N. Lorenzo Martinez [4], A.M. Lory [112], M. Losada [120a], G. Löschcke Centeno [151], O. Loseva [39], X. Lou [49a,49b], X. Lou [14,115c], A. Lounis [68], P.A. Love [94], G. Lu [14,115c], M. Lu [68], S. Lu [132], Y.J. Lu [153], H.J. Lubatti [143], C. Luci [77a,77b], F.L. Lucio Alves [115a], F. Luehring [70], O. Lukianchuk [68], B.S. Lunday [132], O. Lundberg [149], B. Lund-Jensen [149,*], N.A. Luongo [6], M.S. Lutz [37], A.B. Lux [26], D. Lynn [30], R. Lysak [135], E. Lytken [101], V. Lyubushkin [40], T. Lyubushkina [40], M.M. Lyukova [150], M.Firdaus M. Soberi [54], H. Ma [30], K. Ma [64a], L.L. Ma [64b], W. Ma [64a], Y. Ma [125], J.C. MacDonald [103], P.C. Machado De Abreu Farias [85e], R. Madar [42], T. Madula [99], J. Maeda [87], T. Maeno [30], P.T. Mafa [34c], H. Maguire [144], V. Maiboroda [139], A. Maio [134a,134b,134d], K. Maj [88a], O. Majersky [50], S. Majewski [127], N. Makovec [68], V. Maksimovic [16], B. Malaescu [131], Pa. Malecki [89], V.P. Maleev [39], F. Malek [62,m], M. Mali [96], D. Malito [98], U. Mallik [82,*], S. Maltezos[10], S. Malyukov[40], J. Mamuzic [13], G. Mancini [55], M.N. Mancini [27], G. Manco [75a,75b], J.P. Mandalia [97], S.S. Mandarry [151], I. Mandić [96], L. Manhaes de Andrade Filho [85a], I.M. Maniatis [174], J. Manjarres Ramos [92], D.C. Mankad [174], A. Mann [112], S. Manzoni [37], L. Mao [64c], X. Mapekula [34c], A. Marantis [157,r], G. Marchiori [5], M. Marcisovsky [135], C. Marcon [73a], M. Marinescu [21], S. Marium [50], M. Marjanovic [124], A. Markhoos [56], M. Markovitch [68], M.K. Maroun [106], E.J. Marshall [94], Z. Marshall [18a], S. Marti-Garcia [168], J. Martin [99], T.A. Martin [138], V.J. Martin [54], B. Martin dit Latour [17], L. Martinelli [77a,77b], M. Martinez [13,t], P. Martinez Agullo [168], V.I. Martinez Outschoorn [106], P. Martinez Suarez [13], S. Martin-Haugh [138], G. Martinovicova [137], V.S. Martoiu [28b], A.C. Martyniuk [99], A. Marzin [37], D. Mascione [80a,80b], L. Masetti [103], J. Masik [104], A.L. Maslennikov [39], S.L. Mason [43], P. Massarotti [74a,74b], P. Mastrandrea [76a,76b], A. Mastroberardino [45b,45a], T. Masubuchi [128], T.T. Mathew [127], T. Mathisen [166], J. Matousek [137], D.M. Mattern [51], J. Maurer [28b], T. Maurin [61], A.J. Maury [68], B. Maček [96], D.A. Maximov [39], A.E. May [104], R. Mazini [34g], I. Maznas [119], M. Mazza [110], S.M. Mazza [140], E. Mazzeo [73a,73b], J.P. Mc Gowan [170], S.P. Mc Kee [109], C.A. Mc Lean [6], C.C. McCracken [169], E.F. McDonald [108], A.E. McDougall [118], L.F. Mcelhinney [94], J.A. Mcfayden [151], R.P. McGovern [132], R.P. Mckenzie [34g], T.C. Mclachlan [50], D.J. Mclaughlin [99], S.J. McMahon [138], C.M. Mcpartland [95], R.A. McPherson [170,x], S. Mehlhase [112], A. Mehta [95], D. Melini [168], B.R. Mellado Garcia [34g], A.H. Melo [57], F. Meloni [50], A.M. Mendes Jacques Da Costa [104], H.Y. Meng [159], L. Meng [94], S. Menke [113], M. Mentink [37], E. Meoni [45b,45a], G. Mercado [119], S. Merianos [157], C. Merlassino [71a,71c], L. Merola [74a,74b], C. Meroni [73a,73b], J. Metcalfe [6], A.S. Mete [6], E. Meuser [103], C. Meyer [70], J-P. Meyer [139], R.P. Middleton [138], L. Mijović [54], G. Mikenberg [174], M. Mikestikova [135], M. Mikuž [96], H. Mildner [103], A. Milic [37], D.W. Miller [41], E.H. Miller [148], L.S. Miller [35], A. Milov [174], D.A. Milstead[49a,49b], T. Min[115a], A.A. Minaenko [39], I.A. Minashvili [154b], A.I. Mincer [121], B. Mindur [88a], M. Mineev [40], Y. Mino [90], L.M. Mir [13], M. Miralles Lopez [61], M. Mironova [18a], M.C. Missio [117], A. Mitra [172], V.A. Mitsou [168], Y. Mitsumori [114], O. Miu [159], P.S. Miyagawa [97], T. Mkrtchyan [65a], M. Mlinarevic [99], T. Mlinarevic [99], M. Mlynarikova [37], S. Mobius [20], P. Mogg [112], M.H. Mohamed Farook [116], A.F. Mohammed [14,115c], S. Mohapatra [43], G. Mokgatitswane [34g], L. Moleri [174], B. Mondal [146], S. Mondal [136], K. Mönig [50], E. Monnier [105], L. Monsonis Romero[168], J. Montejo Berlingen [13], A. Montella [49a,49b], M. Montella [123], F. Montereali [79a,79b], F. Monticelli [93], S. Monzani [71a,71c], A. Morancho Tarda [44], N. Morange [68], A.L. Moreira De Carvalho [50], M. Moreno Llácer [168], C. Moreno Martinez [58],

J.M. Moreno Perez[23b], P. Morettini[59b], S. Morgenstern[37], M. Morii[63], M. Morinaga[158], M. Moritsu[91], F. Morodei[77a,77b], P. Moschovakos[37], B. Moser[130], M. Mosidze[154b], T. Moskalets[46], P. Moskvitina[117], J. Moss[32,j], P. Moszkowicz[88a], A. Moussa[36d], Y. Moyal[174], E.J.W. Moyse[106], O. Mtintsilana[34g], S. Muanza[105], J. Mueller[133], D. Muenstermann[94], R. Müller[37], G.A. Mullier[166], A.J. Mullin[33], J.J. Mullin[132], A.E. Mulski[63], D.P. Mungo[159], D. Munoz Perez[168], F.J. Munoz Sanchez[104], M. Murin[104], W.J. Murray[172,138], M. Muškinja[96], C. Mwewa[30], A.G. Myagkov[39,a], A.J. Myers[8], G. Myers[109], M. Myska[136], B.P. Nachman[18a], K. Nagai[130], K. Nagano[86], R. Nagasaka[158], J.L. Nagle[30,ae], E. Nagy[105], A.M. Nairz[37], Y. Nakahama[86], K. Nakamura[86], K. Nakkalil[5], H. Nanjo[128], E.A. Narayanan[46], Y. Narukawa[158], I. Naryshkin[39], L. Nasella[73a,73b], S. Nasri[120b], C. Nass[25], G. Navarro[23a], J. Navarro-Gonzalez[168], A. Nayaz[19], P.Y. Nechaeva[39], S. Nechaeva[24b,24a], F. Nechansky[135], L. Nedic[130], T.J. Neep[21], A. Negri[75a,75b], M. Negrini[24b], C. Nellist[118], C. Nelson[107], K. Nelson[109], S. Nemecek[135], M. Nessi[37,g], M.S. Neubauer[167], F. Neuhaus[103], J. Neundorf[50], J. Newell[95], P.R. Newman[21], C.W. Ng[133], Y.W.Y. Ng[50], B. Ngair[120a], H.D.N. Nguyen[111], R.B. Nickerson[130], R. Nicolaidou[139], J. Nielsen[140], M. Niemeyer[57], J. Niermann[37], N. Nikiforou[37], V. Nikolaenko[39,a], I. Nikolic-Audit[131], K. Nikolopoulos[21], P. Nilsson[30], I. Ninca[50], G. Ninio[156], A. Nisati[77a], N. Nishu[2], R. Nisius[113], N. Nitika[71a,71c], J-E. Nitschke[52], E.K. Nkadimeng[34g], T. Nobe[158], T. Nommensen[152], M.B. Norfolk[144], B.J. Norman[35], M. Noury[36a], J. Novak[96], T. Novak[96], L. Novotny[136], R. Novotny[116], L. Nozka[126], K. Ntekas[163], N.M.J. Nunes De Moura Junior[85b], J. Ocariz[131], A. Ochi[87], I. Ochoa[134a], S. Oerdek[50,u], J.T. Offermann[41], A. Ogrodnik[137], A. Oh[104], C.C. Ohm[149], H. Oide[86], R. Oishi[158], M.L. Ojeda[37], Y. Okumura[158], L.F. Oleiro Seabra[134a], I. Oleksiyuk[58], S.A. Olivares Pino[141d], G. Oliveira Correa[13], D. Oliveira Damazio[30], J.L. Oliver[163], Ö.O. Öncel[56], A.P. O'Neill[20], A. Onofre[134a,134e], P.U.E. Onyisi[11], M.J. Oreglia[41], D. Orestano[79a,79b], N. Orlando[13], R.S. Orr[159], L.M. Osojnak[132], Y. Osumi[114], G. Otero y Garzon[31], H. Otono[91], P.S. Ott[65a], G.J. Ottino[18a], M. Ouchrif[36d], F. Ould-Saada[129], T. Ovsiannikova[143], M. Owen[61], R.E. Owen[138], V.E. Ozcan[22a], F. Ozturk[89], N. Ozturk[8], S. Ozturk[84], H.A. Pacey[130], A. Pacheco Pages[13], C. Padilla Aranda[13], G. Padovano[77a,77b], S. Pagan Griso[18a], G. Palacino[70], A. Palazzo[72a,72b], J. Pampel[25], J. Pan[177], T. Pan[66a], D.K. Panchal[11], C.E. Pandini[118], J.G. Panduro Vazquez[138], H.D. Pandya[1], H. Pang[15], P. Pani[50], G. Panizzo[71a,71c], L. Panwar[131], L. Paolozzi[58], S. Parajuli[167], A. Paramonov[6], C. Paraskevopoulos[55], D. Paredes Hernandez[66b], A. Pareti[75a,75b], K.R. Park[43], T.H. Park[159], M.A. Parker[33], F. Parodi[59b,59a], V.A. Parrish[54], J.A. Parsons[43], U. Parzefall[56], B. Pascual Dias[111], L. Pascual Dominguez[102], E. Pasqualucci[77a], S. Passaggio[59b], F. Pastore[98], P. Patel[89], U.M. Patel[53], J.R. Pater[104], T. Pauly[37], F. Pauwels[137], C.I. Pazos[162], M. Pedersen[129], R. Pedro[134a], S.V. Peleganchuk[39], O. Penc[37], E.A. Pender[54], S. Peng[15], G.D. Penn[177], K.E. Penski[112], M. Penzin[39], B.S. Peralva[85d], A.P. Pereira Peixoto[143], L. Pereira Sanchez[148], D.V. Perepelitsa[30,ae], G. Perera[106], E. Perez Codina[160a], M. Perganti[10], H. Pernegger[37], S. Perrella[77a,77b], O. Perrin[42], K. Peters[50], R.F.Y. Peters[104], B.A. Petersen[37], T.C. Petersen[44], E. Petit[105], V. Petousis[136], C. Petridou[157,d], T. Petru[137], A. Petrukhin[146], M. Pettee[18a], A. Petukhov[84], K. Petukhova[37], R. Pezoa[141f], L. Pezzotti[37], G. Pezzullo[177], A.J. Pfleger[37], T.M. Pham[175], T. Pham[108], P.W. Phillips[138], G. Piacquadio[150], E. Pianori[18a], F. Piazza[127], R. Piegaia[31], D. Pietreanu[28b], A.D. Pilkington[104], M. Pinamonti[71a,71c], J.L. Pinfold[2], B.C. Pinheiro Pereira[134a], J. Pinol Bel[13], A.E. Pinto Pinoargote[139,139], L. Pintucci[71a,71c], K.M. Piper[151], A. Pirttikoski[58], D.A. Pizzi[35], L. Pizzimento[66b], A. Pizzini[118], M.-A. Pleier[30], V. Pleskot[137], E. Plotnikova[40], G. Poddar[97], R. Poettgen[101],

L. Poggioli [131], S. Polacek [137], G. Polesello [75a], A. Poley [147,160a], A. Polini [24b], C.S. Pollard [172], Z.B. Pollock [123], E. Pompa Pacchi [124], N.I. Pond [99], D. Ponomarenko [70], L. Pontecorvo [37], S. Popa [28a], G.A. Popeneciu [28d], A. Poreba [37], D.M. Portillo Quintero [160a], S. Pospisil [136], M.A. Postill [144], P. Postolache [28c], K. Potamianos [172], P.A. Potepa [88a], I.N. Potrap [40], C.J. Potter [33], H. Potti [152], J. Poveda [168], M.E. Pozo Astigarraga [37], A. Prades Ibanez [78a,78b], J. Pretel [170], D. Price [104], M. Primavera [72a], L. Primomo [71a,71c], M.A. Principe Martin [102], R. Privara [126], T. Procter [61], M.L. Proffitt [143], N. Proklova [132], K. Prokofiev [66c], G. Proto [113], J. Proudfoot [6], M. Przybycien [88a], W.W. Przygoda [88b], A. Psallidas [48], J.E. Puddefoot [144], D. Pudzha [56], D. Pyatiizbyantseva [39], J. Qian [109], R. Qian [110], D. Qichen [104], Y. Qin [13], T. Qiu [54], A. Quadt [57], M. Queitsch-Maitland [104], G. Quetant [58], R.P. Quinn [169], G. Rabanal Bolanos [63], D. Rafanoharana [56], F. Raffaeli [78a,78b], F. Ragusa [73a,73b], J.L. Rainbolt [41], J.A. Raine [58], S. Rajagopalan [30], E. Ramakoti [39], L. Rambelli [59b,59a], I.A. Ramirez-Berend [35], K. Ran [50,115c], D.S. Rankin [132], N.P. Rapheeha [34g], H. Rasheed [28b], V. Raskina [131], D.F. Rassloff [65a], A. Rastogi [18a], S. Rave [103], S. Ravera [59b,59a], B. Ravina [57], I. Ravinovich [174], M. Raymond [37], A.L. Read [129], N.P. Readioff [144], D.M. Rebuzzi [75a,75b], G. Redlinger [30], A.S. Reed [113], K. Reeves [27], J.A. Reidelsturz [176], D. Reikher [127], A. Rej [51], C. Rembser [37], M. Renda [28b], F. Renner [50], A.G. Rennie [163], A.L. Rescia [50], S. Resconi [73a], M. Ressegotti [59b,59a], S. Rettie [37], J.G. Reyes Rivera [110], E. Reynolds [18a], O.L. Rezanova [39], P. Reznicek [137], H. Riani [36d], N. Ribaric [53], E. Ricci [80a,80b], R. Richter [113], S. Richter [49a,49b], E. Richter-Was [88b], M. Ridel [131], S. Ridouani [36d], P. Rieck [121], P. Riedler [37], E.M. Riefel [49a,49b], J.O. Rieger [118], M. Rijssenbeek [150], M. Rimoldi [37], L. Rinaldi [24b,24a], P. Rincke [57,166], T.T. Rinn [30], M.P. Rinnagel [112], G. Ripellino [166], I. Riu [13], J.C. Rivera Vergara [170], F. Rizatdinova [125], E. Rizvi [97], B.R. Roberts [18a], S.S. Roberts [140], S.H. Robertson [107,x], D. Robinson [33], M. Robles Manzano [103], A. Robson [61], A. Rocchi [78a,78b], C. Roda [76a,76b], S. Rodriguez Bosca [37], Y. Rodriguez Garcia [23a], A.M. Rodríguez Vera [119], S. Roe [37], J.T. Roemer [37], O. Røhne [129], R.A. Rojas [106], C.P.A. Roland [131], J. Roloff [30], A. Romaniouk [81], E. Romano [75a,75b], M. Romano [24b], A.C. Romero Hernandez [167], N. Rompotis [95], L. Roos [131], S. Rosati [77a], B.J. Rosser [41], E. Rossi [130], E. Rossi [74a,74b], L.P. Rossi [63], L. Rossini [56], R. Rosten [123], M. Rotaru [28b], B. Rottler [56], C. Rougier [92], D. Rousseau [68], D. Rousso [50], A. Roy [167], S. Roy-Garand [159], A. Rozanov [105], Z.M.A. Rozario [61], Y. Rozen [155], A. Rubio Jimenez [168], V.H. Ruelas Rivera [19], T.A. Ruggeri [1], A. Ruggiero [130], A. Ruiz-Martinez [168], A. Rummler [37], Z. Rurikova [56], N.A. Rusakovich [40], H.L. Russell [170], G. Russo [77a,77b], J.P. Rutherfoord [7], S. Rutherford Colmenares [33], M. Rybar [137], E.B. Rye [129], A. Ryzhov [46], J.A. Sabater Iglesias [58], H.F-W. Sadrozinski [140], F. Safai Tehrani [77a], B. Safarzadeh Samani [138], S. Saha [1], M. Sahinsoy [84], A. Saibel [168], M. Saimpert [139], M. Saito [158], T. Saito [158], A. Sala [73a,73b], D. Salamani [37], A. Salnikov [148], J. Salt [168], A. Salvador Salas [156], D. Salvatore [45b,45a], F. Salvatore [151], A. Salzburger [37], D. Sammel [56], E. Sampson [94], D. Sampsonidis [157,d], D. Sampsonidou [127], J. Sánchez [168], V. Sanchez Sebastian [168], H. Sandaker [129], C.O. Sander [50], J.A. Sandesara [106], M. Sandhoff [176], C. Sandoval [23b], L. Sanfilippo [65a], D.P.C. Sankey [138], T. Sano [90], A. Sansoni [55], L. Santi [37,77b], C. Santoni [42], H. Santos [134a,134b], A. Santra [174], E. Sanzani [24b,24a], K.A. Saoucha [165], J.G. Saraiva [134a,134d], J. Sardain [7], O. Sasaki [86], K. Sato [161], C. Sauer [37], E. Sauvan [4], P. Savard [159,ac], R. Sawada [158], C. Sawyer [138], L. Sawyer [100], C. Sbarra [24b], A. Sbrizzi [24b,24a], T. Scanlon [99], J. Schaarschmidt [143], U. Schäfer [103], A.C. Schaffer [68,46], D. Schaile [112], R.D. Schamberger [150], C. Scharf [19], M.M. Schefer [20], V.A. Schegelsky [39], D. Scheirich [137], M. Schernau [141e], C. Scheulen [58], C. Schiavi [59b,59a], M. Schioppa [45b,45a], B. Schlag [148], S. Schlenker [37], J. Schmeing [176], M.A. Schmidt [176], K. Schmieden [103], C. Schmitt [103],

N. Schmitt[103], S. Schmitt[50], L. Schoeffel[139], A. Schoening[65b], P.G. Scholer[35], E. Schopf[130], M. Schott[25], J. Schovancova[37], S. Schramm[58], T. Schroer[58], H-C. Schultz-Coulon[65a], M. Schumacher[56], B.A. Schumm[140], Ph. Schune[139], A.J. Schuy[143], H.R. Schwartz[140], A. Schwartzman[148], T.A. Schwarz[109], Ph. Schwemling[139], R. Schwienhorst[110], F.G. Sciacca[20], A. Sciandra[30], G. Sciolla[27], F. Scuri[76a], C.D. Sebastiani[95], K. Sedlaczek[119], S.C. Seidel[116], A. Seiden[140], B.D. Seidlitz[43], C. Seitz[50], J.M. Seixas[85b], G. Sekhniaidze[74a], L. Selem[62], N. Semprini-Cesari[24b,24a], A. Semushin[178,39], D. Sengupta[58], V. Senthilkumar[168], L. Serin[68], M. Sessa[78a,78b], H. Severini[124], F. Sforza[59b,59a], A. Sfyrla[58], Q. Sha[14], E. Shabalina[57], A.H. Shah[33], R. Shaheen[149], J.D. Shahinian[132], D. Shaked Renous[174], L.Y. Shan[14], M. Shapiro[18a], A. Sharma[37], A.S. Sharma[169], P. Sharma[30], P.B. Shatalov[39], K. Shaw[151], S.M. Shaw[104], Q. Shen[64c], D.J. Sheppard[147], P. Sherwood[99], L. Shi[99], X. Shi[14], S. Shimizu[86], C.O. Shimmin[177], I.P.J. Shipsey[130,*], S. Shirabe[91], M. Shiyakova[40,v], M.J. Shochet[41], D.R. Shope[129], B. Shrestha[124], S. Shrestha[123,af], I. Shreyber[39], M.J. Shroff[170], P. Sicho[135], A.M. Sickles[167], E. Sideras Haddad[34g,164], A.C. Sidley[118], A. Sidoti[24b], F. Siegert[52], Dj. Sijacki[16], F. Sili[93], J.M. Silva[54], I. Silva Ferreira[85b], M.V. Silva Oliveira[30], S.B. Silverstein[49a], S. Simion[68], R. Simoniello[37], E.L. Simpson[104], H. Simpson[151], L.R. Simpson[109], S. Simsek[84], S. Sindhu[57], P. Sinervo[159], S. Singh[30], S. Sinha[50], S. Sinha[104], M. Sioli[24b,24a], I. Siral[37], E. Sitnikova[50], J. Sjölin[49a,49b], A. Skaf[57], E. Skorda[21], P. Skubic[124], M. Slawinska[89], I. Slazyk[17], V. Smakhtin[174], B.H. Smart[138], S.Yu. Smirnov[39], Y. Smirnov[39], L.N. Smirnova[39,a], O. Smirnova[101], A.C. Smith[43], D.R. Smith[163], E.A. Smith[41], J.L. Smith[104], R. Smith[148], H. Smitmanns[103], M. Smizanska[94], K. Smolek[136], A.A. Snesarev[39], H.L. Snoek[118], S. Snyder[30], R. Sobie[170,x], A. Soffer[156], C.A. Solans Sanchez[37], E.Yu. Soldatov[39], U. Soldevila[168], A.A. Solodkov[39], S. Solomon[27], A. Soloshenko[40], K. Solovieva[56], O.V. Solovyanov[42], P. Sommer[52], A. Sonay[13], W.Y. Song[160b], A. Sopczak[136], A.L. Sopio[54], F. Sopkova[29b], J.D. Sorenson[116], I.R. Sotarriva Alvarez[142], V. Sothilingam[65a], O.J. Soto Sandoval[141c,141b], S. Sottocornola[70], R. Soualah[165], Z. Soumaimi[36e], D. South[50], N. Soybelman[174], S. Spagnolo[72a,72b], M. Spalla[113], D. Sperlich[56], G. Spigo[37], B. Spisso[74a,74b], D.P. Spiteri[61], M. Spousta[137], E.J. Staats[35], R. Stamen[65a], A. Stampekis[21], E. Stanecka[89], W. Stanek-Maslouska[50], M.V. Stange[52], B. Stanislaus[18a], M.M. Stanitzki[50], B. Stapf[50], E.A. Starchenko[39], G.H. Stark[140], J. Stark[92], P. Staroba[135], P. Starovoitov[65a], S. Stärz[107], R. Staszewski[89], G. Stavropoulos[48], A. Stefl[37], P. Steinberg[30], B. Stelzer[147,160a], H.J. Stelzer[133], O. Stelzer-Chilton[160a], H. Stenzel[60], T.J. Stevenson[151], G.A. Stewart[37], J.R. Stewart[125], M.C. Stockton[37], G. Stoicea[28b], M. Stolarski[134a], S. Stonjek[113], A. Straessner[52], J. Strandberg[149], S. Strandberg[49a,49b], M. Stratmann[176], M. Strauss[124], T. Strebler[105], P. Strizenec[29b], R. Ströhmer[171], D.M. Strom[127], R. Stroynowski[46], A. Strubig[49a,49b], S.A. Stucci[30], B. Stugu[17], J. Stupak[124], N.A. Styles[50], D. Su[148], S. Su[64a], W. Su[64d], X. Su[64a], D. Suchy[29a], K. Sugizaki[158], V.V. Sulin[39], M.J. Sullivan[95], D.M.S. Sultan[130], L. Sultanaliyeva[39], S. Sultansoy[3b], T. Sumida[90], S. Sun[175], W. Sun[14], O. Sunneborn Gudnadottir[166], N. Sur[105], M.R. Sutton[151], H. Suzuki[161], M. Svatos[135], M. Swiatlowski[160a], T. Swirski[171], I. Sykora[29a], M. Sykora[137], T. Sykora[137], D. Ta[103], K. Tackmann[50,u], A. Taffard[163], R. Tafirout[160a], J.S. Tafoya Vargas[68], Y. Takubo[86], M. Talby[105], A.A. Talyshev[39], K.C. Tam[66b], N.M. Tamir[156], A. Tanaka[158], J. Tanaka[158], R. Tanaka[68], M. Tanasini[150], Z. Tao[169], S. Tapia Araya[141f], S. Tapprogge[103], A. Tarek Abouelfadl Mohamed[110], S. Tarem[155], K. Tariq[14], G. Tarna[28b], G.F. Tartarelli[73a], M.J. Tartarin[92], P. Tas[137], M. Tasevsky[135], E. Tassi[45b,45a], A.C. Tate[167], G. Tateno[158], Y. Tayalati[36e,w], G.N. Taylor[108], W. Taylor[160b], P. Teixeira-Dias[98], J.J. Teoh[159],

K. Terashi[158], J. Terron[102], S. Terzo[13], M. Testa[55], R.J. Teuscher[159,x], A. Thaler[81], O. Theiner[58], T. Theveneaux-Pelzer[105], O. Thielmann[176], D.W. Thomas[98], J.P. Thomas[21], E.A. Thompson[18a], P.D. Thompson[21], E. Thomson[132], R.E. Thornberry[46], C. Tian[64a], Y. Tian[58], V. Tikhomirov[39,a], Yu.A. Tikhonov[39], S. Timoshenko[39], D. Timoshyn[137], E.X.L. Ting[1], P. Tipton[177], A. Tishelman-Charny[30], S.H. Tlou[34g], K. Todome[142], S. Todorova-Nova[137], S. Todt[52], L. Toffolin[71a,71c], M. Togawa[86], J. Tojo[91], S. Tokár[29a], K. Tokushuku[86], O. Toldaiev[70], G. Tolkachev[105], M. Tomoto[86,114], L. Tompkins[148,l], E. Torrence[127], H. Torres[92], E. Torró Pastor[168], M. Toscani[31], C. Tosciri[41], M. Tost[11], D.R. Tovey[144], I.S. Trandafir[28b], T. Trefzger[171], A. Tricoli[30], I.M. Trigger[160a], S. Trincaz-Duvoid[131], D.A. Trischuk[27], B. Trocmé[62], A. Tropina[40], L. Truong[34c], M. Trzebinski[89], A. Trzupek[89], F. Tsai[150], M. Tsai[109], A. Tsiamis[157], P.V. Tsiareshka[40], S. Tsigaridas[160a], A. Tsirigotis[157,r], V. Tsiskaridze[159], E.G. Tskhadadze[154a], M. Tsopoulou[157], Y. Tsujikawa[90], I.I. Tsukerman[39], V. Tsulaia[18a], S. Tsuno[86], K. Tsuri[122], D. Tsybychev[150], Y. Tu[66b], A. Tudorache[28b], V. Tudorache[28b], A.N. Tuna[63], S. Turchikhin[59b,59a], I. Turk Cakir[3a], R. Turra[73a], T. Turtuvshin[40], P.M. Tuts[43], S. Tzamarias[157,d], E. Tzovara[103], F. Ukegawa[161], P.A. Ulloa Poblete[141c,141b], E.N. Umaka[30], G. Unal[37], A. Undrus[30], G. Unel[163], J. Urban[29b], P. Urrejola[141a], G. Usai[8], R. Ushioda[142], M. Usman[111], F. Ustuner[54], Z. Uysal[84], V. Vacek[136], B. Vachon[107], T. Vafeiadis[37], A. Vaitkus[99], C. Valderanis[112], E. Valdes Santurio[49a,49b], M. Valente[160a], S. Valentinetti[24b,24a], A. Valero[168], E. Valiente Moreno[168], A. Vallier[92], J.A. Valls Ferrer[168], D.R. Van Arneman[118], T.R. Van Daalen[143], A. Van Der Graaf[51], P. Van Gemmeren[6], M. Van Rijnbach[37], S. Van Stroud[99], I. Van Vulpen[118], P. Vana[137], M. Vanadia[78a,78b], U.M. Vande Voorde[149], W. Vandelli[37], E.R. Vandewall[125], D. Vannicola[156], L. Vannoli[55], R. Vari[77a], E.W. Varnes[7], C. Varni[18b], D. Varouchas[68], L. Varriale[168], K.E. Varvell[152], M.E. Vasile[28b], L. Vaslin[86], A. Vasyukov[40], L.M. Vaughan[125], R. Vavricka[103], T. Vazquez Schroeder[37], J. Veatch[32], V. Vecchio[104], M.J. Veen[106], I. Veliscek[30], L.M. Veloce[159], F. Veloso[134a,134c], S. Veneziano[77a], A. Ventura[72a,72b], S. Ventura Gonzalez[139], A. Verbytskyi[113], M. Verducci[76a,76b], C. Vergis[97], M. Verissimo De Araujo[85b], W. Verkerke[118], J.C. Vermeulen[118], C. Vernieri[148], M. Vessella[163], M.C. Vetterli[147,ac], A. Vgenopoulos[103], N. Viaux Maira[141f], T. Vickey[144], O.E. Vickey Boeriu[144], G.H.A. Viehhauser[130], L. Vigani[65b], M. Vigl[113], M. Villa[24b,24a], M. Villaplana Perez[168], E.M. Villhauer[54], E. Vilucchi[55], M.G. Vincter[35], A. Visibile[118], C. Vittori[37], I. Vivarelli[24b,24a], E. Voevodina[113], F. Vogel[112], J.C. Voigt[52], P. Vokac[136], Yu. Volkotrub[88b], E. Von Toerne[25], B. Vormwald[37], V. Vorobel[137], K. Vorobev[39], M. Vos[168], K. Voss[146], M. Vozak[118], L. Vozdecky[124], N. Vranjes[16], M. Vranjes Milosavljevic[16], M. Vreeswijk[118], N.K. Vu[64d], R. Vuillermet[37], O. Vujinovic[103], I. Vukotic[41], I.K. Vyas[35], S. Wada[161], C. Wagner[148], J.M. Wagner[18a], W. Wagner[176], S. Wahdan[176], H. Wahlberg[93], C.H. Waits[124], J. Walder[138], R. Walker[112], W. Walkowiak[146], A. Wall[132], E.J. Wallin[101], T. Wamorkar[6], A.Z. Wang[140], C. Wang[103], C. Wang[11], H. Wang[18a], J. Wang[66c], P. Wang[104], P. Wang[99], R. Wang[63], R. Wang[6], S.M. Wang[153], S. Wang[14], T. Wang[64a], W.T. Wang[82], W. Wang[14], X. Wang[167], X. Wang[64c], Y. Wang[64d], Y. Wang[115a], Y. Wang[64a], Z. Wang[109], Z. Wang[64d,53,64c], Z. Wang[109], A. Warburton[107], R.J. Ward[21], N. Warrack[61], S. Waterhouse[98], A.T. Watson[21], H. Watson[54], M.F. Watson[21], E. Watton[61,138], G. Watts[143], B.M. Waugh[99], J.M. Webb[56], C. Weber[30], H.A. Weber[19], M.S. Weber[20], S.M. Weber[65a], C. Wei[64a], Y. Wei[56], A.R. Weidberg[130], E.J. Weik[121], J. Weingarten[51], C. Weiser[56], C.J. Wells[50], T. Wenaus[30], B. Wendland[51], T. Wengler[37], N.S. Wenke[113], N. Wermes[25], M. Wessels[65a], A.M. Wharton[94], A.S. White[63], A. White[8], M.J. White[1], D. Whiteson[163], L. Wickremasinghe[128],

W. Wiedenmann[175], M. Wielers[138], C. Wiglesworth[44], D.J. Wilbern[124], H.G. Wilkens[37], J.J.H. Wilkinson[33], D.M. Williams[43], H.H. Williams[132], S. Williams[33], S. Willocq[106], B.J. Wilson[104], D.J. Wilson[104], P.J. Windischhofer[41], F.I. Winkel[31], F. Winklmeier[127], B.T. Winter[56], J.K. Winter[104], M. Wittgen[148], M. Wobisch[100], T. Wojtkowski[62], Z. Wolffs[118], J. Wollrath[37], M.W. Wolter[89], H. Wolters[134a,134c], M.C. Wong[140], E.L. Woodward[43], S.D. Worm[50], B.K. Wosiek[89], K.W. Woźniak[89], S. Wozniewski[57], K. Wraight[61], C. Wu[21], M. Wu[115b], M. Wu[117], S.L. Wu[175], X. Wu[58], X. Wu[64a], Y. Wu[64a], Z. Wu[4], J. Wuerzinger[113,aa], T.R. Wyatt[104], B.M. Wynne[54], S. Xella[44], L. Xia[115a], M. Xia[15], M. Xie[64a], A. Xiong[127], J. Xiong[18a], D. Xu[14], H. Xu[64a], L. Xu[64a], R. Xu[132], T. Xu[109], Y. Xu[143], Z. Xu[54], Z. Xu[115a], B. Yabsley[152], S. Yacoob[34a], Y. Yamaguchi[86], E. Yamashita[158], H. Yamauchi[161], T. Yamazaki[18a], Y. Yamazaki[87], S. Yan[61], Z. Yan[106], H.J. Yang[64c,64d], H.T. Yang[64a], S. Yang[64a], T. Yang[66c], X. Yang[37], X. Yang[14], Y. Yang[46], Y. Yang[64a], W-M. Yao[18a], H. Ye[57], J. Ye[14], S. Ye[30], X. Ye[64a], Y. Yeh[99], I. Yeletskikh[40], B. Yeo[18b], M.R. Yexley[99], T.P. Yildirim[130], P. Yin[43], K. Yorita[173], S. Younas[28b], C.J.S. Young[37], C. Young[148], C. Yu[14,115c], Y. Yu[64a], J. Yuan[14,115c], M. Yuan[109], R. Yuan[64d,64c], L. Yue[99], M. Zaazoua[64a], B. Zabinski[89], I. Zahir[36a], E. Zaid[54], Z.K. Zak[89], T. Zakareishvili[168], S. Zambito[58], J.A. Zamora Saa[141d,141b], J. Zang[158], D. Zanzi[56], R. Zanzottera[73a,73b], O. Zaplatilek[136], C. Zeitnitz[176], H. Zeng[14], J.C. Zeng[167], D.T. Zenger Jr[27], O. Zenin[39], T. Ženiš[29a], S. Zenz[97], S. Zerradi[36a], D. Zerwas[68], M. Zhai[14,115c], D.F. Zhang[144], J. Zhang[64b], J. Zhang[6], K. Zhang[14,115c], L. Zhang[64a], L. Zhang[115a], P. Zhang[14,115c], R. Zhang[175], S. Zhang[109], S. Zhang[92], T. Zhang[158], X. Zhang[64c], Y. Zhang[143], Y. Zhang[99], Y. Zhang[115a], Z. Zhang[18a], Z. Zhang[64b], Z. Zhang[68], H. Zhao[143], T. Zhao[64b], Y. Zhao[140], Z. Zhao[64a], Z. Zhao[64a], A. Zhemchugov[40], J. Zheng[115a], K. Zheng[167], X. Zheng[64a], Z. Zheng[148], D. Zhong[167], B. Zhou[109], H. Zhou[7], N. Zhou[64c], Y. Zhou[15], Y. Zhou[115a], Y. Zhou[7], C.G. Zhu[64b], J. Zhu[109], X. Zhu[64d], Y. Zhu[64c], Y. Zhu[64a], X. Zhuang[14], K. Zhukov[70], N.I. Zimine[40], J. Zinsser[65b], M. Ziolkowski[146], L. Živković[16], A. Zoccoli[24b,24a], K. Zoch[63], T.G. Zorbas[144], O. Zormpa[48], W. Zou[43], L. Zwalinski[37].

[1]Department of Physics, University of Adelaide, Adelaide; Australia.
[2]Department of Physics, University of Alberta, Edmonton AB; Canada.
[3](a)Department of Physics, Ankara University, Ankara;(b)Division of Physics, TOBB University of Economics and Technology, Ankara; Türkiye.
[4]LAPP, Université Savoie Mont Blanc, CNRS/IN2P3, Annecy; France.
[5]APC, Université Paris Cité, CNRS/IN2P3, Paris; France.
[6]High Energy Physics Division, Argonne National Laboratory, Argonne IL; United States of America.
[7]Department of Physics, University of Arizona, Tucson AZ; United States of America.
[8]Department of Physics, University of Texas at Arlington, Arlington TX; United States of America.
[9]Physics Department, National and Kapodistrian University of Athens, Athens; Greece.
[10]Physics Department, National Technical University of Athens, Zografou; Greece.
[11]Department of Physics, University of Texas at Austin, Austin TX; United States of America.
[12]Institute of Physics, Azerbaijan Academy of Sciences, Baku; Azerbaijan.
[13]Institut de Física d'Altes Energies (IFAE), Barcelona Institute of Science and Technology, Barcelona; Spain.
[14]Institute of High Energy Physics, Chinese Academy of Sciences, Beijing; China.
[15]Physics Department, Tsinghua University, Beijing; China.
[16]Institute of Physics, University of Belgrade, Belgrade; Serbia.

[17]Department for Physics and Technology, University of Bergen, Bergen; Norway.
[18(a)]Physics Division, Lawrence Berkeley National Laboratory, Berkeley CA;[(b)]University of California, Berkeley CA; United States of America.
[19]Institut für Physik, Humboldt Universität zu Berlin, Berlin; Germany.
[20]Albert Einstein Center for Fundamental Physics and Laboratory for High Energy Physics, University of Bern, Bern; Switzerland.
[21]School of Physics and Astronomy, University of Birmingham, Birmingham; United Kingdom.
[22(a)]Department of Physics, Bogazici University, Istanbul;[(b)]Department of Physics Engineering, Gaziantep University, Gaziantep;[(c)]Department of Physics, Istanbul University, Istanbul; Türkiye.
[23(a)]Facultad de Ciencias y Centro de Investigaciónes, Universidad Antonio Nariño, Bogotá;[(b)]Departamento de Física, Universidad Nacional de Colombia, Bogotá; Colombia.
[24(a)]Dipartimento di Fisica e Astronomia A. Righi, Università di Bologna, Bologna;[(b)]INFN Sezione di Bologna; Italy.
[25]Physikalisches Institut, Universität Bonn, Bonn; Germany.
[26]Department of Physics, Boston University, Boston MA; United States of America.
[27]Department of Physics, Brandeis University, Waltham MA; United States of America.
[28(a)]Transilvania University of Brasov, Brasov;[(b)]Horia Hulubei National Institute of Physics and Nuclear Engineering, Bucharest;[(c)]Department of Physics, Alexandru Ioan Cuza University of Iasi, Iasi;[(d)]National Institute for Research and Development of Isotopic and Molecular Technologies, Physics Department, Cluj-Napoca;[(e)]National University of Science and Technology Politechnica, Bucharest;[(f)]West University in Timisoara, Timisoara;[(g)]Faculty of Physics, University of Bucharest, Bucharest; Romania.
[29(a)]Faculty of Mathematics, Physics and Informatics, Comenius University, Bratislava;[(b)]Department of Subnuclear Physics, Institute of Experimental Physics of the Slovak Academy of Sciences, Kosice; Slovak Republic.
[30]Physics Department, Brookhaven National Laboratory, Upton NY; United States of America.
[31]Universidad de Buenos Aires, Facultad de Ciencias Exactas y Naturales, Departamento de Física, y CONICET, Instituto de Física de Buenos Aires (IFIBA), Buenos Aires; Argentina.
[32]California State University, CA; United States of America.
[33]Cavendish Laboratory, University of Cambridge, Cambridge; United Kingdom.
[34(a)]Department of Physics, University of Cape Town, Cape Town;[(b)]iThemba Labs, Western Cape;[(c)]Department of Mechanical Engineering Science, University of Johannesburg, Johannesburg;[(d)]National Institute of Physics, University of the Philippines Diliman (Philippines);[(e)]University of South Africa, Department of Physics, Pretoria;[(f)]University of Zululand, KwaDlangezwa;[(g)]School of Physics, University of the Witwatersrand, Johannesburg; South Africa.
[35]Department of Physics, Carleton University, Ottawa ON; Canada.
[36(a)]Faculté des Sciences Ain Chock, Université Hassan II de Casablanca;[(b)]Faculté des Sciences, Université Ibn-Tofail, Kénitra;[(c)]Faculté des Sciences Semlalia, Université Cadi Ayyad, LPHEA-Marrakech;[(d)]LPMR, Faculté des Sciences, Université Mohamed Premier, Oujda;[(e)]Faculté des sciences, Université Mohammed V, Rabat;[(f)]Institute of Applied Physics, Mohammed VI Polytechnic University, Ben Guerir; Morocco.
[37]CERN, Geneva; Switzerland.
[38]Affiliated with an institute formerly covered by a cooperation agreement with CERN.
[39]Affiliated with an institute covered by a cooperation agreement with CERN.
[40]Affiliated with an international laboratory covered by a cooperation agreement with CERN.
[41]Enrico Fermi Institute, University of Chicago, Chicago IL; United States of America.
[42]LPC, Université Clermont Auvergne, CNRS/IN2P3, Clermont-Ferrand; France.
[43]Nevis Laboratory, Columbia University, Irvington NY; United States of America.

[44]Niels Bohr Institute, University of Copenhagen, Copenhagen; Denmark.
[45(a)]Dipartimento di Fisica, Università della Calabria, Rende;[(b)]INFN Gruppo Collegato di Cosenza, Laboratori Nazionali di Frascati; Italy.
[46]Physics Department, Southern Methodist University, Dallas TX; United States of America.
[47]Physics Department, University of Texas at Dallas, Richardson TX; United States of America.
[48]National Centre for Scientific Research "Demokritos", Agia Paraskevi; Greece.
[49(a)]Department of Physics, Stockholm University;[(b)]Oskar Klein Centre, Stockholm; Sweden.
[50]Deutsches Elektronen-Synchrotron DESY, Hamburg and Zeuthen; Germany.
[51]Fakultät Physik , Technische Universität Dortmund, Dortmund; Germany.
[52]Institut für Kern- und Teilchenphysik, Technische Universität Dresden, Dresden; Germany.
[53]Department of Physics, Duke University, Durham NC; United States of America.
[54]SUPA - School of Physics and Astronomy, University of Edinburgh, Edinburgh; United Kingdom.
[55]INFN e Laboratori Nazionali di Frascati, Frascati; Italy.
[56]Physikalisches Institut, Albert-Ludwigs-Universität Freiburg, Freiburg; Germany.
[57]II. Physikalisches Institut, Georg-August-Universität Göttingen, Göttingen; Germany.
[58]Département de Physique Nucléaire et Corpusculaire, Université de Genève, Genève; Switzerland.
[59(a)]Dipartimento di Fisica, Università di Genova, Genova;[(b)]INFN Sezione di Genova; Italy.
[60]II. Physikalisches Institut, Justus-Liebig-Universität Giessen, Giessen; Germany.
[61]SUPA - School of Physics and Astronomy, University of Glasgow, Glasgow; United Kingdom.
[62]LPSC, Université Grenoble Alpes, CNRS/IN2P3, Grenoble INP, Grenoble; France.
[63]Laboratory for Particle Physics and Cosmology, Harvard University, Cambridge MA; United States of America.
[64(a)]Department of Modern Physics and State Key Laboratory of Particle Detection and Electronics, University of Science and Technology of China, Hefei;[(b)]Institute of Frontier and Interdisciplinary Science and Key Laboratory of Particle Physics and Particle Irradiation (MOE), Shandong University, Qingdao;[(c)]School of Physics and Astronomy, Shanghai Jiao Tong University, Key Laboratory for Particle Astrophysics and Cosmology (MOE), SKLPPC, Shanghai;[(d)]Tsung-Dao Lee Institute, Shanghai;[(e)]School of Physics, Zhengzhou University; China.
[65(a)]Kirchhoff-Institut für Physik, Ruprecht-Karls-Universität Heidelberg, Heidelberg;[(b)]Physikalisches Institut, Ruprecht-Karls-Universität Heidelberg, Heidelberg; Germany.
[66(a)]Department of Physics, Chinese University of Hong Kong, Shatin, N.T., Hong Kong;[(b)]Department of Physics, University of Hong Kong, Hong Kong;[(c)]Department of Physics and Institute for Advanced Study, Hong Kong University of Science and Technology, Clear Water Bay, Kowloon, Hong Kong; China.
[67]Department of Physics, National Tsing Hua University, Hsinchu; Taiwan.
[68]IJCLab, Université Paris-Saclay, CNRS/IN2P3, 91405, Orsay; France.
[69]Centro Nacional de Microelectrónica (IMB-CNM-CSIC), Barcelona; Spain.
[70]Department of Physics, Indiana University, Bloomington IN; United States of America.
[71(a)]INFN Gruppo Collegato di Udine, Sezione di Trieste, Udine;[(b)]ICTP, Trieste;[(c)]Dipartimento Politecnico di Ingegneria e Architettura, Università di Udine, Udine; Italy.
[72(a)]INFN Sezione di Lecce;[(b)]Dipartimento di Matematica e Fisica, Università del Salento, Lecce; Italy.
[73(a)]INFN Sezione di Milano;[(b)]Dipartimento di Fisica, Università di Milano, Milano; Italy.
[74(a)]INFN Sezione di Napoli;[(b)]Dipartimento di Fisica, Università di Napoli, Napoli; Italy.
[75(a)]INFN Sezione di Pavia;[(b)]Dipartimento di Fisica, Università di Pavia, Pavia; Italy.
[76(a)]INFN Sezione di Pisa;[(b)]Dipartimento di Fisica E. Fermi, Università di Pisa, Pisa; Italy.
[77(a)]INFN Sezione di Roma;[(b)]Dipartimento di Fisica, Sapienza Università di Roma, Roma; Italy.
[78(a)]INFN Sezione di Roma Tor Vergata;[(b)]Dipartimento di Fisica, Università di Roma Tor Vergata, Roma; Italy.

[79(a)]INFN Sezione di Roma Tre;[(b)]Dipartimento di Matematica e Fisica, Università Roma Tre, Roma; Italy.
[80(a)]INFN-TIFPA;[(b)]Università degli Studi di Trento, Trento; Italy.
[81]Universität Innsbruck, Department of Astro and Particle Physics, Innsbruck; Austria.
[82]University of Iowa, Iowa City IA; United States of America.
[83]Department of Physics and Astronomy, Iowa State University, Ames IA; United States of America.
[84]Istinye University, Sariyer, Istanbul; Türkiye.
[85(a)]Departamento de Engenharia Elétrica, Universidade Federal de Juiz de Fora (UFJF), Juiz de Fora;[(b)]Universidade Federal do Rio De Janeiro COPPE/EE/IF, Rio de Janeiro;[(c)]Instituto de Física, Universidade de São Paulo, São Paulo;[(d)]Rio de Janeiro State University, Rio de Janeiro;[(e)]Federal University of Bahia, Bahia; Brazil.
[86]KEK, High Energy Accelerator Research Organization, Tsukuba; Japan.
[87]Graduate School of Science, Kobe University, Kobe; Japan.
[88(a)]AGH University of Krakow, Faculty of Physics and Applied Computer Science, Krakow;[(b)]Marian Smoluchowski Institute of Physics, Jagiellonian University, Krakow; Poland.
[89]Institute of Nuclear Physics Polish Academy of Sciences, Krakow; Poland.
[90]Faculty of Science, Kyoto University, Kyoto; Japan.
[91]Research Center for Advanced Particle Physics and Department of Physics, Kyushu University, Fukuoka ; Japan.
[92]L2IT, Université de Toulouse, CNRS/IN2P3, UPS, Toulouse; France.
[93]Instituto de Física La Plata, Universidad Nacional de La Plata and CONICET, La Plata; Argentina.
[94]Physics Department, Lancaster University, Lancaster; United Kingdom.
[95]Oliver Lodge Laboratory, University of Liverpool, Liverpool; United Kingdom.
[96]Department of Experimental Particle Physics, Jožef Stefan Institute and Department of Physics, University of Ljubljana, Ljubljana; Slovenia.
[97]School of Physics and Astronomy, Queen Mary University of London, London; United Kingdom.
[98]Department of Physics, Royal Holloway University of London, Egham; United Kingdom.
[99]Department of Physics and Astronomy, University College London, London; United Kingdom.
[100]Louisiana Tech University, Ruston LA; United States of America.
[101]Fysiska institutionen, Lunds universitet, Lund; Sweden.
[102]Departamento de Física Teorica C-15 and CIAFF, Universidad Autónoma de Madrid, Madrid; Spain.
[103]Institut für Physik, Universität Mainz, Mainz; Germany.
[104]School of Physics and Astronomy, University of Manchester, Manchester; United Kingdom.
[105]CPPM, Aix-Marseille Université, CNRS/IN2P3, Marseille; France.
[106]Department of Physics, University of Massachusetts, Amherst MA; United States of America.
[107]Department of Physics, McGill University, Montreal QC; Canada.
[108]School of Physics, University of Melbourne, Victoria; Australia.
[109]Department of Physics, University of Michigan, Ann Arbor MI; United States of America.
[110]Department of Physics and Astronomy, Michigan State University, East Lansing MI; United States of America.
[111]Group of Particle Physics, University of Montreal, Montreal QC; Canada.
[112]Fakultät für Physik, Ludwig-Maximilians-Universität München, München; Germany.
[113]Max-Planck-Institut für Physik (Werner-Heisenberg-Institut), München; Germany.
[114]Graduate School of Science and Kobayashi-Maskawa Institute, Nagoya University, Nagoya; Japan.
[115(a)]Department of Physics, Nanjing University, Nanjing;[(b)]School of Science, Shenzhen Campus of Sun Yat-sen University;[(c)]University of Chinese Academy of Science (UCAS), Beijing; China.
[116]Department of Physics and Astronomy, University of New Mexico, Albuquerque NM; United States of

America.
[117]Institute for Mathematics, Astrophysics and Particle Physics, Radboud University/Nikhef, Nijmegen; Netherlands.
[118]Nikhef National Institute for Subatomic Physics and University of Amsterdam, Amsterdam; Netherlands.
[119]Department of Physics, Northern Illinois University, DeKalb IL; United States of America.
[120(a)]New York University Abu Dhabi, Abu Dhabi;[(b)]United Arab Emirates University, Al Ain; United Arab Emirates.
[121]Department of Physics, New York University, New York NY; United States of America.
[122]Ochanomizu University, Otsuka, Bunkyo-ku, Tokyo; Japan.
[123]Ohio State University, Columbus OH; United States of America.
[124]Homer L. Dodge Department of Physics and Astronomy, University of Oklahoma, Norman OK; United States of America.
[125]Department of Physics, Oklahoma State University, Stillwater OK; United States of America.
[126]Palacký University, Joint Laboratory of Optics, Olomouc; Czech Republic.
[127]Institute for Fundamental Science, University of Oregon, Eugene, OR; United States of America.
[128]Graduate School of Science, Osaka University, Osaka; Japan.
[129]Department of Physics, University of Oslo, Oslo; Norway.
[130]Department of Physics, Oxford University, Oxford; United Kingdom.
[131]LPNHE, Sorbonne Université, Université Paris Cité, CNRS/IN2P3, Paris; France.
[132]Department of Physics, University of Pennsylvania, Philadelphia PA; United States of America.
[133]Department of Physics and Astronomy, University of Pittsburgh, Pittsburgh PA; United States of America.
[134(a)]Laboratório de Instrumentação e Física Experimental de Partículas - LIP, Lisboa;[(b)]Departamento de Física, Faculdade de Ciências, Universidade de Lisboa, Lisboa;[(c)]Departamento de Física, Universidade de Coimbra, Coimbra;[(d)]Centro de Física Nuclear da Universidade de Lisboa, Lisboa;[(e)]Departamento de Física, Universidade do Minho, Braga;[(f)]Departamento de Física Teórica y del Cosmos, Universidad de Granada, Granada (Spain);[(g)]Departamento de Física, Instituto Superior Técnico, Universidade de Lisboa, Lisboa; Portugal.
[135]Institute of Physics of the Czech Academy of Sciences, Prague; Czech Republic.
[136]Czech Technical University in Prague, Prague; Czech Republic.
[137]Charles University, Faculty of Mathematics and Physics, Prague; Czech Republic.
[138]Particle Physics Department, Rutherford Appleton Laboratory, Didcot; United Kingdom.
[139]IRFU, CEA, Université Paris-Saclay, Gif-sur-Yvette; France.
[140]Santa Cruz Institute for Particle Physics, University of California Santa Cruz, Santa Cruz CA; United States of America.
[141(a)]Departamento de Física, Pontificia Universidad Católica de Chile, Santiago;[(b)]Millennium Institute for Subatomic physics at high energy frontier (SAPHIR), Santiago;[(c)]Instituto de Investigación Multidisciplinario en Ciencia y Tecnología, y Departamento de Física, Universidad de La Serena;[(d)]Universidad Andres Bello, Department of Physics, Santiago;[(e)]Instituto de Alta Investigación, Universidad de Tarapacá, Arica;[(f)]Departamento de Física, Universidad Técnica Federico Santa María, Valparaíso; Chile.
[142]Department of Physics, Institute of Science, Tokyo; Japan.
[143]Department of Physics, University of Washington, Seattle WA; United States of America.
[144]Department of Physics and Astronomy, University of Sheffield, Sheffield; United Kingdom.
[145]Department of Physics, Shinshu University, Nagano; Japan.
[146]Department Physik, Universität Siegen, Siegen; Germany.

[147]Department of Physics, Simon Fraser University, Burnaby BC; Canada.
[148]SLAC National Accelerator Laboratory, Stanford CA; United States of America.
[149]Department of Physics, Royal Institute of Technology, Stockholm; Sweden.
[150]Departments of Physics and Astronomy, Stony Brook University, Stony Brook NY; United States of America.
[151]Department of Physics and Astronomy, University of Sussex, Brighton; United Kingdom.
[152]School of Physics, University of Sydney, Sydney; Australia.
[153]Institute of Physics, Academia Sinica, Taipei; Taiwan.
[154(a)]E. Andronikashvili Institute of Physics, Iv. Javakhishvili Tbilisi State University, Tbilisi;[(b)]High Energy Physics Institute, Tbilisi State University, Tbilisi;[(c)]University of Georgia, Tbilisi; Georgia.
[155]Department of Physics, Technion, Israel Institute of Technology, Haifa; Israel.
[156]Raymond and Beverly Sackler School of Physics and Astronomy, Tel Aviv University, Tel Aviv; Israel.
[157]Department of Physics, Aristotle University of Thessaloniki, Thessaloniki; Greece.
[158]International Center for Elementary Particle Physics and Department of Physics, University of Tokyo, Tokyo; Japan.
[159]Department of Physics, University of Toronto, Toronto ON; Canada.
[160(a)]TRIUMF, Vancouver BC;[(b)]Department of Physics and Astronomy, York University, Toronto ON; Canada.
[161]Division of Physics and Tomonaga Center for the History of the Universe, Faculty of Pure and Applied Sciences, University of Tsukuba, Tsukuba; Japan.
[162]Department of Physics and Astronomy, Tufts University, Medford MA; United States of America.
[163]Department of Physics and Astronomy, University of California Irvine, Irvine CA; United States of America.
[164]University of West Attica, Athens; Greece.
[165]University of Sharjah, Sharjah; United Arab Emirates.
[166]Department of Physics and Astronomy, University of Uppsala, Uppsala; Sweden.
[167]Department of Physics, University of Illinois, Urbana IL; United States of America.
[168]Instituto de Física Corpuscular (IFIC), Centro Mixto Universidad de Valencia - CSIC, Valencia; Spain.
[169]Department of Physics, University of British Columbia, Vancouver BC; Canada.
[170]Department of Physics and Astronomy, University of Victoria, Victoria BC; Canada.
[171]Fakultät für Physik und Astronomie, Julius-Maximilians-Universität Würzburg, Würzburg; Germany.
[172]Department of Physics, University of Warwick, Coventry; United Kingdom.
[173]Waseda University, Tokyo; Japan.
[174]Department of Particle Physics and Astrophysics, Weizmann Institute of Science, Rehovot; Israel.
[175]Department of Physics, University of Wisconsin, Madison WI; United States of America.
[176]Fakultät für Mathematik und Naturwissenschaften, Fachgruppe Physik, Bergische Universität Wuppertal, Wuppertal; Germany.
[177]Department of Physics, Yale University, New Haven CT; United States of America.
[178]Yerevan Physics Institute, Yerevan; Armenia.
[a] Also Affiliated with an institute covered by a cooperation agreement with CERN.
[b] Also at An-Najah National University, Nablus; Palestine.
[c] Also at Borough of Manhattan Community College, City University of New York, New York NY; United States of America.
[d] Also at Center for Interdisciplinary Research and Innovation (CIRI-AUTH), Thessaloniki; Greece.
[e] Also at CERN, Geneva; Switzerland.
[f] Also at CMD-AC UNEC Research Center, Azerbaijan State University of Economics (UNEC); Azerbaijan.

[g] Also at Département de Physique Nucléaire et Corpusculaire, Université de Genève, Genève; Switzerland.
[h] Also at Departament de Fisica de la Universitat Autonoma de Barcelona, Barcelona; Spain.
[i] Also at Department of Financial and Management Engineering, University of the Aegean, Chios; Greece.
[j] Also at Department of Physics, California State University, Sacramento; United States of America.
[k] Also at Department of Physics, King's College London, London; United Kingdom.
[l] Also at Department of Physics, Stanford University, Stanford CA; United States of America.
[m] Also at Department of Physics, Stellenbosch University; South Africa.
[n] Also at Department of Physics, University of Fribourg, Fribourg; Switzerland.
[o] Also at Department of Physics, University of Thessaly; Greece.
[p] Also at Department of Physics, Westmont College, Santa Barbara; United States of America.
[q] Also at Faculty of Physics, Sofia University, 'St. Kliment Ohridski', Sofia; Bulgaria.
[r] Also at Hellenic Open University, Patras; Greece.
[s] Also at Imam Mohammad Ibn Saud Islamic University; Saudi Arabia.
[t] Also at Institucio Catalana de Recerca i Estudis Avancats, ICREA, Barcelona; Spain.
[u] Also at Institut für Experimentalphysik, Universität Hamburg, Hamburg; Germany.
[v] Also at Institute for Nuclear Research and Nuclear Energy (INRNE) of the Bulgarian Academy of Sciences, Sofia; Bulgaria.
[w] Also at Institute of Applied Physics, Mohammed VI Polytechnic University, Ben Guerir; Morocco.
[x] Also at Institute of Particle Physics (IPP); Canada.
[y] Also at Institute of Physics, Azerbaijan Academy of Sciences, Baku; Azerbaijan.
[z] Also at National Institute of Physics, University of the Philippines Diliman (Philippines); Philippines.
[aa] Also at Technical University of Munich, Munich; Germany.
[ab] Also at The Collaborative Innovation Center of Quantum Matter (CICQM), Beijing; China.
[ac] Also at TRIUMF, Vancouver BC; Canada.
[ad] Also at Università di Napoli Parthenope, Napoli; Italy.
[ae] Also at University of Colorado Boulder, Department of Physics, Colorado; United States of America.
[af] Also at Washington College, Chestertown, MD; United States of America.
[ag] Also at Yeditepe University, Physics Department, Istanbul; Türkiye.
[*] Deceased